FACULDADE DE ENGENHARIA DA UNIVERSIDADE DO PORTO

FEUP

Dynamic Analysis of Upper Limbs Movements after Breast Cancer Surgery

Ana Rita Carvalho Moreira

MASTER THESIS

Mestrado Integrado em Bioengenharia

Supervisor: Hélder Filipe Pinto de Oliveira (PhD)

Co-Supervisor: Jaime dos Santos Cardoso (PhD)

June 2014

Resumo

A qualidade de vida dos pacientes com cancro de mama tem vindo a tornar-se um fator de importante consideração aquando da escolha do tipo de tratamento a ser utilizado. Contudo, técnicas de tratamento comuns, como o caso da radioterapia ou da remoção cirúrgica dos nódulos linfáticos da axila, resultam em vários danos no funcionamento dos membros superior das mulheres. Estas deficiências incluem uma limitada mobilidade do braço e o seu inchaço, o que normalmente precede o aparecimento linfedema crónico. Estas morbidades afetam as várias atividades diárias dos pacientes e, consequentemente, contribuem para uma menor qualidade de vida.

Assim, é de extrema importância avaliar as restrições funcionais derivadas do tratamento do cancro, de modo a avaliar a qualidade dos procedimentos e a evitar complicações posteriores. Sendo assim, este trabalho tem como objetivo desenvolver um método eficaz para a avaliação do funcionamento dos membros superior do corpo, aplicável a pacientes com cancro da mama. Para este fim, é investigado o uso de informação de profundidade e de esqueleto, adquiridos com a Microsoft Kinect, para extrair atributos que caracterizam o movimento dos membros superiores. São utilizados algoritmos de classificação supervisionados para construir um modelo de classificação, obtendo-se resultados muito promissores, com elevada precisão de classificação. Deste modo, o método desenvolvido parece ser uma solução adequada ao objetivo proposto.

Após tratamento do cancro de mama, é fundamental para as mulheres manter uma atividade física contínua de modo a recuperar a mobilidade dos membros superiores. Dessa forma, normalmente é recomendado um conjunto de exercícios para efectuar em casa, mas as pacientes nem sempre os fazem como deveriam. Isto reforça a importância de um modelo de cuidado para reabilitação dos pacientes de cancro da mama, de modo a promover e apoiar a atividade física. Desta forma, neste trabalho foi também investigado um modelo de reabilitação para pacientes com cancro de mama. Recorrendo à Kinect, desenvolveu-se uma aplicação neste sentido, que instrui o paciente na execução dos exercícios e realiza uma avaliação da sua performance. Os resultados preliminares são bastante satisfatórios, mas ainda é necessário um trabalho mais aprofundado nesta área.

Abstract

The quality of life of breast cancer patients has increasingly become an important factor of consideration in choosing the type of treatment used. However, common treatment techniques, as the case of radiation therapy or the surgical removal of the axillary lymphatic nodes, result in several impairments in women's upper-body function. These impairments include restricted shoulder mobility and arm swelling, which usually precedes chronic lymphedema. As consequence, several daily life activities of the women will be affected and, consequently, contribute to a decreased QOL.

Therefore, is of extreme importance to assess the functional restrictions caused by cancer treatment, in order to evaluate the quality of procedures and to avoid further complications. In this manner, the present work aims to develop an effective method for the evaluation of the upper-body function, suitable for breast cancer patients. For this purpose, it is investigated the use of both depth and skeleton data, provided by the Microsoft Kinect, to extract features that characterize the upper-limbs motion. Supervised classification algorithms are used to construct a predictive model of classification and very promising results are obtained, with high classification accuracy. Therefore, the developed method appears to be a proper solution for the proposed goal.

After breast cancer treatment, it is essential for the women to maintain a continuous physical activity in order to recover the upper-limb mobility. In that way, a home-base exercise program is normally recommended, but the patients not always perform the exercises as they should. This highlights the importance of a surveillance rehabilitation model for breast cancer patients to promote and support physical activity and exercise behaviors. Further in this research, it was investigated a rehabilitation model for breast cancer patients. Taking advantage of the Kinect device, an application was developed in this direction, that instructs the patient on how to execute the exercises and makes an evaluation of their performance. Preliminary results are quite satisfactory, but further work is still needed.

Acknowledgments

This work would not be possible without the contribution, help and support of several people to whom I owe a sincere gratitude.

First of all, I am eternally grateful to Hélder, for his continuous support, motivation, friendship and for being always available. Without him nothing of this would be possible! Also, I have to thank to Professor Jaime for his helpful and pertinent advising, whenever needed. Furthermore, I am very thankful to Dr. André Magalhães from the *Hospital São João*, for the medical support. My gratitude goes also to INESC TEC and the VCMI (Visual Computing and Machine Intelligence) group, for the work environment provided, which allowed the development of this thesis.

To Inês, Sofia and Filipa, my daily mates, for working by me side, for all the lunches together and, more important, for all the confidences, chats and laughs. To M&B for all the things it taught me. For make me understand that the bacon is better than the egg. To 09, for those who entered with me and the did this journey by me side. To C'amelias for all the unforgettable moments we had together. All the tears and laughs and tears by laughs. All the dinners, beers and cheers. All the Porto and *fados*. From here I did friends for life. Some deserve a special word: to Xiló, for the unconditional friendship, always being there to hear me; to Joana, my timeless roommate; to Rita and Dani, or the embreast-it would not be complete. To João, despite everything, for all the *inrideo ut pervenio lux*. To all the others who accompanied me in these five years and made part of the best times of my life, a sincere thank you.

To Pedro, for being by my side every single day, for all the patience with my bad mood and my craziness moments, for making me stand up when I was almost falling. For all the love and encouragement, for everything that is not possible to thank.

To my mother, my role model, for all the efforts that I know she did so I could accomplish this, for always taking care of me, for the unconditional love and eternal support. To my father, for never stop believing on my capabilities and always trust that I could it. To my brother, for all the support and advisement and for never doubt of my success. To Lu, my second mother. To Koda and Woody, or the family would not be complete.

Rita Moreira

"We must try not to sink beneath our anguish, Harry, but battle on."

Albus Dumbledore

To my mother,

x

Contents

List of Figures

List of Tables

Acronyms

2D	Two-Dimensional
3D	Three-Dimensional
ALND	Axillary Lymph Node Dissection
BCCT	Breast Cancer Conservative Treatment
BCCT.core	Breast Cancer Conservative Treatment.Cosmetic result
BCS	Breast Conserving Surgery
BIS	Bioelectrical Impedance Spectroscopy
CAD	Computer Aided Design
CAML	Computer Aided Measurement Laser
CCs	Cue Circles
CT	Computed tomography
DASH	Disabilities of the Arm, Shoulder and Hand
DCIS	Ductal Carcinoma *in situ*
DEXA	Dual Energy X-ray Absorptiometry
DNA	Deoxyribonucleic acid
EORTC QLQ BR23	European Organization for Research and Treatment of Cancer Quality of Life Questionnaire-Breast Cancer Module
FACT-B	Functional Assessment of Cancer Therapy-Breast
FN	False Negative
FP	False Positive
GT	Ground Truth
GUI	Graphical User Interface
ICP	Iterative Closest Points
IDC	Invasive Ductal Carcinoma
ILC	Invasive Lobular Carcinoma
IR	Infra-Red
KAPS	Kwan's arm problem scale
LDA	Linear Discriminant Analysis
MRI	Magnetic Resonance Imaging
NUI	Natural User Interface
QOL	Quality-of-Life
RBF	Radial Basis Function
ROM	Range of Motion
RT	Radiotherapy
PS	Proximity Space
PSFS	Patient-Specific Functional Scale
SDK	Software Development Kit
SLN	Sentinel Lymph Node
SLND	Sentinel Lymph Node Dissection
SVM	Support Vector Machine
TP	True Positive
UBF	Upper-Body Function
UEFI	Upper Extremity Functional Index
VR	Virtual reality

Chapter 1

Introduction

Breast cancer is the most common cancer both in developed and developing regions, representing 23% of all cancers [35]. Nevertheless, due to effective earlier diagnosis methods and effective adjuvant therapies, the mortality rate is 27% or less in the more developed regions [35]. These high probabilities of long term disease survival mean that the women need to live daily with the consequences of the treatment. Consequently, the interest in the psychological adaptation and Quality of Life (QOL) of women after treatment has been growing. Increased psychiatric morbidity is associated with patients who experience unpleasant side effects of treatment for breast cancer. Women diagnosed with this disease have an higher risk of developing severe anxiety, depression and potential mood disorders, mainly due to worries regarding fear of death and altered body image, sexuality and attractiveness [115].

Approximately, 25% of women diagnosed with breast cancer present cancer cells in the axillary lymph node system [42]. Thus, besides the tumor removal, treatments generally includes the removal of axillary lymph nodes, as well as radiotherapy to the axilla [40]. However, this type of procedures are normally responsible for several upper-limb problems, including restricted shoulder mobility, lymphedema and/or arm/shoulder pain. Furthermore, at the 5 year follow-up the prevalence of arm/shoulder pain is 30-40%, of lymphedema 10–15%, and of restricted arm/shoulder mobility is 15–30% [80]. These upper-body morbidities are highly correlated with decreased QOL in breast cancer patients, since it disrupts valuable daily life activities [66, 102]. Therefore, studies support a timely screening as part of follow-up care and early management of the cancer-related physical impairments, with an appropriated rehabilitation program, can improve the the upper-limbs function and patients' QOL [104].

1.1 Motivation

Breast cancer survivors normally experience long-term sequelae that include psychological distress, related with suboptimal cosmetic results, and physical impairments, which will contribute to a poor QOL. There is a diversity of strategies used is breast cancer treatment, both in surgery and in radiation therapy, which will result in different outcomes [83]. Therefore, it would be useful to have an objective and standard assessment of the final outcome of treatment, in order to identify which procedures have the less morbidity associated and to standardize these treatments. In this direction, a large research has been done and several methods were proposed for the evaluation of breast cancer treatment [15, 16, 32, 51, 82]. However, almost all the studies only focused on the cosmetic appearance, and the functional status has received much less attention. It is claimed by some authors [66, 102] that the upper-body morbidity, such as arm edema and restricted

shoulder mobility, are correlated more strongly with QOL indicators than cosmetic status, due to their ability to disrupt valued life activities. So, it would be appropriate to include an Upper-Body Function (UBF) evaluation, besides the cosmetic assessment, in the evaluation of the breast cancer treatment.

The assessment of functional limitations in breast cancer patients can be performed by the identification of arm edema and by the evaluation of arm/shoulder mobility. However, this evaluation is not always done, and when it happens, the methods used have problems regarding the lack of objectivity or inaccuracy. The common procedures include subjective questionnaires [13], circumference measurements [103] or the use of a goniometer [38]. For that reason, there is a need of an simple, accurate, low-cost and reproducible method for the evaluation of UBF.

An early diagnosis of upper-limbs impairments is also important to have an identification of adequate therapies that can lead to greater success in managing functional morbidity, as well as prevention of progression, with improved outcomes and QOL for breast cancer survivors. It has been well documented the benefits of physiotherapy and physical activity on the recovering of upper-extremity range-of-motion (ROM), strength, and function on women's QOL [19, 26, 76, 77, 100]. Therefore, it would be also useful a comprehensive model of care to identify exercise prescription and to guide the rehabilitation of breast cancer-related physical impairments.

1.2 Objectives

The main purpose of the present study is the development of a new methodology to assess objectively the upper-limbs functional status on breast cancer patients, using a low cost equipment, the Microsoft Kinect (Microsoft Corp., Redmond, WA, USA). On the other hand, it is also intended the use of the Kinect for the creation of a home-based rehabilitation system for physical impairments related to breast cancer treatment.

The Kinect sensor provides RGB and depth data, and allows a simplified skeleton tracking. To evaluate the upper-extremity function it will be assessed the limb volume and the temporal motion of the upper-arm and shoulder, using the depth camera and the tracking capabilities of the Kinect device. With this system it will be possible to extract movements' features, including the upper-arm volume and the shoulder ROM, in order to evaluate the motion of the upper-limb over time. Thus, it will be possible to have a complete functional evaluation of the upper-body status of breast cancer patients, and identify reduced UBF caused by the treatment.

Also, it will be investigated a possible upper-body exercise system for home environment, using the Kinect device, that can be helpful in the rehabilitation of the arm/shoulder mobility and reduce the risk of lymphedema.

All the research depends on the availability of training and testing examples used in the development of the models. Therefore, this project included the collection of a data set with the help of an expert in breast cancer.

1.3 Contributions

The proposed work had four main contributions:

- Using the Kinect for Windows SDK it was developed a windows application for the collection of medical data. With this application is possible to acquire and record RGB and depth frames, as well as information about the skeleton's joints positions over time.

- It was created a database comprising color, depth and skeleton data of breast cancer patients performing adduction/abduction movements. This database is a unique tool and can lead to new developments in the area.
- A new methodology is proposed, suitable for the evaluation of the upper-body function and lymphedema detection in breast cancer patients.
- Finally, taking advantage of the Kinect capabilities, it was developed an application that can be used as home-based rehabilitation system to recover the upper-body function.

1.4 Document Structure

Besides the introduction, this document is composed by five more chapters. In chapter 2, a global introduction to the breast cancer problem is presented. In chapter 3, the literature review is provided on all the topics related to upper-body functional evaluation assessment. It includes methods used to measure the limb volume, subjective scales to evaluate the effects of injury in upper-body function and vision-based systems used to track human movements. Also, some insights are provided regarding virtual reality systems in home-based rehabilitation models. Chapter 4 describes the proposed method for upper-body function evaluation and the main results obtained. The application developed for rehabilitation is presented on Chapter 5. Finally, Chapter 6 serves as a conclusion to the presented research.

Chapter 2

Breast Cancer

2.1 Breast Anatomy and Physiology

The breast is a highly efficient organ mainly used to produce milk. It is a mass of glandular, fatty, and fibrous tissues positioned over the pectoralis major muscles of the chest wall [29]. The shape of the breast is similar to a tear-drop and has an extension toward the axilla, known as the tail of Spencer. Each adult female mammary gland usually consists of 15–20 glandular lobes. On the other hand, each lobe is composed by more than 40 smaller lobules, also known as the terminal ductal lobular units. The lobules terminate in many tiny bulbs which are the milk-secreting cells. The lobes, lobules and bulbs are all linked by the ducts [97] (see Figure 2.1).

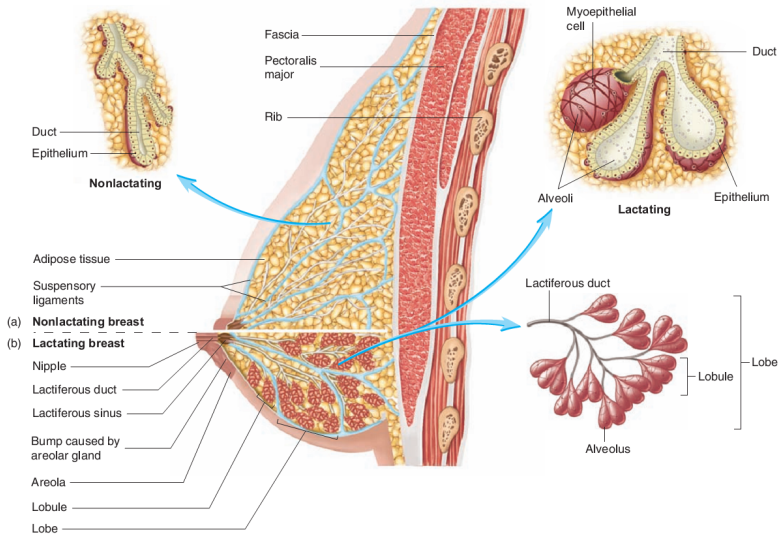

Figure 2.1: Breast Anatomy: the mammary gland consists of lobes, which are made up of lobules. Ducts from the lobules converge to form lactiferous ducts. (a) Nonlactating breast, only with the duct system (b) Lactating breast, with alveoli at the ends of the ducts, which produce milk (From [97]).

2.1.1 Breast Lymphatic System

The lymphatic system is part of the body's defense system against pathogens. In addition, it helps to maintain fluid balance in tissues and to absorb fat from the digestive tract. It is a network of tissue and organs that primarily consists of lymph vessels and lymph nodes [97]. Lymph nodes are small, oval-shaped structures distributed along the course of the lymphatic vessels. They filter the lymph, removing bacteria and other materials. The lymphatic vessels carry the lymph, which contains tissue fluid and waste products, as well as immune system cells.

In the upper-limbs, all the lymph vessels drain into the lymph nodes in the axilla. In addition, axillary nodes receive fluid from the upper back and shoulder, the lower neck, the chest, and the upper anterolateral abdominal wall. Regarding the breast, approximately 75% of the drainage of lymph fluid of the mammary gland is performed via lymphatic vessels into axillary nodes (see Figure 2.2) [29].

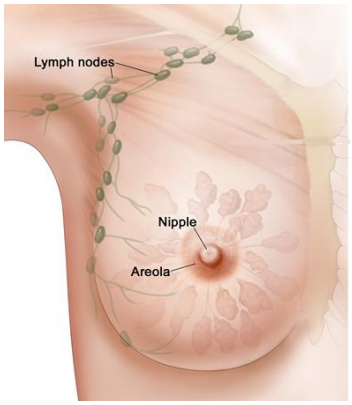

Figure 2.2: Brest Lymphatic System. Adapted from [120]

2.2 Breast Carcinoma

Cancer begins when cells in a part of the body start to grow out of control. These cells have a tightly regulated cell cycle that controls their growth, maturity, division and death. Cell division and growth is controlled by Deoxyribonucleic acid (DNA) and genes that lie within the cell's nucleus, so any changes to DNA affects the cell. A cancer cell appears when a normal cell undergoes damage to the DNA that it is not repaired and the cell does not die, as it should. Instead, the cell undertakes division and the damage is propagated by the out-of-control growth of abnormal cells. This leads to formation of a tumor that may be benign (not dangerous to health) or malignant (has the potential to be dangerous) [57].

Breast cancer is a malignant tumor arising from the cells of the breast. Usually breast cancer either develops in the cells of the lobules or the lactiferous ducts. Less commonly, breast cancer can begin in the stromal tissues, which include the fatty and fibrous connective tissues of the breast [29].

There are different types of breast cancer, often divided into non-invasive and invasive. Non-invasive breast cancer, also known as carcinoma *in situ*, is when the cancer remain within the place of origin. The cancer do not grow into or invade normal tissues within or beyond the breast. One type of non-invasive cancer called ductal carcinoma *in situ* (DCIS) is considered a pre-cancerous lesion. This means that, although the abnormal cells have not spread out, they can eventually develop into invasive breast cancer. In invasive breast cancer, the abnormal cells spread outside the membrane that lines a duct or lobule, invading the surrounding

tissues. The cells can travel through the bloodstream or the lymphatic system to other parts of the body such as the bones, liver or lungs, creating metastasis. Invasive ductal carcinoma (IDC) and invasive lobular carcinoma (ILC) are the most common types of invasive breast cancer [69].

2.3 Breast Cancer Treatments

Besides disease control, breast cancer treatments aims to reduce the risk of distant metastases and/or local recurrence, obtain better aesthetic outcomes, relief of symptoms and restoring the QOL prior to diagnosis [91]. The type of treatment chosen by the clinicians depends on several factors, such as women's health and age, position and size of the cancer and how far it has spread. The treatments options normally include chemotherapy, radiotherapy and surgery.

Depending on factors such as the position and size of the cancer, the treatment chosen may be the surgical removal of the tumor by a mastectomy or a more conservative approach by Breast Cancer Conservative Treatment (BCCT). Non-surgical treatments, as chemotherapy and radiotherapy, may be used before surgery to help shrink the tumor or after surgery.

Mastectomy is the surgical removal of the entire breast. There are five different types: simple or total mastectomy, partial mastectomy, subcutaneous (nipple-sparing) mastectomy, modified radical mastectomy and radical mastectomy [56]. Total mastectomy involves removal of the breast, nipple, areola, and sentinel lymph nodes. The partial mastectomy removes the part of the breast that has cancer and some normal tissue around it. During subcutaneous mastectomy, all of the breast tissue is removed, but the nipple is left alone. A modified radical mastectomy consists in the removal of the entire breast, nipple, areola, and axillary lymph nodes but often leaves the chest wall intact. When the tumor is large and has spread to the muscles of the chest wall, a radical mastectomy may be necessary [57]. Although mastectomy may significantly reduce the recurrence risk of the cancer, it is a radical surgical intervention, so the psychological costs are very high. Patients who experienced a mastectomy fell less attractive, less sexually desirable and ashamed of their body. Other side effects may include weight gain, breast sensitivity, muscle stiffness and joint pain [4].

BCCT was created as an attempt to preserve the breast without compromising the survival of the patient. BCCT is defined as a combination of a breast conserving surgery (BCS) for resection of the primary tumour, followed by moderate-dose radiation therapy to eradicate any microscopic residual disease [91]. In breast conserving surgery it is only removed the breast tumor and some of the normal tissue that surrounds it, while preserving the natural shape and appearance of the breast.

Radiation therapy is normally used after the surgical removal of the tumor in order to eradicate any residual cancer cells. However, side effects of this treatment, caused by interference on lymphatic drainage, include swelling and heaviness of the arm, that will affect its mobility [34].

2.3.1 Lymph Node Dissection

The primary route of lymphatic drainage of breast is through the axillary lymph node group. The lymphatic system facilitate cancer spread, since cancer cells can enter lymphatic vessels and begin to grow in lymph nodes. In that case, there is a higher chance that the cancer metastasized to other places in the body.

About 40% of women diagnosed with breast cancer have cancer cells in their axillary lymph nodes [43]. Therefore, in addition to the removal of breast cancer through surgery, sometimes is needed the removal of one or more axillary lymph nodes to discover if the cancer has spread beyond the breast. Lymph node biopsy

and dissection is also important to determine the stage of the breast cancer and decide the type of treatment needed.

Axillary lymph node dissection (ALND) has been part of breast cancer surgery since the description of the radical mastectomy [40]. This technique involves the removal of, at least, six of the lymph nodes of axilla (see Figure 2.3).

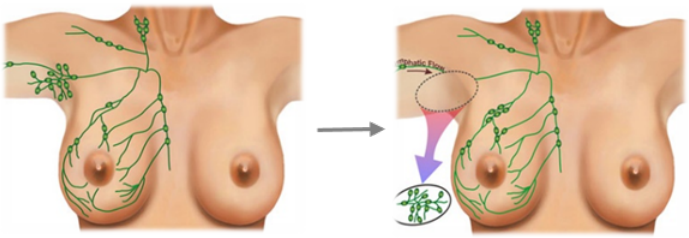

Figure 2.3: Axillary Lymph Node Dissection (ALND). Adapted from [81].

Sentinel lymph node dissection (SLND) was designed to accurately stage tumor-draining axillary nodes with less morbidity than ALND [65]. The first lymph node to receive lymphatic drainage from the breast is called sentinel lymph node (SLN). Therefore, a tumor-free SLN can indicate the absence of cancer metastasis in the rest of the lymphatic system [88]. Otherwise, ALND remains the standard procedure of care for patients with metastases in SLN [40].

About 25% of women with breast cancer undergoing SLND presented cancer cells in the axillary lymph nodes and, therefore, needed a complete dissection of the remaining nodes [42]. These women subjected to ALND will probably be affected by severe morbidities in upper-extremity function since the removal of lymph nodes will affect the drainage of the limbs. The interruption of the axillary lymphatic system will result in the accumulation of fluid in subcutaneous tissue in the arm, with decreased distensibility of tissue around the joints and increased weight of the limb [34]. In this manner, significant impairments in UBF are associated with ALND, such as restricted arm and/or shoulder motion and arm edema [34, 88].

2.4 Conclusion

Breast cancer treatment approaches have been improving, moving towards a more conservative treatment. Following this line of thought, surgical procedures as the radical mastectomy and ALND were replaced by a conservative treatment and the use of a SLND to reduce the number of unnecessary lymph node dissections. However, these less extensive procedures still result in considerable morbidity in several patients, such as restricted upper-body function, caused either by the lymph node removal [34, 109] or by the use of additional radiation therapy of the axilla [34], since both procedures will interfere with the axillary lymphatic system.

Upper-body impairments include reduced motion of the arm/shoulder, strength and flexibility, arm/shoulder pain and/or arm edema. Restricted UBF is typically associated with alterations in the use and function of the upper-body and adverse physical, psychosocial, and social implications that profoundly influence all aspects of daily life and, therefore, QOL [48, 62].

An extensive research has been done regarding the effect of BCCT in the physical appearance of the breast, and several methods were proposed to objectively evaluate the aesthetic results of the treatment [83], as a mean to improve patients' QOL. However, upper-extremity functional impairments are, in most cases, considered for the treatment evaluation. Some authors [66, 102] defend that upper-body morbidity caused

by breast cancer treatments, as indexed by arm edema, are correlated more strongly with QOL indicators than cosmetic status, due to their ability to disrupt valued life activities. Thereby, although concerns related to the impact of BCCT on appearance may be important, the upper-body functional limitations also deserve attention. Unfortunately, limited research and conflicting results characterize the work undertaken to assess the UBF problems related to breast cancer treatment [13, 45].

In other words, there is a lack of practical and cost-effective methodologies to assess changes in upper-body function caused by BCCT, that have a relevant influence in women's QOL. Therefore, the objective evaluation of UBF restrictions can be an helpful tool in the determination and quantification of the sequel related to breast cancer treatment. This functional evaluation is essential to identify which procedures have the less morbidity associated and to standardize these treatments. Moreover, with an early identification and diagnosis of impairments, therapeutic interventions can lead to greater success in managing upper-limb morbidity, with improved outcomes and QOL for breast cancer survivors [8].

Chapter 3

Literature Review

In the previous Chapter it was discussed the main causes and consequences of the breast cancer treatments regarding the UBF. It was stated the importance of a functional evaluation of the upper-body motion, in order to identify the procedures that present better results and, more important, to have a timely diagnosis in order to prevent further complications and, thereby, improve women's QOL. In this way, this Chapter discusses several methods that are, or could be, used to address this purpose.

3.1 Functional Evaluation: Methods of Assessment

The assessment of UBF alterations caused by breast cancer treatment can be divided in two different ways:

1. Firstly, it can be evaluated the change of upper-limbs shape, namely, the identification of an higher volume in the affected limb. These findings can indicate the presence of a arm swelling related to lymphedema.

2. Secondly, although objective methods of functional evaluation has focus on arm swelling detection, it is possible to identify other aspects of interest in functional evaluation [80]. Other limitations, as the restricted shoulder ROM and the reduced strength and flexibility, affect upper-extremity functional capacity and, therefore, daily-life activities. Thereby, it is also important to assess motion limitations.

When deciding which method of assessment is the most adequate, several factors should be considered, such as the sensitivity and specificity of the measure, if it is able to identify early edema (before patient report advanced symptoms), and if the method is affordable, transportable, practical for clinical use, non invasive and time efficient [47].

3.1.1 Upper-Limb Volume Measurements

For many women diagnosed with breast cancer, lymphedema is one of the several morbidities associated to the upper-limbs and that adversely affect the function status and QOL [108]. Lymphedema is regarded as incurable, progressive, disfiguring and disabling disorder that is difficult to treat [46]. Therefore, the early detection of arm edema indicators allow an early intervention, with an appropriated therapy, in acute lymphedema that can be reversible, reducing the risk of chronic lymphedema development [3, 84].

Lymphedema was previously diagnosed clinically by medical history and physical examination [34, 107]. However, this type of diagnosis is only effective for advanced sustained disease since the detection is more

difficult to ascertain in the early stages, particularly when edema is mild or intermittent [107]. Currently, methodologies for edema diagnosis often focus on limb volume assessment [9]. Ideally, the evaluation should be performed by the comparison between measurements of the limb before and after the treatment. However, there is no habit of performing these measures before the surgery, thereby bilateral limb comparisons are usually made [9].

3.1.1.1 Methods for Limb Edema Assessment

Lymphedema detection is normally assessed by the comparison of the limb volume with the unaffected limb. Several volume methodologies currently used for this goal include water displacement, circumference measurements, bioimpedance or imaging techniques (see Table 3.1).

Table 3.1: Comparison of the most significant methods for limb edema assessment. Adapted from [72].

System	Time to operate	Home/Travel	Accuracy	Cost	Complex
Water Displacement: The limb is immersed into a container and the amount of the displaced water represents the volume of the limb [108].	High	No	High	Low	Medium
Circumferential Measurements: The volume can be estimated assuming cylindrical/conic volumes between several measures taken along the limb [103].	High	Yes	Low	Low	Low
Perometer ® : The device scans the limb with IR light and assess limb volume at small intervals [21].	Medium	No	High	Medium	High
CT: Determines of the overall cross-section area and quantify the density of the tissues [27].	Low	No	High	High	High
DEXA: Uses a tissue-specific mode with attenuation of X-ray dependent on the thickness, density, and chemical structure of the tissue examined [92].	Low	No	High	High	High
BIS: Small current passes through the body. Measures volumes by comparing impedance values of both arms [22].	Medium	No	Medium	High	Medium

The water displacement is based in a simple physical principle. The limb is immersed into a container and, therefore, the amount of the displaced water will represent the volume of the limb. When performed properly, water displacement is accurate [103], however, it is time-consuming, non portable and can be nonhygienic [108]. On the other hand, there are difficulties in the definition and implementation of the upper level for immersion [108].

The volume can also be obtained indirectly from multiple circumferential measurements of the limb by a tape measure, assuming cylindrical/conic shapes. Accuracy will depend on the spacing between the measurements. Sources of error in this method arise from the assumption of circular cross-section of the limb and from the way the operator uses it [103].

Arm circumferences can also be measured with the use of a Perometer ® [21]. The Perometer ® is an opto-electronic device that depends on the interruption of infra-red (IR) light beams by the limb. The arm

is positioned in a frame with a mobile source of IR light: emitting diodes on two adjacent sides and rows of corresponding sensors on the opposite two sides. The movement of the frame along the limb allows the automatic calculation of the volume from a large number of vertical and horizontal diameter measurements at 0.31 mm interval. This method allows reliable and highly reproducible measurements [108], however the size and the cost of the equipment limits its usability and portability.

In the review of Stanton *et al.* [103] addressing non-invasive methods for lymphedema detection, it was also assessed the use of imaging techniques for this purpose. Computed tomography (CT) has been used to evaluate limb swelling, since this technique allows the determination of the overall cross-section area and quantify the density of the tissues. In lymphedema, CT has shown that subcutaneous compartment increases in volume [27]. The radiation dose is a particular drawback for the repeated use of CT. Magnetic resonance imaging (MRI) was compared with CT for the investigation of limb swelling after breast cancer treatment [27]. Differences between the two methods were small and, although no use of radiation with MRI, the use of CT is cheaper and more readily available.

Dual energy x-ray absorptiometry (DEXA) is typically used to study soft tissue composition as well as bone mineral density. It uses a tissue-specific mode (fat, lean tissue, and bone) with attenuation of X-ray dependent on the thickness, density, and chemical structure of the tissue examined [92]. A criticism similar with CT is applied in this case because of the radiation dose that is used.

Bioelectrical impedance spectroscopy (BIS) as a lymphedema measure has been previously well described [22, 103]. The procedure involves passing an small current through the body at a range of frequencies that can be used to provide information on the amount of total body water and extracellular water. The working principle assumes that extracellular and intracellular fluids act as a network of resistors with the cell membranes behaving as an imperfect capacitor [103]. Comparing the impedance values between the treated and untreated sides, it is possible to measure lymphedema in a accurate manner [22].

3.1.1.2 Three-dimensional approaches for Limb Edema Assessment

Some of the methods described above can provide an objective and accurate measure of the limb volume, however they are time-consuming, complicated or expensive. Therefore, the search for an accurate, reproducible, low-cost and easy-to-use system is still on going.

The fast evolution of 3D technology over the last decade allowed the development of several efficient and cost-effective applications in medicine and health care. Therefore, traditional methods to assess health status, are being replaced by the use of more sophisticated systems. Low-cost, non-invasive and ease of use 3D body-surface scanners are transforming the ability to accurately measure the body size, shape, and skin-surface area. These features make them appealing for widespread clinical applications [112].

In the recent years, some systems comprising 3D laser scanning for limb volume measurement in edema detection were proposed (see Table 3.2).

In 2007, McKinnon *et al.* [75] evaluated the use of digital scanning (Polhemus FastSCAN™ [59]) (Figure 3.1) for lymphedema measurement by comparison to the method of water displacement. The Polhemus FastSCAN system combines laser scanning with 3D spatial orientation. McKinnon concluded that laser scanning is a method that combines precision and reproducibility in tissue volume measurement and may have clinical utility for measuring lymphedema. Harrison *et al.* [44] also validated the clinically use of FastSCAN™ for the assessment of postoperative facial swelling.

More recently, the use of Insignia™ laser scanning system [87] (Figure 3.1) was assessed by Vukotich *et al.* [117] as a mean to obtain limb volume. In comparison with water displacement method, the use of the scanner proved to be suitable for assessing volume in any patient.

Table 3.2: Comparison of 3D methods proposed for arm edema assessment.

System	Papers	Time to operate	Home/Travel	Accuracy	Cost	Complex
FastSCAN™: 3D Laser scanner embedded with FASTRAK® unit, used to determine position and orientation	McKinnon *et al.* [75], Harrison *et al.* [44]	Low	Yes	High	High	High
Insignia™: 3D Laser Scanner embedded with two motion-tracking devices.	Vukotich *et al.* [117]	Low	Yes	High	High	High
CAML: 3D Laser Scanner (FastSCAN™) with CAD software	Trombetta *et al.* [113]	Low	Yes	High	High	Medium
IR Sensor (Microsoft Kinect) with gyroscopes and accelerometers attached.	Lu *et al.* [72]	Medium	Yes	High	Low	High

In 2012, the use of a Computer Aided Measurement Laser (CAML) technique was proposed by Trombetta *et al.* [113] to quantify post-surgery lymphedema. They defend that the use of IR laser scanning and computer aided design (CAD) is a more sensitive and accurate method that provides a fast, precise and non invasive technique to quantify arm edema. The 3D scanner analyzes the limb and collects data on its size, shape and appearance. This data is processed in CAD software to create a model through which it is possible to determine circumferential and limb volume measurements. In their study, the FastSCAN™ was used, in conjugation with a CAD software, to acquire circumferential and volume data for phantoms and upper arm of enrolled patients. The data was compared with circumferential measurements and minimal errors were obtained.

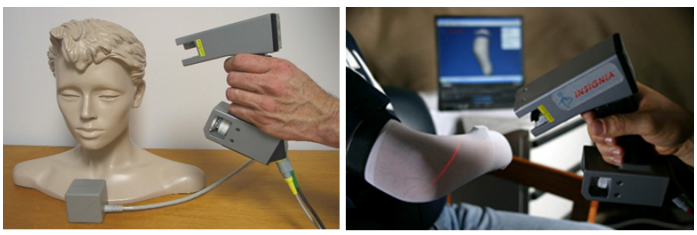

Figure 3.1: (a) Polhemus FastSCAN™ [59] and (b) Insignia™ laser scanner [87].

Lu *et al.* [72], on the other hand, proposed a method for measuring limb volume and for detecting early swelling that relies in IR imaging sensors, such as Microsoft Kinect. The IR sensor is used to capture different views of the human arm while its moved around the subject. A constrained imposed in this method is the fact that the user needs to hold the sensor at 80 cm of the target limb, approximately, while moving the device around. After image acquisition, it is needed to perform a coarse and a fine registration in order to register pairs of consecutive depth images into the same 3D coordinate frame, and iteratively to register all pairs into a single reference coordinate frame. The coarse registration is performed manually (the user needs to click on a set of four corresponding points on two consecutive images), but the authors intend to automate this method with the implementation of gyroscopes and accelerometers attached to the sensor. The fine registration is

accomplished by the use of Iterative Closest Points (ICP) algorithm. The first results confirm the robustness of the system and the ability to detect small and localized differences in limb volume. But in a future work the authors still intend to compare the results with tradition methodologies for limb volume measurement, such as water displacement method.

Several other identical approaches were studied, including 3D scanners and 3D image acquisition, for body swelling detection and volume measurement with different goals than lymphedema evaluation. For example, Kau *et al.* [63], described the use of laser scanners for monitoring facial swelling following orthognathic surgery. In a different manner, Hayn *et al.* [49] assessed the use of a 3D camera-based measurement in order to detect and quantify leg edema. The goal of their study was the evaluation 3D imaging techniques used as an extension of home monitoring for heart failure patients.

3.1.1.3 Summary

Traditional methods for the assessment of arm edema include water displacement, circumference measurements, bioimpedance or imaging techniques. Although accurate, water displacement methods are time-consuming and the apparatus limits its portability. Methods based on multiple circumferential measurements, on the other hand, have limited accuracy and several sources of error. The Perometer has more accurate results but is more expensive. Imaging techniques, such as CT or MRI, require equipment that is not commonly available in clinics due to cost and the need for specialized training. Also, BIS involve the use of several electrodes placed along the arm, which leads to a high lifetime operational cost.

Therefore, all these constrains limit the practical use on clinical settings of these procedures. In this way, research is been done to test the application of the arising 3D technologies on body volume estimation. Several authors [75, 113, 117] validated the used of 3D scanners for limb volume assessment, as the case of Polhemus FastSCAN™ and Insignia™ laser scanner. These 3D scanners allow an easy and efficient way for upper-limb modeling and volume assessment, however they are very expensive devices and are quite difficult to be handled by non-professionals. On the other hand, Lu *et al.* [72] explored the use of a low-cost system, the Microsoft Kinect, for arm modeling and volume measurement. However, the proposed method is quite complex since it depends on gyroscopes and accelerometers attached to the sensor, and its time-consuming since it is necessary to move the device around the limb. Moreover, it is operator-dependent, so its reproducibility is limited.

It remains to find the most suitable method for clinical use, low-cost and easy to operate, in order to assess limb volume and identify arm edema in breast cancer patients. But the investigation of these new 3D technologies, with great potential application in health care, may be the right path to follow.

3.1.2 Upper-Limb Motion Evaluation: Non-vision systems

The assessment of functional status after breast cancer treatment has been concentrated on lymphedema detection [80]. However, it is also important to go beyond the limb size and evaluate the UBF impairments, activity limitations and participation restriction that patients of breast cancer normally experience. In 2003, the study of Engel *et al.* [33] about long-term upper-body morbidity and patient QOL, found that restrictions on upper-limbs motion is the most important source of decreased QOL after breast cancer treatment. Therefore, more clinical attention should be given to other aspects of UBF morbidity, such as limited shoulder ROM.

In that way, as for edema detection, there is a need for an objective, reproducible and low-cost method for evaluation of women's upper-body motion after breast cancer treatment. This method should be sensitive to

the unique issues of breast cancer patients, this is shoulder mobility, and responsive to change in the patients' status [13].

3.1.2.1 Subjective Methods for UBF Evaluation

Normally, UBF evaluation rely on subjective measurements of patients experiences, symptomatology and function limitation [13]. In that way, several generic self-report questionnaires have been developed to capture the effects of injury in upper-body function (see Table 3.3).

Table 3.3: Self-report scales used for upper-body function assessment of breast cancer patients. Adapted from [13]

Scale	Paper	Type of Measure	Description	Clinical interpretation	Comments
PSFS	Stratford *et al.* [105]	Clinical measure of function	3 items; 11-point scale	Higher score - better function	For use clinical setting: measures change in function specific to the individual survivor.
DASH	Hudak *et al.* [55]	Pain-related upper extremity disability	30 items; 5-point scale	Higher score - poorer function	Has not been validated in the breast cancer patients.
UEFI	Stratford *et al.* [106]	Upper extremity function	20 items; 5-point scale	Higher score - better function	Valid and sensitive to change in the breast cancer population.
KAPS	Kwan *et al.* [67]	Upper extremity symptoms and function	13-items; 5-point scale	Higher score - more symptoms and poorer function	Developed to identify shoulder and arm problems during breast cancer treatment.
FACT-B	Coster *et al.* [23]	Multidimensional QOL in breast cancer survivors	36 items; 5-point scale	Higher score - better QOL	Focuses on nonsurgical treatment-related issues.
FACT-B+4	Coster *et al.* [23]	Upper extremity impairment	4 items with arm subscale; 5-point scale	Higher score - better QOL,less impairments	Measures impairment not function.

Specific scales for UBF assessment include the Patient-Specific Functional Scale (PSFS) [105], developed as a clinical measure of functional status limitations related to the effect of a treatment/intervention. Patients are asked to identify up to 5 daily life activities which they are unable to perform or are having difficulty with as a consequence of the treatment. Indicated items are rated according to the current level of difficulty and are followed to provide a comparison of activities level performance over time.

Disabilities of the Arm, Shoulder and Hand (DASH) scale [55], in turn, was designed to measure physical function and symptoms in patients with any disorder affecting the upper-extremity. This self-report covers symptoms such as pain, weakness and numbness, and the degree of difficult performing work and recreational activities [13].

The Upper Extremity Functional Index (UEFI) [106] aims to evaluate patients' upper-extremity functional status in a variety of activities. On the other hand, Kwan's arm problem scale (KAPS) [67] was developed to identify shoulder and arm problem in breast cancer patients, including arm/shoulder motion, pain, stiffness, swelling and impairments performing daily activities.

Self-report questionnaires are also used to evaluate QOL indicators of breast cancer survivors. As an example, there is the Functional Assessment of Cancer Therapy-Breast (FACT-B) scale [23]. It is composed

with a Breast Cancer Subscale, which complements the general scale. The FACT-B+4 [23] is a subscale of the FACT-B designed to capture the impact of arm morbidity in a greater extent. Other examples include the European Organization for Research and Treatment of Cancer Quality of Life Questionnaire-Breast Cancer Module (EORTC QLQ BR23) [101] and the BREAST-Q [89].

3.1.2.2 Objective Methods for UBF Evaluation

For the objective assessment of upper-extremity functional limitations there are several methods that include tests of flexibility, strength and endurance. From these tests, the most common for the evaluation of UBF in breast cancer patients is the goniometry [38, 80, 109], used to assess active and passive shoulder ROM in all planes. Comparing measurements of the affected and unaffected limb is possible to detect restricted mobility or impaired shoulder function. The movements that are normally evaluated are: abduction, flexion, extension, internal rotation and external rotation [38].

Other approaches for upper-extremity functional measurement can include the evaluation of strength and endurance assessed by the use of isometric and isokinetic dynamometry and/or maximal performance of a set of tasks/exercises using the repetition maximum method [45, 47, 48]. So, strength and endurance can be measured by means of an incremental exercise protocol where each stage lasts one minute in duration and increments are made by increasing speed of movement and weight held [48]. The movements normally combine a traditional "upright row" and "shoulder press", with the range of movements specified for each patient and each arm [45, 48]. The use of a isokinetic dynamometer for strength and endurance assessment was also reported [45]. The patients are asked to perform sets of repetitions, with 15 seconds of rest between sets, using the dynamometer. The assessment of the grip strength can also be relevant since this is an important requisite for good arm function. A standard hand dynamometer can be used for this purpose, where the patient is normally asked to perform a maximum contraction three times for each side [45, 48].

There are several other methods to test speed and accuracy movement. Box and Block, for example, is used to measure gross unilateral manual dexterity. It is asked to the patient to move the maximum number of small blocks from one compartment of a box to another within 1 minute [25]. On other hand, Nine-hole Peg Test is used to assess dexterity and upper-extremity function. The requirement is to insert 9 dowels into a board and then removes them in the shortest time possible [25]. However, these methods, and other similar, were not tested in breast cancer context, so it is not known its sensitivity for functional limitations related to breast cancer treatment.

3.1.2.3 Summary

Normally, the assessment of upper-limb function in women diagnosed with breast cancer is performed through broad-based questionnaires that measures psychological, social, and physical functioning aspects of QOL in diverse patient populations, including breast cancer survivors. Although easy-to-use and useful to provide reference data, these subjective methods are generally not accurate and adequately sensitive to UBF issues of breast cancer patients. Moreover, a qualitative evaluation like this has problems related to impartiality and poor reproducibility. Nevertheless, these self-reports can be an useful tool as a validation method for the results obtained in this study.

There is also some studies that report the use of flexibility, strength and endurance tests for the evaluation of UBF in breast cancer patients. However, the use of these methods is not a clinical standard in breast cancer so, it is not well known its sensitivity for functional limitations related to the treatment. The one

that is most commonly used is the ROM assessment by a manual goniometer. But, it is operator-dependent, time-consuming, it presents several sources of error, and has low accuracy and reliability.

Thus, to overcome these limitations, other methods should be considered in order to have an efficient, time-adequate and objective method for assessment of patient's UBF after breast cancer treatment.

3.1.3 Upper-Limb Motion Evaluation: Vision-based systems

As stated before, traditional clinical methods for upper-extremity function evaluation can include either subjective scales obtained by patient's self-report, or more objective measures, such as range of motion and strength tests, which still present several sources of error and low reliability.

So, to have a better understanding on upper-limb function, a more objective and accurate analysis of motion is needed. Human movement tracking systems have demonstrated to be able to to generate real-time data that dynamically represents the human movement. This field has been in constant research in the last decades, due to its promising application in many areas, including medical diagnosis. In that way, this area of research should be considered, since it can provide objective information on the upper-limb movement patterns. Human movements are normally detected using systems with visual sensors (e.g. cameras) either assisted by visual markers placed upon the human body or marker-free [125].

3.1.3.1 Marker-based human motion tracking systems

In marker-based tracking systems, cameras are used to track human movements, with identifiers placed upon the body [125]. The work of Johansson in 1973 [60] is the milestone in human motion tracking. He used his Moving Light Display system to perceive human motion. The tracking during trajectories was possible due to small reflective markers attached in the joints of human subjects.

Nowadays, several marker-tracking systems are commercially available. For example, VICON [71] (see Figure 3.2) is a passive optical system, designed for motion capture in virtual and immersive environments. It uses several cameras emitting a beam of IR light and a set of reflective markers placed on the objected to be tracked. The markers reflect the IR radiation that is recognized by the system. In that way, is possible to construct a 3D representation of the object. A similar technique is used in Qualisys system [90]. Codamotion [70] (see Figure 3.2), on the other hand, is an active visual tracking system. This technology uses miniature infra-red markers, to track the key positions on the subject. Signals from these markers are emitted to three linear arrays inside a CODA unit which provides an immediate and precise 3D measurement. Another example is Polaris [58], an optical systems that measure the 3D positions of either active or passive markers affixed to a object. Using this information, each Polaris System is able to determine the position and orientation of the object based on the information received from the markers.

(a) (b)

Figure 3.2: (a) VICON [71] and (b) Codamotion capture systems [70].

However, all these technologies have several drawbacks associated. The use of markers can be unreliable, they can move and wobble, giving rise to noisy data. Also, all the systems require calibration and professional intervention. Moreover, these methods are expensive and very complex, and the space requirements often limit their usability in clinical settings [125]. To overcome these restrictions, a lot of research has been done in order to develop marker-free motion tracking systems.

3.1.3.2 2D Markerless human motion tracking systems

Markerless tracking systems only exploit optical sensors to measure movements of the human body. On 2D motion tracking, it is only considered the human movement in an image plane. This approach can be employed with or without the use of explicit shape models.

Model-based approaches use *a priori* an human body model to match with the acquired image data. This method uses the knowledge of the movement in 2D for feature correspondence and body structure recovery. The models used are usually stick figures (see Figure 3.3), the simplest representation of a human body, which consists of line segments linked by joints, wrapped around with ribbons or blobs [39].

An early attempt to segment and track body parts was made in Akita work [1]. It assumes that the order of human movement and the spatial relationships between the body parts can be approximated by the use of a key frame sequence of stick figure poses. The stick figure contain the legs, head, arms, and trunk elements, and the cone model is used to provide knowledge of the rough shape of the body parts.

Leung and Yang [68], on the other hand, applied a 2D ribbon model to gather motion information of a moving human object. The system implements two main processes. The first, extracts moving human outlines from an image sequence using a 2D ribbon model. The second, interprets the outline and determines if an extracted 2D ribbon belongs to a part of the body or to the background.

Wren *et al.* [122] proposed a region-based approach, where the human body is considered as a set of blobs that can be described using a spacial and color Gaussian distribution (see Figure 3.3).

In the work of Ju *et al.* [61] it is assumed that a person can be represented by a set of connected planar patches: the cardboard person mode. The parametrized image motion of these patches is constrained to enforce articulated motion. The recovered motion parameters provide a good description of the movement that can be used for recognition.

Figure 3.3: Representation of (a) 2D stick-figure model with ribbons by Leung and Yang [68], and the demonstration of the work by Wren *et al.* [122]: (b) Video input; (c) Segmentation; (d) 2D representation of the blob statistics.

In a different manner, other approaches were described without the use of shape models. In this case, the pose recovery step is ignored, and the human movement is characterized in terms of a simple low-level, 2D features from a region of interest. The motion models are then described in statistical terms normally derived from the low-level features. An example is the work of Baumberg and Hogg [5], where active shape models

are applied to track pedestrians (see Figure 3.4). The tracking is initiated in the foreground region, obtained by background subtraction. A Kalman filter is used for spatio-temporal control, similar to the work of Blake *et al.* [6].

Figure 3.4: Human tracking results using the approach proposed by Baumberg and Hogg [5].

Chang *et al.* [17] proposed a method for tracking cyclic human motion based on decomposing complex cyclic motion into components and maintaining coupling between components. The decomposition reduces the dimensionality of the problem and enables a graphical modeling of the articulated human body.

Finally, in the work of Wong and Wong [121], is presented a system were is used a wavelet estimator. The human body is located within a small search window, using color and motion as heuristics.

3.1.3.3 3D Markerless human motion tracking systems

2D approaches have several restrictions for the addressed purposed, due to their viewing angle. On the contrary, the use of 3D techniques for human motion identification has the advantage of the knowledge available *a priori* about the kinematic and shape properties of the human body.

The use of 3D shape models simplify the tracking process and allows the prediction of events such as (self) occlusion and (self) collision. Model-based methods contain stick figures, volumetric, and a mixture of models [125]. In this case, the stick figure is regarded as a collection of segments and joint angles with various degree of freedom at the articulation sites.

In the work of Huber [54], for 3D segment tracking and recognition of human pose and gestures, it is used a stick figure representation, where the joints are connected by line segments. The author studies the behavior of a Proximity Space (PS) method, developed for tracking objects, in the recognition of human poses and gestures as a person moves through a cluttered environment. The PS method uses LoG filtered images and relies on stereo measurements to spatially distinguish between objects in 3D.

Ronfard *et al.* [94] developed a method to find people in static video frames using learned models of both the appearance of body parts (head, limbs, hands), and of the geometry of their assemblies. The system is built on Forsyth & Fleck's general "body plan" methodology and Felzenszwalb & Huttenlocher's dynamic programming approach for efficiently assembling candidate parts into "pictorial structures".

Instead of stick figures, it can also be used volumetric models, such as elliptical cylinders. Ivana *et al.* [78] presented an automated system for motion capture that includes both the model acquisition and the motion tracking, using multiple synchronized video streams (see Figure 3.5). It is computed the 3D voxel reconstructions of the body shape at each frame which then are used as input to the model acquisition and tracking. The human body model consists of ellipsoids and cylinders. Model acquisition starts with localization of body part based on template fitting and growing, which uses prior knowledge of average body part shapes and dimensions. This initial model is then refined using a Bayesian network that imposes human body proportions onto the body part size estimation. The tracking procedure is an extended Kalman filter that estimates model parameters based on the measurements made on the labeled voxel data.

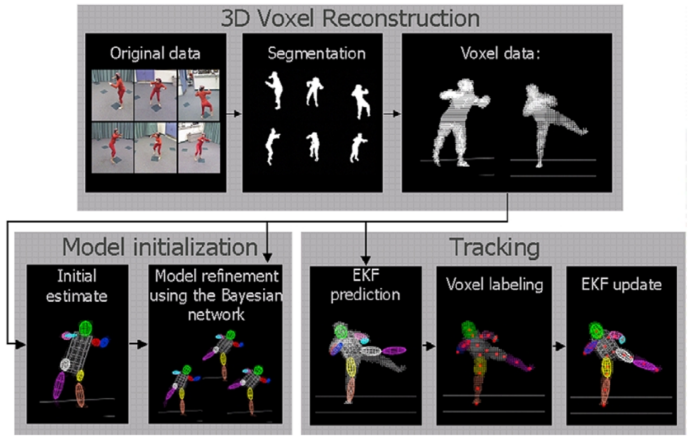

Figure 3.5: Representation of the automated system for motion capture proposed by Ivana *et al.* [78].

Rohr [93] introduced a model-based approach for the recognition of pedestrians. The human body is represented by a 3D-model of cylinders. The estimation of model parameters in consecutive images is done by applying a Kalman filter.

Gonçalves *et al.* [41] studied the position and motion of a human arm in 3D without any constraints on its behavior. The arm was modeled as two truncated right-circular cones connected with spherical joints. A recursive estimator for arm position is used to predict the appearance of the arm on the image, and the difference between the predicted and actual images is then used as an error measurement for the estimator.

In the work of Chung *et al.* [20], on the other hand, the human body is simplified as a stick model represented by connections of several circular cylinders. The authors proposed a new image feature called cue circles (CCs). Using CCs, 3D motion of the human body is measured from a sequence of boundary contour image pairs, which is obtained by an active binocular sensor system. Stereo matching for recovering the body model is carried out by finding pairs of CCs between the pair of contour images under consideration.

Theobalt *et al.* [110] described a system to capture human motion, where is applied a 2D feature tracking algorithm and a silhouette-based 3D volumetric scene reconstruction (see Figure 3.6). The person is recorded by multiple synchronized cameras, and a multi-layer hierarchical kinematic skeleton is fitted to each frame in a two-stage process. The pose of a first model layer at every time step is determined from the tracked 3D locations of hands, head and feet. A more sophisticated second skeleton layer is fitted to the motion data by applying a volume registration technique.

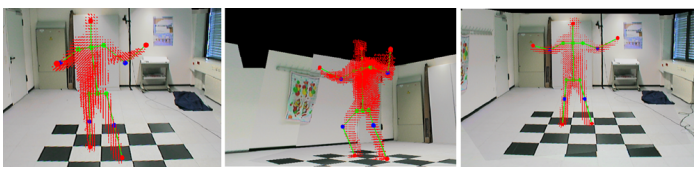

Figure 3.6: System proposed by Theobalt *et al.* [110] to capture human motion: representation of the skeleton fitted to visual hulls (rendered as point sets) of a moving person.

3.1.3.4 Summary

The visual analysis of human motion has become a major application area in computer vision. Existing systems, to some extent, are able to support human motion tracking, therefore, they could possibly be used for tracking of upper-limbs' movement.

It was addressed some of the existing commercial technologies for human tracking based on markers placed upon the body. Although efficient in this task, all these systems have the drawback of the use of markers that can be unreliable. Also, it is needed professional collaboration, the equipment are very expensive and complex, and have large space requirement.

On the other hand, it is also described above some of the existent marker-free methods for motion tracking. Most of them have been partially successful in real situations so, they may have a useful application for motion tracking of upper-limbs. However, some of the proposed algorithms/systems have problems related to robustness and efficiency that need to be improved. Moreover, most of them use complex systems of image acquisition, with multiple cameras and large space requirements.

Therefore, is still missing a simple, portable, and cost-effective functional assessment of upper-body movements that can be used practically in various clinical settings, or in home environment.

3.2 Rehabilitation Model for Breast Cancer Patients

Upper-body function is often compromised through surgical procedures used for breast cancer treatment. The functional problems, that can persist beyond the post-operative recovery period, include deficits in upper-limb range of motion, strength and flexibility, as well as arm edema and pain. These impairments in the upper-limbs limit their function, which is essential for the successfully execution of activities of daily living, as well a most household chores and occupational demands [36]. Breast cancer patients may also experience feelings of loss, lack of control, and diminished self-efficacy related to functional deficits caused by the physical limitations [36]. Therefore, these physical and psychological impairments will negatively impact women's QOL.

After surgical treatment, patients are normally advise on how to use the upper-limbs and how to avoid acute infection and edema or the risks of chronic lymphedema. An early study of Burdick [10] defended that an appropriated function rehabilitation should be indicated to the women, in order to restore normal function of the hand, arm and shoulder. As soon as drains and sutures are removed, instructions related to limb exercises are given to the patient, that is early encouraged to wash, brush her teeth, feed herself, and brush her hair. A regular exercise program should also be outlined with emphasis on stretching or reaching movements to increase mobility and strength of the arm and shoulder [10].

Several studies demonstrated the efficacy of physical activity and rehabilitation intervention on the improvement of women's UBF and, consequently, QOL [19, 26, 76, 77, 100]. Stretching exercises improves upper-limb range of motion and shoulder function, increases tendon flexibility and also enhances muscular performance (Figure 3.7). A study of McKenzie *et al.* [74] also reported very important findings regarding the effect of physical exercise on arm edema. Participation in an upper-body exercise program caused no changes in arm circumference or arm volume in women with lymphedema, and increased patients' QOL.

A recent research of Stout *et al.* [104] defend the use of a prospective surveillance for early identification and treatment of breast cancer-related physical impairments, as a means to prevent or reduce many of the functional problems reported. Moreover, they propose a prospective surveillance model for physical rehabilitation and exercise that can be integrated with disease treatment to create a more comprehensive approach

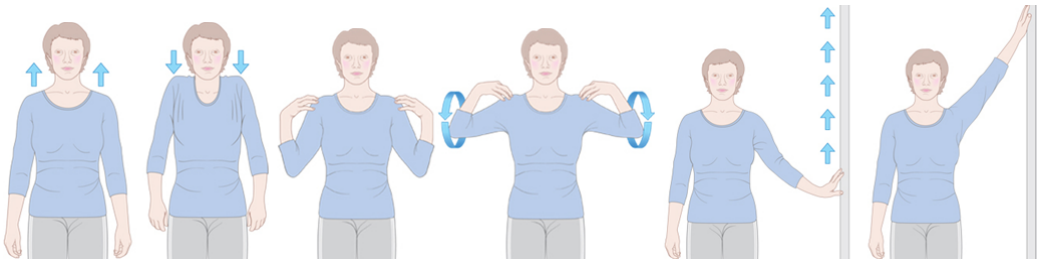

Figure 3.7: Example of exercises that are normally advised to breast cancer patients in order to recover the the full range of movement. Adapted from [114].

for breast cancer survivors. This model aims to promote surveillance for common physical impairments and functional limitations associated with breast cancer treatment; to provide patients education to facilitate early identification of impairments; to introduce rehabilitation and exercise intervention when impairments are identified; and to promote and support physical activity and exercise behaviours through the trajectory of disease treatment and survivorship.

Therefore, breast cancer patients should have a continuous surveillance of upper-body function after breast surgery, in order to detect any impairment caused by the treatment. When these restrictions are detected, it is also important to have an appropriated method for rehabilitation in order to recover any decreased functionality of the upper-limbs.

3.2.1 Home-Based exercise intervention on breast cancer patients

Evidence has supported that exercise intervention reduces fatigue, increases functional performance and improves patients' QOL. Thereby, simple, effective, and inexpensive physical therapy for cancer survivors is needed. Some investigation was done on the hypothesis of a home-based program of exercises for breast cancer patients, with similar results but overcoming limitations related to supervised programs. Home-based rehabilitation mitigates transportation and scheduling difficulties, is less expensive than supervised programs, and does not require patients to attend classes or maintain a health club membership to sustain physical activity [85].

A research of Pinto *et al.* [85] evaluated the efficacy of a home-based physical activity intervention for early-stage breast cancer patients. The results showed that women who receive physical activity intervention not only increased functional performance and improved their fitness, but also reported increased vigor and reduced fatigue, and improvement on specific aspects of psychological well-being.

Matthew *et al.* [73], in turn, evaluated the effect of a 12-week home-based walking intervention, among breast cancer survivors, in physical activity behaviors, body weight, and body composition. Objective measures of activity proved the efficacy of the proposed programs, since intervention participants increased their activity levels over time. A similar study of Mock *et al.* [79] with women following a treatment of radiation therapy, also reported a home-based walking exercise program, as an effective, convenient, and low-cost self-care activity that reduces symptoms and facilitates adaptation to breast cancer treatment.

On the other hand, Crowley *et al.* [24] tested the effectiveness of a structured home-based exercise program in decreasing fatigue, increasing strength and endurance, increasing physical self-efficacy, and enhancing perceptions of functional wellness in women undergoing adjuvant chemotherapy. The program includes aerobic (walking) and resistance exercises, 3-5 times/week during 13 weeks. Preliminary findings supported

the positive role of the exercise program in increasing endurance and physical self-efficacy for early stage breast cancer patients.

Home-based rehabilitation programs are particularly subject to questions about whether participants adhere to exercise recommendations in the absence of direct supervision [86]. Findings of a study of adherence in a 12-week randomized controlled trial, reveal that participants significantly increased their minutes of exercise from week 1 to 12 [86]. However, it was also concluded that adherence to exercise interventions changes over time and may be related to baseline levels of exercise self-efficacy. Therefore, home-based programs requires close examination, even in trials that have demonstrated positive effects on exercise behavior and psychological well-being [86].

These findings suggests the use of a home-base rehabilitation intervention for the restoration of function and activity for women diagnosed with and treated for breast cancer, due to its simple and inexpensive application. But, it is also important to have an ongoing clinical monitoring, in order to have a complete guidance on patients' rehabilitation.

3.2.2 Virtual Reality in Upper-Body Function Rehabilitation

Breast cancer patients are normally instructed to perform a set of exercises in order to restore the function of the arm and shoulder. Exercises are simple but must be repeated daily, and not always the patients perform the exercises as they should. Studies indicate that only 31% of subjects with motor disabilities perform the exercises as recommended [98], which may limit the effectiveness of the rehabilitation attributed to the patient. Lack of motivation is normally identified as an impediment to them performing the exercises regularly [53].

Thereby, research has been done in order to identify motivating and effective methods of encouraging people with motor disabilities to perform exercises, in order to help them retain or enhance their motor control and increase their independence [53]. Virtual reality (VR) systems for motor rehabilitation is one of the strategies studied in the past years with this goal [18, 50, 53, 64, 96]. VR provides an interactive interface to a computer generated environment, where the individual can see, hear and dynamically navigate through scenarios according to his or her action. The use of virtual reality technologies can be helpful in different rehabilitation contexts. VR systems can be used as training tools to promote intensive training directed towards specific deficits and guide the patients in task-oriented activities. Moreover, it allows a real-time high-resolution monitoring, where is possible to have a quantitative assessment of relevant properties of the impairment, performance and recovery [11]. On the other hand, VR environment demand focus and attention of the patient, motivate him to perform the exercises, and provide a sense of achievement to the user [50]. VR based rehabilitation systems can easily transfer clinical training to home-based application for telerehabilitation, creating a set of diagnostic and training possibilities [11]. Cost was certainly an issue when this technology was first created. But, the gaming industry is been developing a variety of VR systems for home use, making this technology both affordable and accessible for clinical settings with potential application for home environment [96].

Several groups of research are investigating the use of VR systems for upper-extremity rehabilitation, using a variety of approaches. Holden *et al.* [52] developed a VR motor training system based on the concept of "learning by imitation". The system relies on a virtual teacher, whose movements are followed by the user, to retrain a wide variety of arm movements (including shoulder, elbow, wrist, and hand). It consists of computer, a VR software and an electromagnetic motion-tracking device. The difference between the two

trajectories of both limbs is used to provide the patient with augmented feedback designed to enhance motor learning.

Regarding arm reaching training, a setup proposed by Broeren *et al.* [7] combines VR training with haptic feedback. The systems includes a haptic force feedback interface (PHANToM) connected to a virtual environment and a stereoscopic view setup, allowing a sense of touch with virtual solid objects. It is asked to the user to knock down bricks in a pile with a ball in a variable velocity, where the force feedback is provided by a haptic stylus.

Other systems also proposed the use of exoskeletons, that allows arm gravity support. T-WREX, developed by Sanchez *et al.* [95], is one of these examples. It is comprised by an orthosis that assists the arm movement in a broad range, a grip sensor for grasp training, and a software to train functionality. Patients can train arm function with different games related to daily-life activities, with emphasis on the repetitive training of different ranges of movements and grips. The software include tasks such as "Shopping", "Washing the Stove", "Cracking eggs", and "Making Lemonade" (see Figure 3.8).

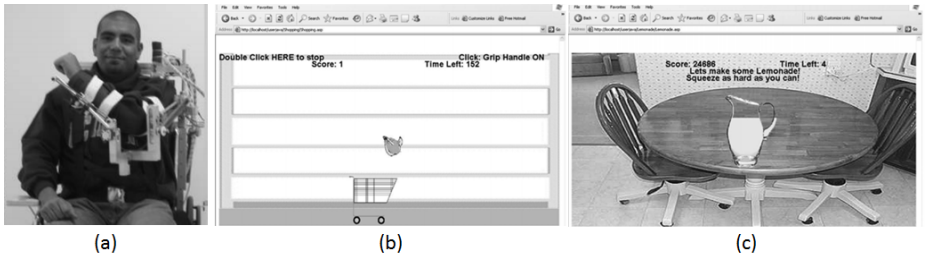

Figure 3.8: (a) T-WREX exoskeletons apparatus developed by Sanchez *et al.* [95]. Display screens of the (b) "Shopping" and (c) "Making Lemonade" tasks.

Weiss *et al.* [119] use video capture to track the user's movements and mapping them onto an image that is embedded in a virtual environment. The patients can see themselves in a mirror image in the virtual scenario. Therefore, a feedback about body posture and quality of movement is given to the patient. The authors modified the VividGroup's Gesture Xtreme VR [116], a platform formerly used for entertainment and education, in order to use it in neurological rehabilitation.

On the other hand, Cameirão *et al.* [12] based their work on the hypothesis that action execution coupled with motor imagery and action observation can promote the functional recovery by taking advantage of the life-long plasticity of the brain. The authors developed the Rehabilitation Gaming System (see Figure 3.9), that combines movement execution with observation of correlated action of virtual limbs that are displayed in a first-person perspective. All these proposed systems, and others, demonstrated to have positive results in functional recovery of the upper-extremity, mainly in stroke patients.

3.2.3 Summary

It is well stated the importance of physical activity of patients during and after breast cancer treatment, in order to overcome functional limitations of the upper-limbs caused by treatments. For practical reasons, home-based rehabilitation programs for breast cancer patients are defended and have shown to be as efficient as supervised treatments. So, women are normally advised on how to use the upper-limbs and which exercises should perform at home. However, there is no standard of follow-up after treatment and patients not always perform the exercises as they should. This highlights the importance of a close and regular examination by clinicians.

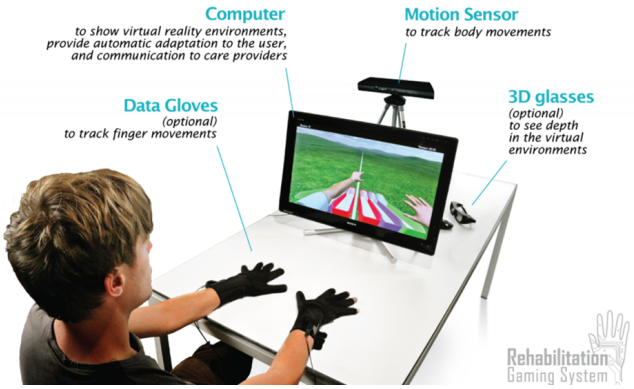

Figure 3.9: The Rehabilitation Gaming System proposed by Cameirão [12]: Arm movements are tracked by a Kinect sensor mounted on top of the display. Two data gloves are used to detect finger movements. On the display two virtual arms mimic the movements of the subject's arms, hands and fingers.

In this direction, the use of virtual reality in rehabilitation context was deeply studied. VR systems can be tailored to the needs of the patient and have an attractive environment that demand focus and attention, and motivate the user to perform the exercises. Moreover, VR allows a real-time quantitative monitoring of patients' performance. Several research groups reported the potential application of these systems in rehabilitation of upper-extremity function, mainly in stroke patients. Although the lack of tests in breast cancer field, VR technologies can be an important tool with relevant applications for UBF rehabilitation in breast cancer survivors, since it overcomes limitations of home-based programs by promoting patient motivation and allowing clinical monitoring.

3.3 Conclusion

Breast cancer patients report several impairments in the upper-body function due to the surgical removal of the lymph nodes and the use of radiation therapy. These impairments are characterized by reduced ROM of shoulder and swelling of the limb that can be an early indication of lymphedema.

Traditionally, the assessment of limb volume for the detection of arm edema is done, objectively, using methodologies as water displacement and circumferential measurements. However, these methods are either non-practical for clinical use, as the case of water displacement, or with low accuracy, as with the circumferential measures. In order to overcome these limitations, some groups investigated the use of more sophisticated technologies to accurately measure body's size and shape, as 3D body-scanners. However, most of the proposed methods are either complex or expensive.

On the other hand, to evaluate restricted motion of upper-limbs caused by breast cancer treatment, self-report questionnaires are traditionally used. Although obvious limitations of these subjective approaches, they are useful to provide reference data and, so, can be a valuable tool for validation of the results in this research. Other methods include the use of goniometry to assess shoulder ROM, that although objective, incorrect use limits its accuracy, it is time-consuming and not reproducible.

Human motion tracking systems have demonstrated to be able to generate real-time data that dynamically represents the human movement and, therefore, it has promising application in medical diagnosis. Several systems developed had shown to be efficient for upper-limbs motion tracking and evaluation and, so, could have an application in assessment of UBF of breast cancer survivors. However, most of them are still missing

improvements regarding robustness and efficiency or use complex systems of image acquisition, which limits its application in clinical settings or home environment.

Therefore, when performed by clinicians, methods of assessment of upper-body functional status are non-practical for clinical use, time-consuming, non reproducible and/or non accurate. So, the lack of a practical and standard clinical tool in this area leads to the need for a simple, portable and objective system for the assessment of UBF in breast cancer patients. Recently, advances in 3D image acquisition technologies make them an attractive tool with potential applications in this field.

Several research is been done in order to find a standard evaluation of breast cancer treatments, as a mean to evaluate its quality. This evaluation is important to enable the identification of variables that affect the final outcome and to improve current strategies. However, all the methods proposed only focused on cosmetic appearance, and much less attention has been given to the patients' functional status, more strongly correlated to decreased QOL since it disrupts valued life activities. Therefore, any evaluation of breast cancer treatments should also have in consideration functional impairments that may be caused to the patient. In this way, there is still missing a complete system that, besides cosmetic outcomes, has in attention the UBF of the patient through an evaluation of upper-limb motion and arm swelling.

After breast cancer treatment, women are normally advised with a set of exercises that should performed at home in order to avoid UBF impairments. However, there is no standard of follow-up care and patients not always perform the recommended exercises as they should. So, although efficient and practical, home-based rehabilitation programs still need a close and regular examination by clinicians.

More recently, virtual reality systems appeared as an useful tool in the rehabilitation context since it allows a training session tailored to the needs of the patient and have an attractive environment that demand focus and attention, and motivate the user to perform the exercises. Moreover, a real-time quantification of users' performance allows the clinicians to have a constant monitoring of patients rehabilitation. Therefore, these systems can be integrated in a home-based rehabilitation program for breast cancer patients, where women can perform the exercises prescribed while the performance is recorded and, later, the clinicians can evaluate if the exercises are done as recommended.

Chapter 4

Upper-Body Function Evaluation

In Chapter 2 it was discussed the consequences of breast cancer treatments on upper-body function, such as limited limb mobility and arm edema, affecting patients' QOL. Also, in the Literature Review, it was verified a lack of a practical and standard clinical tool for this purpose, which increases the need for a simple, portable and objective system for the assessment of the upper-limbs motion. Therefore, one of the main goals of this research was the development of a method for the evaluation of UBF, important either for an timely diagnosis or for the assessment of treatment procedures.

In this chapter, we start to present the database created in order to make possible all the developed work. After, it is described the proposed method, followed by the obtained results an conclusions.

4.1 Database

The present research depends on the availability of training and testing examples used in the development of the models. However, the acquisition of pictures in medical environment is not always easy to perform. In this case, the process was possible thanks the collaboration of an expert in breast cancer of the Hospital S. João. Therefore, this project included the development of an application for the collection of training data, using the Microsoft Kinect.

4.1.1 Application for medical data acquisition

The Kinect incorporates a RGB camera and a depth sensor (a laser based near IR projector and an IR camera), which combined provide full-body 3D motion capture and gesture recognition capabilities. The default RGB video stream uses 8-bit VGA resolution (640×480 pixels), while the monochrome depth sensor has a 11-bit VGA resolution which allows 2048 sensibility levels. Both video outputs work at 30 frames per second (fps).

Microsoft released a software development kit (SDK), with a set of libraries that allows the development of applications on a variety of Microsoft platforms using the Kinect sensor as an input [118]. Since one of the goals of this research was the development of a markerless motion tracking system of the upper-limbs, we took advantage of the SDK, which allows the tracking of skeletons using a very fast and accurate recognition. Skeletal tracking is accomplished by processing the depth data to determine the position of several joints on an human form [118]. The systems allows the detection of a complete set of positioned points (20 total) that represent the skeleton's joints (see Figure 4.1) [118]. Each joints is defined as a point with a position (x, y, z)

expressed in skeleton space. This space is defined around the sensor, which is considered the origin, looking in the direction of the positive z-axis (see Figure 4.1).

There are several Natural User Interface (NUI) libraries available for the Kinect development (see Table 4.1), but we choose the SDK since it is relatively simple to integrate all the functionalities needed and has a bigger number of joints (20 total) when compared, for example, with the OpenNI.

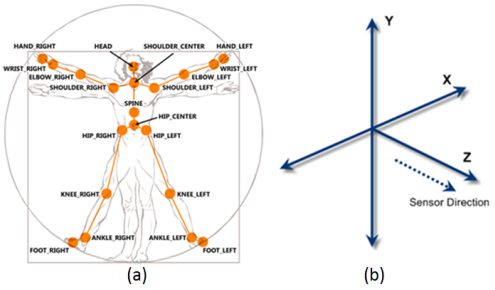

Figure 4.1: (a) Skeleton Joints tracked by the Kinect device and (b) Skeleton space axes. Adapted from [28].

Table 4.1: A comparison table for Natural User Interface (NUI) libraries. Adapted from [99].

Techniques	**Pros**	**Cons**
Microsoft Kinect SDK	1. Easy to install, fairly widespread. 2. Support skeleton tracking (20 joints). 3. Does not require camera calibration. 4. Predictive tracking of joints. 5. Skeleton Recognition is done very fast. 6. Joints occlusion handled.	1. Support for windows only. 2. Limited language support, only for C/C++ and C#. 3. Higher processing power.
OpenNI	1. Support skeleton tracking (15 Joints). 2. Available for most languages. 3. Any OS compatible.	1. Difficult to install. 2. No predictive tracking. 3. Joints occlusion not handled properly. 4. Gets confused with very fast movements.
Libfreenect	1. Available for most languages. 2. Any OS compatible.	1. Difficult to install. 2. No skeleton tracking.
Evoluce SDK	1. Support various gesture recognition methods. 2. Easy to install. 3. Support skeleton tracking.	1. Only for Windows 7. 2. Calibration pose is required. 3. Limited language support (C/C++ and C#).
Delicode NImate	1. Quite fast. 2. Support skeleton tracking. 3. Does not require camera calibration.	1. Skeleton tracking not done properly. 2. Only for Windows.

In this way, it was developed an application for the data acquisition, using the Microsoft SDK. With this application is possible to acquire and record RGB and depth frames each 30 fps, as well as, information with the skeleton joints position. In the Figure 4.2 is possible to visualize the Graphical User Interface (GUI) of the developed application, where is present a color and depth stream. Also, it is allowed to the user to introduce the name of the patient, pertinent comments and control the tilt of the Kinect. Moreover, the complete human skeleton can also be visualized, along with a graphical representation of the X and Y positions of a joint chosen by the user.

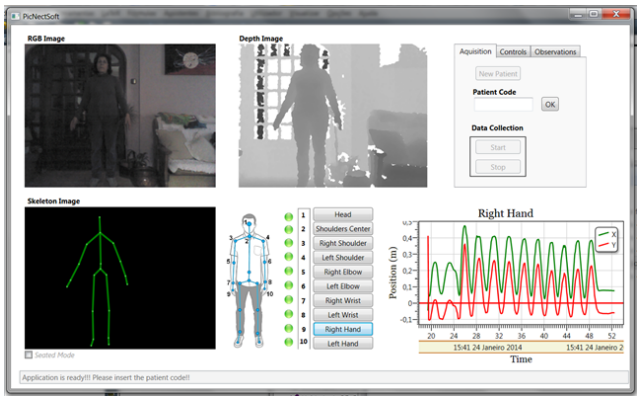

Figure 4.2: Graphical User Interface of the application developed for the data acquisition.

4.1.2 Dataset

Currently, the database includes 48 patients, from which 24 were diagnosed with lymphedema. The acquired data include several color and depth map images (resolution of 640x480 pixels), captured while the patient was performing simple exercises of abduction and adduction of the arms (see Figure 4.4), as well as information of the upper-body joints position while performing these exercises (see Figure 4.3 and Table 4.2). The complete information of each acquired patient can be found in Table 4.3, where is possible to consult medical information regarding the treatment used: the type and year of the surgery used to remove the tumor (Mastectomy or BCS), the type of surgery performed to the axilla (SLN or ALND), which type of radiotherapy was included in the treatment (Breast and/or Axilla), if the patient has lymphedema and if she has done physiotherapy.

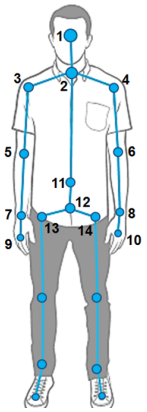

Figure 4.3: Skeleton Joints saved on the database.

Table 4.2: List of the skeleton joints saved on the database.

#	Name	#	Name
1	Head	8	Left Wrist
2	Shoulder Center	9	Right Hand
3	Right Shoulder	10	Left Hand
4	Left Shoulder	11	Spine
5	Right Elbow	12	Hip Center
6	Left Elbow	13	Right Hip
7	Right Wrist	14	Left Hip

Subjective evaluation of the patients' upper-body functional status was performed by the UEFI self-report questionnaire. This questionnaire consists of 20 items that are rated on a 5-point Likert scale and inquires about the patient's current upper functional status in a variety of activities (see Figure A.1 in Appendix A). The total score ranges from 0 (lowest functional status) to 80 (highest functional status). UEFI was chosen since it is relatively simple and fast to fill and has demonstrated to be valid and sensitive to change in the breast cancer population [13]. However, the patients reported some confusion on the understanding of some

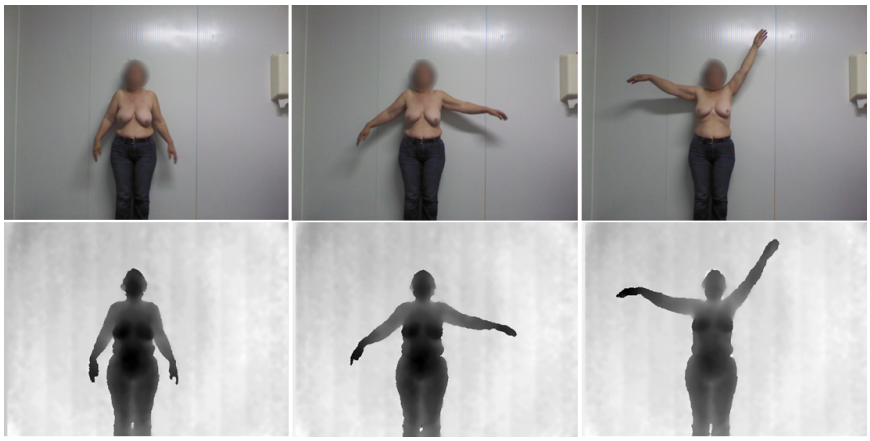

Figure 4.4: Data acquired using the Kinect device (Patient # 42). Color and corresponding depth-map image.

items of the form. Also, this report has weaknesses when the location of the affected limb is on the opposite side of the dominant hand, since the person never used that arm before to perform some of the tasks evaluated. For that reasons, in part of the cases, it was not possible to assign all the 20 items with a rating. Thus, to have a concordant score for all the patients, it was computed the ratio between the rating obtained and the total items filled (for example, a patient with 18 items filled and with a final rate of 30, will have a score of $30/72 = 0.42$). It is possible to consult the scoring data of the UEFI for each patient in Table 4.3, with a score range from 0 to 1, where 1 represents an highest functional status. On the other hand, there is minimal information available about the scoring, interpretation, and functional implications of the results of this self-report.

During the acquisition process it was verified an increasing learning by the medical expert, regarding the acquisition with the Kinect and the filling of the UEFI forms, which led to more accurate data acquired.

Table 4.3: Medical information of the patients presented in the Database: type and year of surgery (*Mast* or *BCS*), surgery to axilla (*SLN* or *ALND*), use of radiotherapy (*RT*), lymphedema (*Lymph.*), physiotherapy (*Phisio.*) and the UEFI score.

Pat.#	**Surgery Breast**	**Year**	**Surgery Axilla**	**RT Breast**	**RT Axilla**	**Lymph.**	**Physio.**	**UEFI (ratio)**	**Nº frames**
1	BCS	2013	SLN	Yes	No	No	No	1.00	132
2	BCS	2008	ALND	No	No	Yes	Yes	0.50	84
3	BCS	2008	ALND	Yes	Yes	No	No	0.84	99
4	BCS	2011	SLN	Yes	No	No	No	0.87	120
5	BCS	2012	SLN	Yes	No	No	No	1.00	109
6	BCS	2011	SLN	Yes	No	No	No	1.00	126
7	BCS	2005	SLN	Yes	No	No	No	0.53	163
8	Mast	2013	SLN	No	No	No	No	1.00	198
9	BCS	2012	SLN	Yes	No	No	No	0.88	241
10	Mast	2011	ALND	No	No	No	Yes	0.75	242
11	BCS	2011	ALND	Yes	Yes	No	No	1.00	203
12	Mast	2010	SLN	Yes	No	No	No	0.50	226
13	Mast	2013	SLN	No	No	No	Yes	0.57	385

Pat.#	Surgery Breast	Year	Surgery Axilla	RT Breast	RT Axilla	Lymph.	Physio.	UEFI (ratio)	Nº frames
14	Mast	2012	SLN	No	No	No	No	0.80	136
15	Mast	2012	ALND	No	No	No	Yes	0.71	202
16	Mast	2008	ALND	No	No	No	Yes	1.00	162
17	BCS	2004	ALND	Yes	No	No	Yes	0.82	114
18	Mast	2006	SLN	No	No	No	Yes	1.00	123
19	Mast	2014	SLN	No	No	No	No	1.00	153
20	BCS	2011	SLN	Yes	No	No	Yes	0.73	403
21	BCS	2012	ALND	Yes	Yes	Yes	Yes	0.88	159
22	BCS	2013	ALND	Yes	?	Yes	Yes	0.44	413
23	Mast	2009	SLN	No	No	No	Yes	1.00	245
24	Mast	2012	SLN	No	No	No	No	1.00	187
25	BCS	2010	SLN	Yes	No	No	No	0.78	329
26	Mast	2013	ALND	Yes	Yes	No	No	0.82	139
27	BCS	2009	ALND	Yes	No	No	Yes	0.46	158
28	Mast	2011	ALND	Yes	Yes	Yes	Yes	0.35	182
29	Mast	2012	ALND	Yes	Yes	Yes	Yes	0.84	225
30	BCS	2011	ALND	Yes	Yes	Yes	Yes	1.00	257
31	Mast	2006	ALND	Yes	Yes	Yes	Yes	0.08	69
32	Mast	2009	ALND	Yes	Yes	Yes	Yes	0.84	288
33	Mast	2010	ALND	Yes	Yes	Yes	Yes	0.24	314
34	BCS	2002	ALND	Yes	Yes	Yes	Yes	0.68	163
35	Mast	2010	ALND	No	No	Yes	Yes	0.23	191
36	BCS	2010	SLN	Yes	Yes	Yes	Yes	0.50	290
37	BCS	2011	ALND	Yes	Yes	Yes	Yes	0.57	243
38	BCS	2011	SLN	Yes	Yes	Yes	Yes	0.35	213
39	Mast	2011	ALND	Yes	No	Yes	Yes	0.70	376
40	Mast	2010	ALND	Yes	Yes	Yes	Yes	0.53	185
41	Mast	2010	ALND	Yes	Yes	Yes	Yes	0.25	236
42	Mast	2012	ALND	No	No	Yes	Yes	0.51	169
43	Mast	2009	ALND	Yes	Yes	Yes	Yes	0.61	188
44	Mast	2011	ALND	Yes	?	Yes	Yes	0.25	190
45	Mast	2009	SLN	No	No	Yes	Yes	0.42	306
46	Mast	2010	ALND	Yes	Yes	Yes	Yes	0.92	276
47	BCS	2009	ALND	Yes	No	Yes	Yes	0.97	173
48	Mast	2008	ALND	Yes	Yes	Yes	Yes	0.59	243

4.2 Methodology

4.2.1 Depth-map noise reduction

Kinect is able to capture real-time depth maps using an IR projector and camera. However, the provided data present significant amount of noise-related issues, due to the limit of working distance, occlusions, multiple reflections, transparent objects or scattering in particular surfaces (such as human tissue and hair). This leads

to missing regions and unstable boundaries in depth maps. Thus, one of the steps of this work was the implementation of a method for recovering missing depth information and noise filtering.

The depth hole filling strategy is based on the depth distribution of neighboring pixels of depth holes, as proposed in the work of Yang *et al.* [123]. First, a binary map is created using the pixels with unknown depth information. Then, the depth holes are labeled by 8-connectivity, creating different blobs corresponding to the different regions to fill. To decide a neighboring region of a depth hole, the blob is dilated with a 5×5 diamond structural element, and the depth values of the expanded area are used to estimate a value to fill the hole (see Figure 4.5).

Figure 4.5: Morphological dilation. (a) example of a labeled region, (b) dilation of (a), (c) boundary extraction by subtracting (a) from (b).

Depth holes are mainly caused by occlusion or non-reflective objects. Therefore, it can be assumed that around the non-filled region there is valid information for the filling process [123]. In the case of the proposed method, a valid value to fill a hole will correspond to a dominant peak that is the most distant depth value among multiple peaks [123]. Hence, the histogram of neighboring pixels of the hole is computed and the dominant peaks are detected (more than 10% of the total number of pixels in the region). Then, it is determined a threshold as an average of these dominant peaks. Finally, a median of the values greater than the threshold is used to fill the hole (see Figure 4.6).

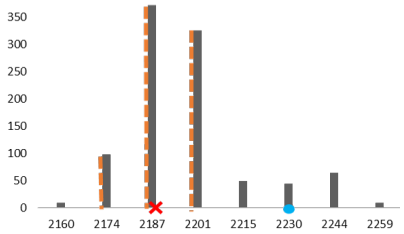

Figure 4.6: Histogram representation of depth values belonging to a neighboring region of a blob. Dotted lines denote dominant peaks, the $\times$ the average threshold value and the circle the estimated depth value.

After filling holes of depth images with valid depth values, there is still the problem of noise around object boundaries. To address this issue, a bilateral filter is used, since it is a non-iterative, local, and relatively simple method. This type of filter combines a domain kernel (σ_d), which gives priority to pixels that are close to the target pixel, with a range kernel (σ_r), which gives priority to the similar pixels to the target pixel [111]. In smooth regions, pixel values in a small neighborhood are similar to each other, so the bilateral filter acts essentially as a standard domain filter, and averages away the small, weakly correlated differences between pixel values caused by noise. On the other hand, considering a sharp boundary between a dark and a bright region, when the bilateral filter is centered on the bright side of the boundary, the pixel will be replaced by an average of the bright pixels in its vicinity, and the dark pixels will be ignored (see Figure 4.7). On Equations 4.1 and 4.2, $k(x)$ is the normalization constant to maintain zero-gain, $f(x,\xi)$ is the Gaussian function, $g(I(\xi) - I(x))$ is the intensity difference, $I(\xi)$ is the current intensity of the current pixel and $J(x)$ represents the output.

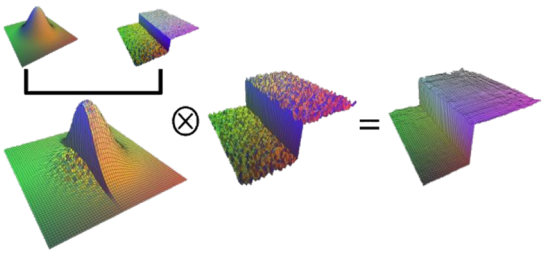

Figure 4.7: Bilateral filter: the shape of the Gaussian kernel is dynamic based on difference of pixel intensity. Adapted from [31].

$$k(x) = \sum_{\xi} f(x,\xi)\ g(I(\xi) - I(x)) \tag{4.1}$$

$$J(x) = \frac{1}{k(x)} \sum_{\xi} f(x,\xi)\ g(I(\xi) - I(x))\ I(\xi) \tag{4.2}$$

4.2.2 Kinect Rotation Correction

In data acquisition, it is important to guarantee the parallelism of the patients to the Kinect device in order to capture valid depth images. However, the conditions of acquisition in medical environment are not always easy to control and this requirement frequently fails. On the other hand, it is easier to assure that the patient is parallel to the wall. Therefore, using the depth information available, it is possible to compensate the rotation of the depth map when the Kinect is not parallel to the patient. For this purpose, it is compared the distance of the wall to the Kinect in different points (in pixels with different widths on the image), in order to estimate the angle of rotation (see Figure 4.8): considering the depth at points 1 and 2 on image width, the distances $d1$ and $d2$ can be assessed, computing the average of the neighboring depth values. In this manner, it is possible to know the difference of distance d between these two points of the wall. Moreover, with the knowledge of the distance w between the points 1 and 2, the angle of rotation θ can be computed (see Equation 4.4).

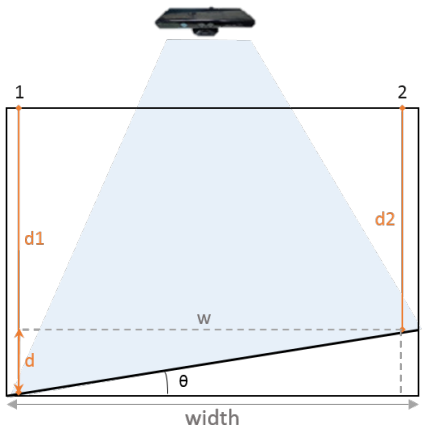

Figure 4.8: Image acquisition sketch when the Kinect is not parallel to the wall.

$$d = d1 - d2 \tag{4.3}$$

$$\theta = \arctan\left(\frac{d}{w}\right) \tag{4.4}$$

The goal is to correct the depth values of the image, in each x, in order to achieve a constant distance to the wall (as represented by the red line in the Figure 4.9) and, in this way, compensate any rotation that may exist between the Kinect and the patient. Thereby, knowing the rotation θ, the image is divide in two sides and the depth at each x can be updated by the Equation 4.5.

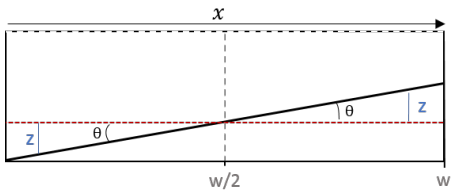

Figure 4.9: Method used to compensate the Kinect rotation.

$$I_{rot}(x,y) = \begin{cases} I(x,y) - (z - w/2) \times \tan\theta & 0 < x < w/2, \forall y \\ I(x,y) + (w/2 - z) \times \tan\theta & w/2 \leq x < w, \forall y \end{cases} \tag{4.5}$$

4.2.3 Patient Segmentation

The conditions of data acquisition are not always regular from patient to patient. Ideally, it would be carried out in a uniform background. However, occasionally there is also the presence of different objects at different depths. In this way, the images captured are normally composed by the background (wall) and the patient, but also with other non-desirable objects (see Figure 4.10 (a)). Therefore, for body segmentation, the application of global traditional thresholding methods, such as Otsu's, are not the most appropriated, as verified in a previous work [82]. In this manner, the information of the 14 upper-body joints available on the database (see Table 4.2) can be very useful, since each joint indicates a position in the depth frame where the body of the patient will be present. Thereby, the pixels values in these positions are assessed, and a double threshold can be defined using the maximum and minimum values of intensity. However, using only these thresholds, several points that probably belong to the body will be consider as background (see Figure 4.10 (b)). Therefore, a margin of 5% above and below the maximum and minimum, respectively, is used in order to consider all the object in the segmentation (see Figure 4.10 (c)).

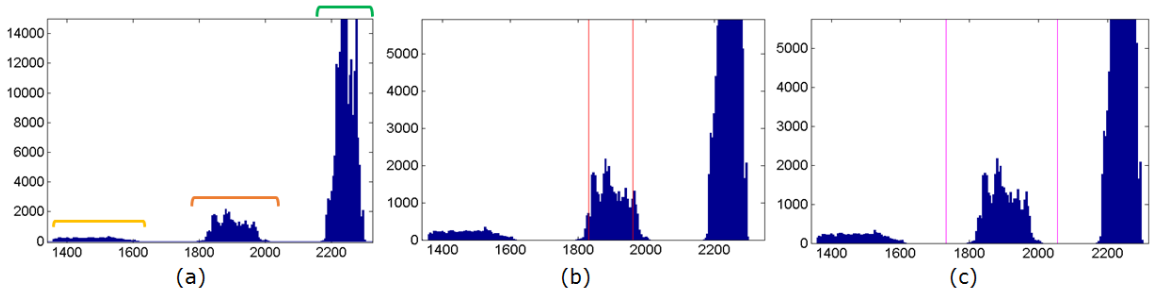

Figure 4.10: (a) Depth image histogram of Patient#42, where is possible to identify the background in green, the patient in orange and an outlier object in yellow. (b) Maximum and minimum values of intensity at joints' positions represented by the red lines (c) 5% of the maximum and minimum values of intensity, represented by the pink lines, used as a double threshold for segmentation

The result of the double threshold for the Patient #42 is presented in Figure 4.11 (a). As can be seen, part of the wall was also consider as foreground (see Figure 4.11 (b)). To solve these cases and select only the body in the binary mask, a flood fill algorithm from the AForge.NET Framework[1] is used in order to fill the area connected in 4 directions (Figure 4.11 (c)). To remove the small holes, a fill holes filter[1] is applied (Figure 4.11 (d)). Finally, to obtain a smoothed body shape, a median filter (11x11) is used to remove the noise of the raw mask (Figure 4.11 (e)).

[1] http://aforgenet.com/framework/

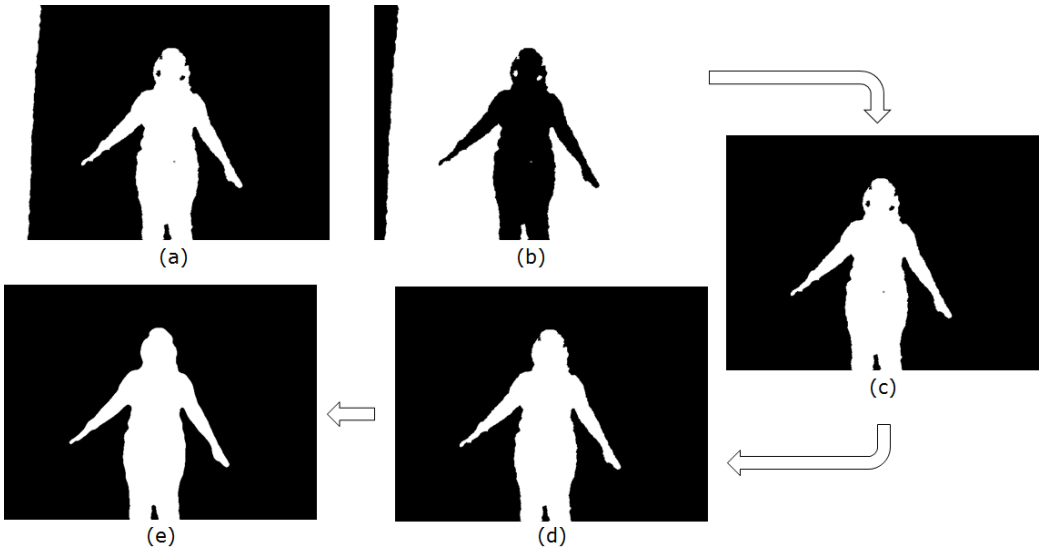

Figure 4.11: Patient segmentation process: (a) Double threshold result and (b) its complement, presented only for better visualization; (c) flood fill; (d) fill holes and (e) median filter.

4.2.4 Arm Segmentation

In order to make possible the characterization of the upper-body motion, the next step on this research was the detection of the region of interest, the upper-arm. This region of the upper-limb is bounded superiorly by the shoulder, inferiorly by the elbow and communicates medially with the axilla [29] (see Figure 4.12 (a)). In accordance with the International Standards for Anthropometric Assessment [37] the arm can be represented by the distance between the Acromiale® and Radiale® landmarks (see Figure 4.12 (b) and (c)).

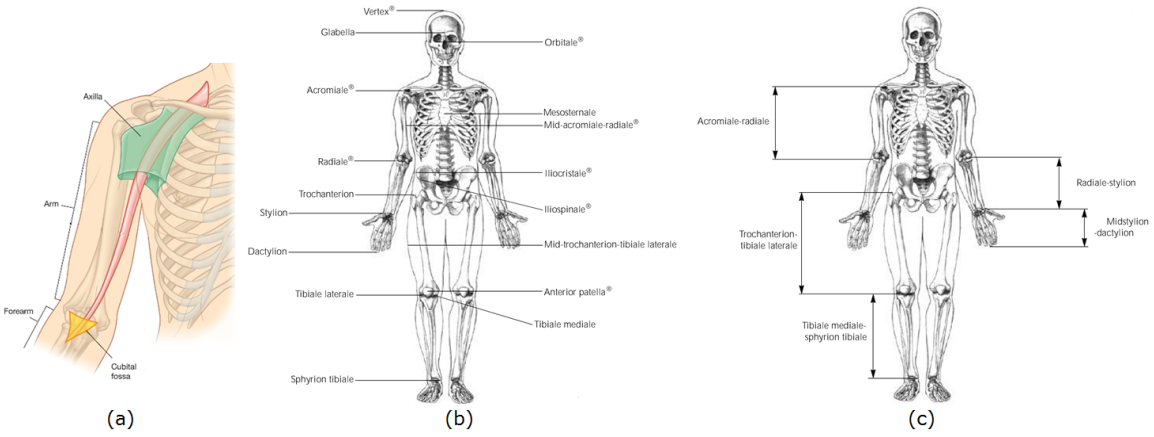

Figure 4.12: (a) Areas of transition of the upper-limb (From [29]). (b) Body anatomical landmarks. (c) Direct lengths: measurements are taken of the segment lengths from landmark to landmark (From [37]).

In this fashion, there are a set of points that can be found in the patient limb, in order to delimit the upper-arm area (see Figure 4.13): the armpit (A_1), the medial (E_1) and the lateral (E_2) elbow point, the medial shoulder point (S_2) and the lateral shoulder point (S_1). If the arm is in a position with ROM of 90º, the points A_1 and S_1 will coincide. With this in mind, we start by the detection of the patient silhouette, accomplished

by a morphological dilation of the mask, using a 3x3 structuring element, and by an exclusive disjunction operation:

$$I_{XOR} = I_M \oplus I_D \tag{4.6}$$

where I_M represents the binary body mask, I_D the outcome of the dilation and I_{XOR} the resultant silhouette. After this process, we have a set of pixels where is possible to find the points to detect. Thus, these pixels will be iteratively assessed in order to find those closest to the points represented in the Figure 4.13. For this purpose, we took advantage of the shoulder and elbow joints given by the Kinect skeleton, represented by a S and E in the Figure 4.14 (a) and (b).

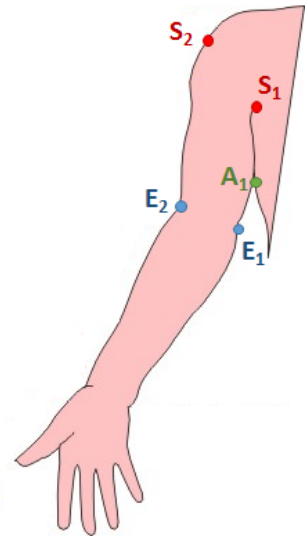

Figure 4.13: Delimitation points of the upper-arm area.

In this way, to detect the point A_1 (see Figure 4.14(c)), we will search the pixels that are below the point S, since the armpit will always be beneath of the Kinect shoulder joint, and select the closer one (flowchart in Figure A.2 (a)). Then, the medial elbow point (E_1) will correspond to the pixel that is closer to the elbow joint E. To guarantee that the point selected is indeed E_1, it is only accepted as valid if the line segment $\overline{A_1E_1}$ does not intersect $\overline{SE}$ (flowchart in Figure A.2 (b)). On the other hand, to detect E_2, it is first determined a line perpendicular to $\overline{SE}$, that contains E_1:

$$m_{E_1} = \frac{-1}{m_{SE}} \tag{4.7}$$

where m_{SE} is the slope of $\overline{SE}$ and m_{E_1} the slop of the line to find. Then, we search the silhouette pixels that are also members of this line. To choose a valid point E_2, it is guaranteed that $\overline{SE}$ intersects $\overline{A_1E_2}$ (flowchart in Figure A.3 (a)). To find S_2, we search the pixel that forms with the shoulder S a line parallel to $\overline{E_1E_2}$. Besides, it is also a condition the intersection of $\overline{S_2E_1}$ and $\overline{SE}$ (flowchart in Figure A.3 (b)). Finally, S_1 will be the point of intersection between $\overline{E_1A_1}$ and $\overline{S_2S}$. This process is done for the right and left arm, and repeated at each frame. Figure 4.14 (c) presents the result of this process for Patient #10 and in Figure 4.14 (d) is is possible to see the result of segmentation on both arms.

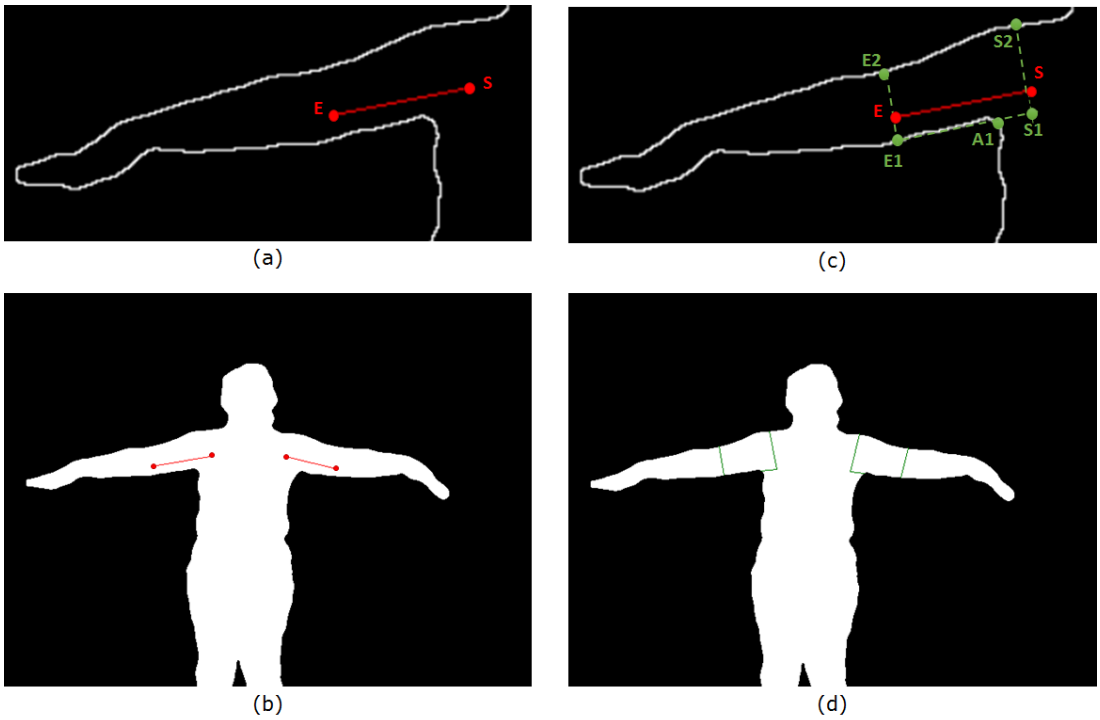

Figure 4.14: (a) Kinect Shoulder and Elbow joints represented by the red dots. (b) Shoulder and Elbow joints on both arms, linked by the red line. (c) Detected points represented by the green dots. (d) Result of the upper-arm segmentation (Patient #10).

4.2.5 Feature Extraction

The next step on this work was the selection of features important to assess, in order to evaluate the upper-body mobility on breast cancer patients. The most significant impairment verified is the appearance of lymphedema, which is also responsible by a reduction of the limb range. In this way, with the information available on the database of the patient skeleton and with the upper-arm segmentation, it is possible to select several aspects that are important to evaluate on both arms:

- Upper-arm volume;
- Shoulder ROM;
- Hands height and width;
- Movement acceleration;
- Elbow flexion.

4.2.5.1 Range of Motion

The decreased ROM of the shoulder is a common consequence observed on patients with limited mobility of the upper-limb. Therefore, this is one of the most important features to assess, and can be obtained by measuring the angle between the upper-limb and the patient body. On the other words, it is computed the angle θ between the line segment $\overline{A_1E_1}$, define by the armpit point and the medial elbow point (see Figure 4.15), and the line $\overline{H_1H_2}$, defined by the head and hip point of the Kinect skeleton (see Figure 4.15).

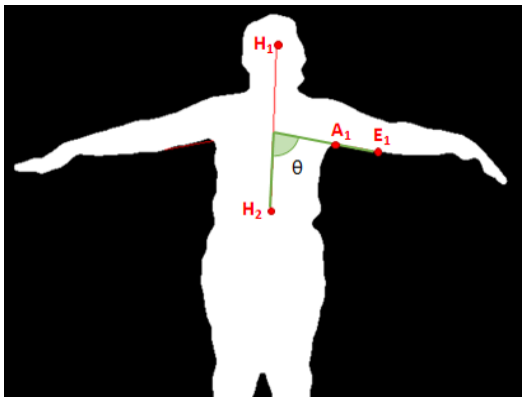

Figure 4.15: Representation of the angle θ measured to evaluate the shoulder ROM

Therefore, the ROM of the right and left shoulder can be measured for each frame of each patient and its ratio can be computed. From this data, two features are selected:

- the ratio of the maximum ROM, which will correspond to the angle at the maximum height achieved by the hand ($maxROM$).
- the average of the ROM ratio along all movement (μROM).

4.2.5.2 Volume

Lymphedema is characterized by an arm swelling. Thus, other feature important to assess is the volume of both limbs, to identify a possible increased size of the affected arm. For this purpose, the depth information is very useful, since it allows the quantification of the volume ratio between the two upper-arms. In this case, it is first determined a plan of reference of the upper-limb, and then the volume is defined as the sum of unit values between the estimated plan and the arm surface (see Figure 4.16). As a reference, it is considered the maximum depth value on the arm (which corresponds to the most distant point) (see Equation 4.8), represented by a red block in Figure 4.16.

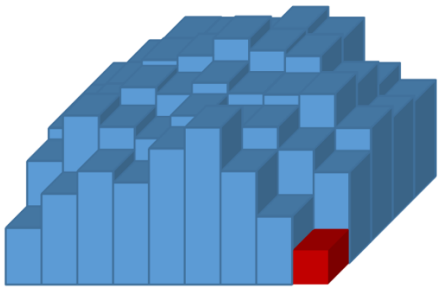

Figure 4.16: Illustration of the volume measurement based on voxels

$$Vol = \sum_{x=1}^{w} \sum_{y=1}^{h} (max(I) - I(x,y)) \tag{4.8}$$

In this manner, the volume of both arms is computed for all frames of each patient. Since it correspond to the most trustful arm segmentation, the volume values are only considered if the shoulder ROM is between 45º and 135º. Moreover, only values between a range of 40% of the median are considered, in order to discard possible outliers. An average value of each arm is then obtained, and their ratio is computed (μVOL).

4.2.5.3 Hand Height and Hand Width

The reduced motion of the limb can also be detected comparing the hand height and, consequently, the width, that the patient reaches during the movement. So, the x and y coordinates of the hands joints are analyzed, and the Shoulder Center (SC) joint is used as a reference point. This means that, for all the frames, it is computed the difference between the hand coordinates (x and y) and the shoulder center point, represented, respectively, by the H and W in Figure 4.17. Thereafter, for each frame, the ratio of the y values of both hands is computed, as well as the the ratio of x values. As with the ROM, two features are obtained for the height and the width, in a total of four:

- the maximum Height ratio ($maxH$), which will correspond to the maximum height achieved by the hand.
- the maximum Width ratio ($maxW$), which will correspond to the width at the maximum height point.
- the average of the Height ratio along all movement (μH).
- the average of the Width ratio along all movement (μW).

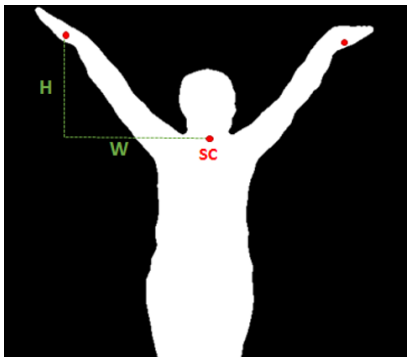

Figure 4.17: Representation of the height (H) and width (W) measurements.

4.2.5.4 Hand Acceleration

The reduced acceleration of the upper-limb movement can also be an indicative of motion problems so, the dynamic of each joint was also computed (see Figure 4.18). This is accomplished measuring the variation of the joints' position over time. The joint chosen was the hand, since it has the biggest variation of position during the movement.

In a first step, each sequence of the joint position is replaced by its difference between each frame. Hence, the instantaneous velocity of motion can be calculated by the Equation 4.9, where T is the sampling interval and n is the number of frames of the movement.

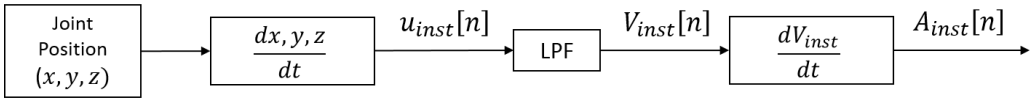

Figure 4.18: Flowchart of the process to obtain the hand instantaneous acceleration. *(x, y, z)* represent the joint coordinates of the hand in meters.

To reduce generated noise from the environment and small body movements, a low-pass filter with cutoff frequency of 2 Hz is applied to $u_{inst}[n]$, since the low frequencies are the main interest. In this way, it is obtained a instantaneous velocity $V_{inst}[n]$, with no phase distortion. The instantaneous acceleration of the

movement is then defined by the Equation 4.10. In this manner, it is possible to compute the average of the movement acceleration for each hand and extract their ratio as a feature (μAcc).

$$u_{inst}[n] = \frac{dx,y,z}{dt}|_{t=nT} = \frac{1}{T}\sqrt{(x[n]-x[n-1])^2+(y[n]-y[n-1])^2+(z[n]-z[n-1])^2} \quad (m/s) \tag{4.9}$$

$$A_{inst}[n] = \frac{V_{inst}}{dt}|_{t=nT} = \frac{1}{T}(V_{inst}[n]-V_{inst}[n-1]) \quad (m/s^2) \tag{4.10}$$

4.2.5.5 Elbow Flexion

Other feature that we thought would be interesting to evaluate is how the elbow behaves during the abduction/adduction movement. In this way, with the knowledge of the position of the shoulder, elbow and wrist joints, it is possible to calculate the angle between the elbow-wrist ($\overline{EW}$) and elbow-shoulder ($\overline{ES}$) lines (see Figure 4.19) and, therefore, assess the elbow flexion. This angle is obtained for the right and left elbow for each frame and their ratio is computed. Once again, the average of the ratio values is used as a feature ($\mu ElbF$).

Figure 4.19: Representation of the angle computed to detected the elbow flexion.

4.2.6 Classification Models

The development of an objective method for the assessment of the upper-body function calls for a gold standard for result comparison (a ground truth). The patients can be divided in two different classes, the ones that present reduction of the upper-limbs mobility, and the ones that do not notice any significant difference. In this way, to select the class of patients with reduced UBF, two approaches are tested as ground truth: the women diagnosed by a clinical expert with lymphedema and the women that present a score above 0.6 in the UEFI.

Machine learning techniques are used to build predictive classification models. In other words, a known dataset (the training dataset), which includes input data and response values, is used to build a model using a supervised learning algorithm. This classification model can then be used to make predictions for a new dataset. In this study, different supervised learning classifiers were tested:

- Fisher Linear Discriminant Analysis (LDA);

- Naive Bayes Classifier;
- Support Vector Machines (SVMs);

For the different classifiers, the models were trained using both the medical diagnosis of lymphedema and the evaluation of the UEFI self-report as a reference. In order to explore all the possibilities and compare performances, the models were trained and tested for all the possible combinations of features, which leads to 2^9 different subsets. In this manner, the model was designed using the selected features, considering all the possible subsets, by means of a Leave One Out (LOO) scheme [30].

4.2.6.1 Fisher Linear Discriminant Analysis

The main goal of Fisher Linear Discriminant Analysis is to find a linear combination of variables which best separates two or more classes by the data projection onto a line, and the classification is performed in this one-dimensional space. The projection maximizes the distance between the means of the two classes while minimizing the variance within each class [2].

Suppose we have 2 classes and d-dimensional samples x_1,...,x_n where n_1 samples come from the first class and n_2 samples come from the second. Fisher's contribution is to find such a projecting that maximize the value J_w, which is the ratio of the between-class (S_B) and within-class scatter matrices (S_W) [2].

$$J_w = \frac{w^T S_B w}{w^T S_W w} \tag{4.11}$$

$$S_B = (m_1 - m_2)(m_1 - m_2)^T \tag{4.12}$$

$$S_w = \sum_{i=1,2} \sum_{x \in C_i} (x - m_i)(x - m_i)^T \tag{4.13}$$

The sample mean of the respective classes, m_i, is defined by the Equation 4.14. Assuming that S_w is a non-singular matrix, it is possible to find an analytic expression for w which maximizes J_w (Equation 4.15). With this expression it is possible to calculate the optimal projection direction w that ensures that the samples belonging to each one of the two classes will be as much separated as possible.

$$m_i = \frac{1}{n_i} \sum_{x \in C_i} x \tag{4.14}$$

$$w = S_w^{-1}(m_1 - m_2) \tag{4.15}$$

4.2.6.2 Naive Bayes Classifier

Naive Bayes is a simple probabilistic classifier based on applying Bayes' theorem with the "naive" assumption of conditional independence between every pair of features [124]. Given a class variable y, composed by two classes y_1 and y_2, and a dependent feature vector $E = (x_1, x_2, ..., x_n)$, Bayes' theorem states the following relationship:

$$p(y|E) = \frac{p(y)p(E|y)}{p(E)} \tag{4.16}$$

E is classified as the class y_1 if and only if

$$f_b(E) = \frac{p(y = y_1|E)}{p(y = y_2|E)} \geq 1, \tag{4.17}$$

Using the naive independence assumption that all attributes are independent given the value of the class variable:

$$p(E|y) = p(x_1, x_2, ..., x_n|y) = \prod_{i=1}^{n} p(x_i|y), \tag{4.18}$$

the resulting classifier is then:

$$f_b(E) = \frac{p(y = y_1)}{p(y = y_2)} \prod_{i=1}^{n} \frac{p(x_i|y = y_1)}{p(x_i|y = y_2)} \tag{4.19}$$

4.2.6.3 Support Vector Machines

Support Vector Machines (SVMs) are a set of supervised learning methods that analyze data and recognize patterns, used for classification and regression analysis. SVMs are based on the concept of decision planes that define decision boundaries. In other words, an SVM classifies data by finding the best hyperplane that separates all data points of one class from another, and the best hyperplane for an SVM means the one with the largest margin between the two classes. The support vectors are the data points that are closest to the separating hyperplane, present on the boundary of the slab (see Figure 4.20).

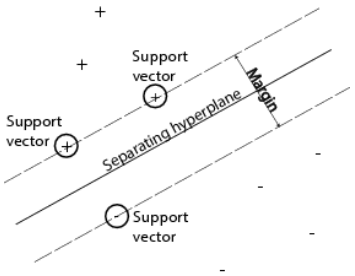

Figure 4.20: Separating hyperplane and margins for an SVM trained with two classes samples. Samples on the margin are called the support vectors.

When the classes are not linearly separable in the feature space, we can no longer find a hyperplane perfectly separating the points of the two classes. In that case, SVM can use a soft margin, meaning a hyperplane that separates many, but not all data points. The goal is to make the margin as large as possible but at the same time to keep the number of points miss-classified as small as possible. In this way, comes the need to control the trade-off between the dual objectives of maximizing the margin and minimizing the miss-classification error. A penalty for miss-classifying an example is added to the objective function, weighted by a parameter C (for the standard C-SVM formulation, as used in this work). A high C value will force the SVM training to avoid classification errors [14].

Some binary classifications do not have a simple hyperplane as a useful separating criterion. For those cases, a more complex classifier, allowing more general boundaries between classes, may be more appropriate. The general methodology is to map the input feature space to a high dimensional feature space where the classes can be satisfactorily separated by a hyper plane. Then, the (linear) SVM method can be mobilized for the design of the hyperplane classifier in the new feature space. However, there is an elegant property in the SVM methodology allowing the implicit mapping into high dimension spaces. This method is based on the idea of kernel functions $k(x, y)$. Thus, it is possible to fit the maximum-margin hyperplane in a transformed

feature space. Common kernels include polynomial ($k(x,y) = (1+(x,y)^d)$, where d is the polynomial order) and radial basis function ($k(x,y) = \exp(-\gamma\|x-y\|^2)$) [14].

4.3 Results

4.3.1 Depth map noise reduction

In order to recover missing depth data, a filling hole strategy is performed, as proposed in the work of Yang *et al.* [123]. Furthermore, to remove the noise of the unstable boundaries of the depth maps, a bilateral filter is implemented. With this type of filter, a Gaussian kernel and the intensity difference on the pixel are combined to obtain image smoothing, thanks to the domain component of the filter, and preserve edges at the same time, thanks to the range component.

Hence, the filter was tested with different parameters, varying the domain kernel (σ_d), the range kernel (σ_r) and, also, the window size. See Figure A.4 and A.5 in Appendix to consult the filter behavior with different parameters. It was only possible to perform the evaluation of these methods by visual observation of the patients point cloud. Nevertheless, the results obtained appear to be very interesting. Using a window of 9×9 it is possible to remove the staircase effect normally present in the Kinect depth maps, but it is verified several small "waves" all over the patient and the wall (see Figure A.4). On the other hand, with a σ_r excessively high important features are over smoothed from the woman's body (see Figure A.4 (c) and Figure A.5 (c)). In this manner, the most interesting result was achieved with $\sigma_r = 5$, $\sigma_d = 15$ and with a 15×15 window. As can be verified in the Figure 4.21, the bilateral filter was capable of smoothing the raw depth data and remove the staircase effect present in the original depth map, while preserving important details.

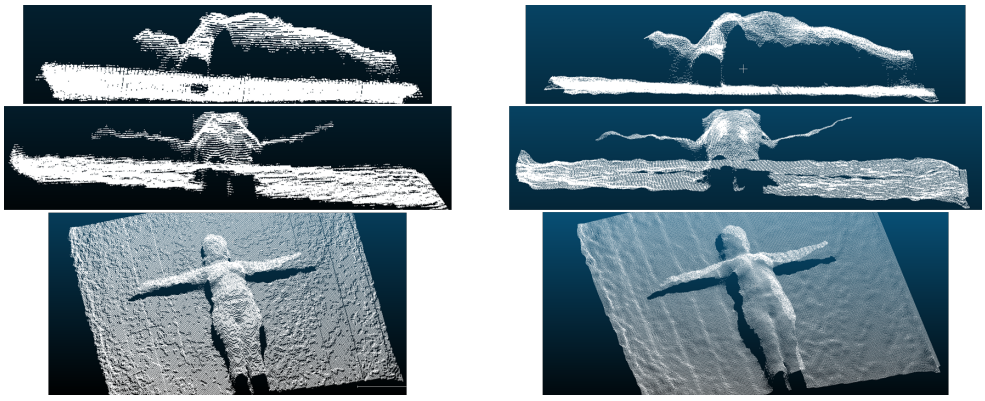

Figure 4.21: Result of the bilateral filter with $\sigma_r = 5$, $\sigma_d = 15$ and with a 15×15 window.

4.3.2 Patient Segmentation

In order to validate this method, a segmentation of the patient was performed using an image editor software, the ImageJ[2]. In this manner, it is manually chosen the best threshold to perform the segmentation and a median filter (11x11) was applied for smoothing. This task was performed for 48 frames randomly chosen among the 48 subjects on the database. Therefore, it was possible to evaluate the automatic segmentation calculating two different similarity indexes: Dice coefficient and Jaccard Index (see Table 4.4).

[2]http://imagej.nih.gov/ij/

Table 4.4: Similarity Indexes used to evaluate the body segmentation.

Name	**Equation**	
Dice coefficient (D)	$D(A,B) = \frac{2(A \bigcap B)}{(A \bigcap B + A \bigcup B)}$ (4.20)	Measures the extent of spatial overlap between two binary images. It gives more weighting to instances where the two images agree. Its values range between 0 (no overlap) and 1 (perfect agreement).
Jaccard Index (J)	$J(A,B) = \frac{\|A \bigcap B\|}{\|A \bigcup B\|}$ (4.21)	Measures similarity between finite sample sets, and is defined as the number of attributes shared divided by the total number of attributes present in either of them. Its values range between 0 (no similarity) and 1 (equal).

Also, the similarity between the two contours of the masks is evaluated by the Hausdorff and average distance. The Hausdorff distance is defined as the maximum distance of a set to the nearest point in the other set. Roughly speaking, it captures the maximum separation between the manual and the automatic contours. Consider the sets of points A and B. First, for each point in A the minimum distance to all points in B is obtained. Then, the directed Hausdorff distance $h(A,B)$ will be the maximum of this set of minimum distances (see Equation 4.22).

$$h(A,B) = \max_{a \in A} \min_{b \in B} \|a - b\| \tag{4.22}$$

The results obtained for the Jaccard Index and Dice coefficient can be consulted in Table 4.5. Regarding the average and Hausdorff distances, the results are presented in Table 4.6.

Table 4.5: Dice coefficient and Jaccard Index results of body segmentation.

	Mean	**Stdev**
Dice coefficient (D)	0.999	0.003
Jaccard Index (J)	0.997	0.005

Table 4.6: Body contour detection error (in pixels) evaluated by the Hausdorff and average distance.

	Automatic ⇒ Ground truth				Ground truth ⇒ Automatic			
	Mean	**Stdev**	**Max**	**Min**	**Mean**	**Stdev**	**Max**	**Min**
h	3.989	7.313	42.755	0	3.601	7.418	38.601	0
Avg	0.094	0.209	1.280	0	0.112	0.332	2.156	0

From the tables presented above it is possible to observe some interesting results. Regarding the Dice and Jaccard coefficients, the indexes are almost 1, which means that the proposed method presents an high similarity and an high overlap with the ground truth. The average distance is relatively low and the Hausdorff distance, which represents the worst case scenario, has an mean around 4 (in pixels). In Figure 4.22 it is possible to consult the automatic segmentation and the ground truth for different patients.

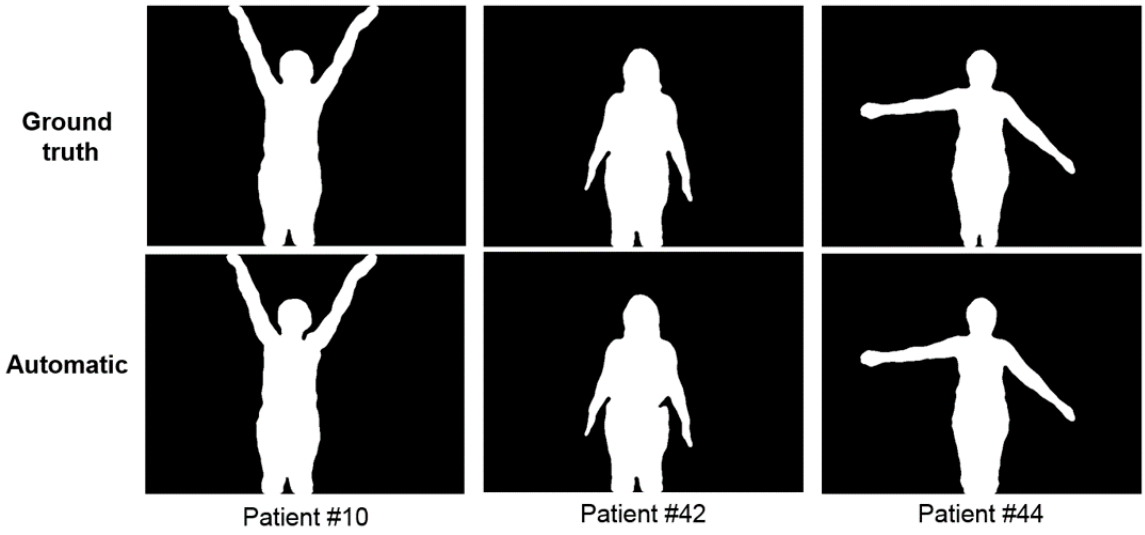

Figure 4.22: Ground truth and body segmentation examples.

4.3.3 Arm Segmentation

For the validation of the method used for upper-arm detection, the upper-arms were manually segmented. This was performed in 48 frames randomly chosen among the 48 subjects on the database. As with the patient segmentation, the Dice coefficient and the Jaccard Index (see Table 4.4), as well as the average and Hausdorff distances, were used for the evaluation of the proposed methodology. These results can be consulted in Table 4.7 and 4.8.

Table 4.7: Dice coefficient and Jaccard Index results of arm segmentation.

	Mean	**Std**
Dice coefficient (D)	0.783	0.048
Jaccard Index (J)	0.646	0.066

Table 4.8: Arm contour detection error (in pixels) evaluated by the Hausdorff and average distance.

	Automatic ⇒ Ground truth				Ground truth ⇒ Automatic			
	Mean	**Std**	**Max**	**Min**	**Mean**	**Std**	**Max**	**Min**
h	12.899	2.800	18.601	6.000	12.707	4.246	22.000	5.831
Avg	4.820	1.031	7.280	2.674	4.912	1.182	7.200	2.830

The similarity indexes present reasonably good results. In average, the Dice coeffient is around 78%, which represents a relatively high overlap between the ground truth and the detected arm, and a similarity of 65%, represented by the Jaccard Index. The average distance present a mean value of almost 5 (in pixels), while the Hausdorff distance has an higher value of around 13 (in pixels). With this results it is possible to conclude that, when compared with the body segmentation, this method is more error prone, but still quite satisfactory. In some cases, the similarity between the ground truth and the automatic detection is quite acceptable, but there are others where the method fails. In Figure 4.23 is possible to consult some examples, including one of the worst cases (Patient #52). It is important to have in attention that the manual

segmentation carried out in this case is harder to control and operator-dependent, so a big source of errors. Furthermore, the automatic detection of the arm points is done based on the Kinect skeleton, which can also have influence in the final result.

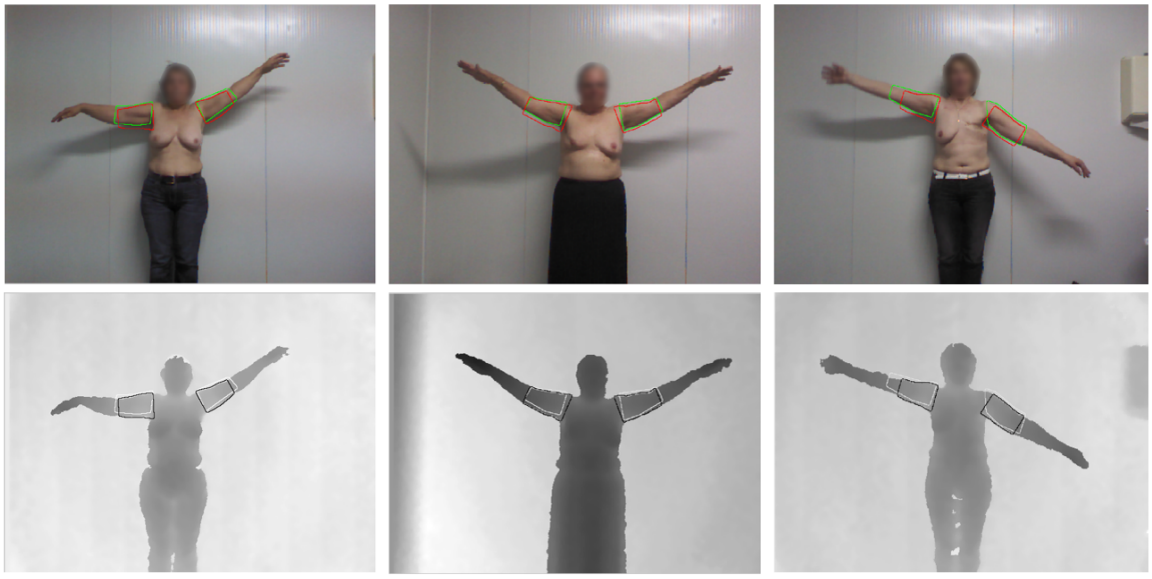

Figure 4.23: Arm contour detection examples. Detected contour (red/black) and ground truth (green/gray).

4.3.4 Upper-Body Functional Evaluation

For the creation of a predictive classification model, different supervised learning classifiers were tested: Fisher Linear Discriminant Analysis, Naive Bayes classifier and Supported Vector Machines.

4.3.4.1 Database Analysis

A ground truth is needed to build and compare the models. Therefore, we test the models using either the subjective evaluation of the UEFI and the medical diagnosis of lymphedema (Table 4.9).

Table 4.9: Distribution of the 48 patients over the two classes.

	Classes		Classes	
	Lymph	**No lymph**	**UEFI < 0.6**	**UEFI > 0.6**
# Cases	24	24	20	28

This is done since some patients that are not diagnosed with lymphedema may also present some limitations on the upper-limbs motion, which can still be a symptom of chronic problems on the UBF. On the other hand, not all patients of the database diagnosed with lymphedema demonstrated difficulties regarding their UBF, since they may already had recover all the mobility on the upper-arms. In this way, the UEFI can be useful, since it allows the identification of difficulties that the patients may have performing daily-life activities. However, there are no training or qualification specifications available for this assessment. So, it is difficult to have an accurate interpretation of the results and their functional implications. Nevertheless, the threshold used to divide the subjects in two classes was 0.6 (UEFI score ratio), chosen having in attention the type of treatment used and resorting to the opinion of a medical expert in breast cancer.

To better understand the disagreement between the evaluation of lymphedema and the UEFI questionnaire, the point-biserial correlation coefficient was assessed (see Equation 4.23). This coefficient is a special case of Pearson correlation in which one variable is quantitative (ratio) and the other variable is dichotomous, as in the present study.

$$r_{pb} = \frac{M_1 - M_0}{s_n} \sqrt{\frac{n_1 n_2}{n^2}}, \tag{4.23}$$

where s_n is the standard deviation:

$$s_n = \sqrt{\frac{1}{n} \sum_{i=1}^{n} (X_i - \overline{X})^2}, \tag{4.24}$$

M_1 being the mean value on the continuous variable X for all data points in group 1, and M_0 the mean value on the continuous variable X for all data points in group 2. Further, n_1 is the number of data points in group 1, n_0 is the number of data points in group 2 and n is the total sample size. Point-biserial values range from -1 to 1, where positive scores closer to 1 are desirable, since it traduces higher reliability. In this fashion, it was obtained a correlation score of $r_{pb} = 0.538$, which means that the disagreement between the self-report and the medical diagnosis is relatively low. This result confirms the validity of using this questionnaire to detect change in the UBF of breast cancer population. Notwithstanding, some of the questions should be revisited and more information about the scoring should be provided.

4.3.4.2 Classification Models

The classification models were designed using the selected features (see Table 4.10), considering all the possible subsets, using a LOO scheme [30]. Models considering two classes were trained using the two different ground truths, in order to verify the one that has lower miss-classification error. SVMs training was performed with linear, polynomial and radial basis function (RBF) kernels. For all this cases, exponentially growing sequences of C were tested, from $C = 2^{-2}$ until $C = 2^6$. For the polynomial kernel the polynomial order varied from 2 to 6, while γ, for the RBF kernel, was tested with: $\gamma = 0.25, 0.5, 0.75, 1$.

Table 4.10: Features used in the classification models.

#	Acronym	Description
1	μVOL	Average of the volume ratio.
2	$maxROM$	ROM at the maximum height achieved by the hand.
3	$maxHeight$	Maximum height achieved by the hand.
4	$maxWidth$	Width at the maximum height point.
5	$\mu ElbF$	Average of the right and left ratio of the elbow angle.
6	μAcc	Average of the hand instantaneous acceleration.
7	μH	Average of the height ratio along the movement.
8	μW	Average of the width ratio along the movement.
9	μROM	Average of the ROM ratio along the movement.

For each classifier, it is presented the parameters and the set of features that lead to lower miss-classification errors. The results considering the ground truth as the diagnosis of lymphedema by an expert can be consulted on Table 4.11. On the other hand, Table 4.17 present the results when the subjective evaluation of the UEFI was used as ground truth. In some of the tests, more than one subset of features obtained the same miss-classification error. For these cases, the ones with less complexity are chosen to present. It is also

possible to consult the confusion matrix of the different models (Tables 4.12-4.22), as well as the precision and recall of each matrix. The precision and recall are defined by the Equations 4.25 and 4.26, where TP are the true positive values, FP the false positive and FN the false negative.

$$Precison(P) = \frac{TP}{TP+FP} \tag{4.25}$$

$$Recall(R) = \frac{TP}{TP+FN} \tag{4.26}$$

Considering the results on Table 4.11, it is possible to verify that the best result obtained was a miss-classification error of 0.19 for the SVM classifier, either with the polynomial and RBF kernel. On the other hand, the maximum error was 0.29 for the LDA classifier. It was expected a better results with the SVMs since it proved to be a good option when there is limited amount of data available. Regarding now the precision and recall, it is possible to compare, for all the models, how many of the positive predictions are actually correct (precision), and how many of the positive labeled instances were actually been matched (recall). High precision values were obtained, which is traduced in a big proportion of cases that are correctly assigned. Although, it can also be noted that the most common miss-classification cases are lymphedema patients that are not considered, traduced by a lower recall value. Either way, considering the models with the best performance (Polynomial and RBF SVMs), the results are still very promising, since the models have proven to be capable of performing a correct classification of patients with reduced UBF, overlooking only 6 cases. As a result, the method developed appears to be a suitable solution for the functional evaluation of the upper-body on breast cancer patients.

The most common features used in almost all the selected models are the *maxW* and the μROM, as well as the *maxROM*, the $\mu ElbF$ and the μAcc. This means that these features are probably the ones that have greater influence in the functional assessment.

Table 4.11: Classification results for the different classifiers tested, using the lymphedema diagnosis as GT.

Classifier	**Kernel**	C	**order**	γ	**MER**	**Feat. Set**
LDA	-	-	-	-	0.29	[2, 4]
NaiveBayes	-	-	-	-	0.27	[5, 6, 9]
SVM	Linear	2^{-1}	-	-	0.25	[2, 5, 6]
SVM	Polynomial	2^{3}	4	-	0.19	[4, 9]
SVM	RBF	2^{4}	-	0.75	0.19	[1, 4, 9]

Table 4.12: Confusion matrix for the LDA model.

LDA

True \ Predict	**No lymph**	**Lymph**
No lymph	23	1
Lymph	13	11
Recall	0.46	
Precision	0.92	

Table 4.13: Confusion matrix for the Naive Bayes model.

Naive Bayes

True \ Predict	**No lymph**	**Lymph**
No lymph	23	1
Lymph	12	12
Recall	0.50	
Precision	0.92	

Table 4.14: Confusion matrix for the linear SVM model.

Linear SVM

True \ Predict	**No lymph**	**Lymph**
No lymph	24	0
Lymph	12	12
Recall	0.50	
Precision	1	

Table 4.15: Confusion matrix for the polynomial SVM model.

Polynomial SVM

True \ Predict	**No lymph**	**Lymph**
No lymph	21	3
Lymph	6	18
Recall	0.75	
Precision	0.86	

Table 4.16: Confusion matrix for the RBF SVM model.

RBF SVM

True \ Predict	**No lymph**	**Lymph**
No lymph	21	3
Lymph	6	18
Recall	0.75	
Precision	0.86	

Regarding now the results on Table 4.17, it is possible to verify that the performance of the classifiers is very similar to the previous approach. Comparing the LDA and Naive Bayes classifier, the errors are smaller, but the SVMs results are practically the same. However, the precision results are globally lower, which means that, in all the classifiers, there are several positive cases ignored.

There is no work in the literature similar to the one presented in this research, so it is not possible to compare the performance of the method developed to assess the upper-body function. In this case, using the UEFI score can be useful. The results are in agreement on both approaches tested, which can be an indication of the strength of the method proposed. More data, both in number and in diversity, would be important to perform a complete validation of the results.

Table 4.17: Classification results for the different classifiers tested, using the UEFI score as GT.

Classifier	**Kernel**	C	**order**	γ	**MER**	**Feat. Set**
LDA	-	-	-	-	0.21	[4, 5, 9]
NaiveBayes	-	-	-	-	0.23	[5, 9]
SVM	Linear	2^1	-	-	0.21	[1, 2, 4]
SVM	Polynomial	2^0	6	-	0.21	[3, 5, 9]
SVM	RBF	2^{-2}	-	0.75	0.21	[4, 9]

Table 4.18: Confusion matrix for the LDA model.

LDA

True \ Predict	**No lymph**	**Lymph**
No lymph	27	1
Lymph	9	11
Recall	0.55	
Precision	0.92	

Table 4.19: Confusion matrix for the Naive Bayes model.

Naive Bayes

True \ Predict	**No lymph**	**Lymph**
No lymph	26	2
Lymph	9	11
Recall	0.55	
Precision	0.85	

Table 4.20: Confusion matrix for the linear SVM model.

Linear SVM

True \ Predict	**No lymph**	**Lymph**
No lymph	27	1
Lymph	9	11
Recall	0.55	
Precision	0.92	

Table 4.21: Confusion matrix for the polynomial SVM model.

Polynomial SVM

True \ Predict	**No lymph**	**Lymph**
No lymph	28	0
Lymph	10	10
Recall	0.50	
Precision	1	

Table 4.22: Confusion matrix for the RBF SVM model.

RBF SVM

True \ Predict	**No lymph**	**Lymph**
No lymph	27	1
Lymph	9	11
Recall	0.55	
Precision	0.92	

In order to ascertain the utility of the self-report questionnaire in this study, another test was performed, using the UEFI score as input feature on the classification models. Table 4.23 present the smaller miss-classification errors, for the set of features that contains the UEFI score. From Table 4.24 to 4.28 are presented their confusion matrices. It is possible to observe that the results obtained are quite similar to the first approach presented. Nevertheless, if we take into account the polynomial and RBF SVMs, the miss-classification error is higher. Moreover, the precision results are quite similar, but the recall values are lower, what is not a desirable effect. In this manner, we can deduce that the UEFI self-report is not a necessary input to the method presented in this research. Therefore, it is possible to decrease the complexity of the UBF evaluation system, once it is no longer necessary to fill this questionnaire. Notwithstanding, in a future work, it would be important to increase the precision of the prediction model and the use of the UEFI data may be a interesting solution.

Table 4.23: Classification results for the different classifiers tested, with the inclusion of the UEFI score as a feature.

Classifier	**Kernel**	C	**order**	γ	**MER**	**Feat. Set**
LDA	-	-	-	-	0.19	[5, 6, 10]
NaiveBayes	-	-	-	-	0.25	[10]
SVM	Linear	2^{-2}	-	-	0.21	[5, 7, 10]
SVM	Polynomial	2^5	5	-	0.21	[10]
SVM	RBF	2^1	-	0.75	0,21	[2, 4, 10]

Table 4.24: Confusion matrix for the LDA model.

LDA

Predict / True	**No lymph**	**Lymph**
No lymph	24	0
Lymph	5	19
Recall	0.79	
Precision	0.83	

Table 4.25: Confusion matrix for the Naive Bayes model.

Naive Bayes

Predict / True	**No lymph**	**Lymph**
No lymph	20	4
Lymph	8	16
Recall	0.67	
Precision	0.80	

Table 4.26: Confusion matrix for the linear SVM model.

Linear SVM

Predict / True	**No lymph**	**Lymph**
No lymph	24	0
Lymph	6	18
Recall	0.75	
Precision	1	

Table 4.27: Confusion matrix for the polynomial SVM model.

Polynomial SVM

Predict / True	**No lymph**	**Lymph**
No lymph	19	5
Lymph	5	19
Recall	0.79	
Precision	0.79	

Table 4.28: Confusion matrix for the RBF SVM model.

RBF SVM

Predict / True	**No lymph**	**Lymph**
No lymph	19	5
Lymph	5	19
Recall	0.79	
Precision	0.79	

4.4 Conclusion

This Chapter presents a potential system for the functional evaluation of the upper-body motion in breast cancer patients, using a low-cost equipment, the Kinect device. This work takes advantage of the depth data and the skeleton information acquired with the Kinect.

Firstly, it was necessary the collection of training data for the development of the classification models. Hence, this work included the creation of a Database that until the present day comprise 48 subjects. The data was acquired with the Kinect and includes RGB and depth frames, as well as information of the skeleton tracking, of patients performing movements of abduction and adduction of the upper-limbs.

The depth and skeleton data are fundamental in this work. Consequently, it was applied a bilateral filter to remove noise from the raw depth data and it was performed a correction of the possible rotation of the Kinect device. Then, an effective segmentation of the patient was accomplished, combining the skeleton information and the depth data. Furthermore, using the patient silhouette and the position of the shoulder and elbow joints, it was possible to perform the detection of arm contour, important for the extraction of movement's features. Thereafter, also using the skeleton data, it is possible to obtain features that relate the

ROM of both shoulders, the volume ratio, the hand height and width, the elbow flexion and the movement acceleration.

Using the extracted features, different supervised classification algorithms (LDA, Naive Bayes and SVMs) were trained and tested for all the possible subsets of features in a LOO scheme. Thus, it was possible to explore all the possibilities and compare performances. The best results were verified with SVMs, with both polynomial and RBF kernels, with a miss-classification error of 0.19. There is no similar work on the literature to compare approaches, but the results are very promising. Notwithstanding, in a future work, it would be important to increase the precision of this prediction model to reduce FN classifications. Therefore, the methodology proposed appear to be suitable for the evaluation of the upper-body functional status in breast cancer patients, but improvements are still needed.

Restricted upper-body motion caused by breast cancer treatment is one of the main causes of decreased QOL among patients. So, there is an increased importance of having an objective and standard assessment of the treatment outcome, in order to identify which procedures have the better results and to standardize these treatments. Moreover, an early diagnosis of upper-limbs impairments is essential for the timely identification of adequate therapies that can lead to greater recovery of functional status, as well as prevention of progression. The visual observation by medial experts is not always enough for the identification of decreased mobility and there is no standard methods used for this assessment. In this manner, the proposed system can be a possible solution since, using a low-cost equipment, it allows the identification of the upper-body restricted motion in simple and efficient way.

Chapter 5

Rehabilitation

Upper-body motion problems caused by breast cancer treatment can persist for several years if an adequate therapy is not conducted. The upper-limbs motion is essential for the successfully execution of daily live activities and are a strong indicative of women's QOL. Thereby, it is important for the patients to have an indication of an appropriated exercise program, with emphasis on stretching or reaching movements, in order to increase the mobility and strength of the arm and shoulder.

In this fashion, this research included a preliminary study which aimed to integrate the method develop for the UBF evaluation with an exercise system, proper for the rehabilitation on breast cancer patients. The goal is to provide to the clinicians an efficient diagnosis method with the possibility of therapy prescription, where they would be able to indicate suitable exercises for the women perform at home. This rehabilitation program should be able to record and evaluate the women's performance in order to have a continuous follow-up of the patients status (see Figure 5.1).

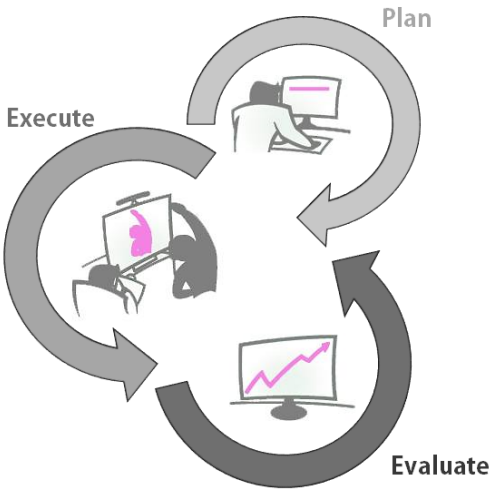

Figure 5.1: Proposed rehabilitation model for breast cancer patients.

Due to time issues, it was only possible the development of a first prototype of the rehabilitation system, and only preliminary tests were conducted.

5.1 Rehabilitation Model

This rehabilitation system was thought as a Windows application with pre-defined exercises available, recommended by a physiotherapy specialist. In this manner, the clinician would be able to select the ones adequate to the patient's therapy. At home, the women can perform the exercises recommended by mimicking the actions of an avatar. To perform an evaluation of the upper-limbs movement the skeleton tracking capabilities of the Kinect are used and, in this way, it is possible to record the women's performance and have a continuous clinical monitoring.

5.1.1 Avatar

The first step on this work was the creation of an avatar, possible to animate with the exercises needed. For this purpose, it was used a free open-source software called KMotion Capturer by Akira32[1](see Figure 5.2). This software captures the skeleton from the Kinect and saves it into a *.ms* (MaxScript) file for use in 3ds Max®[2]. In this way, it is possible to capture the real-time movements and export it to an animation software.

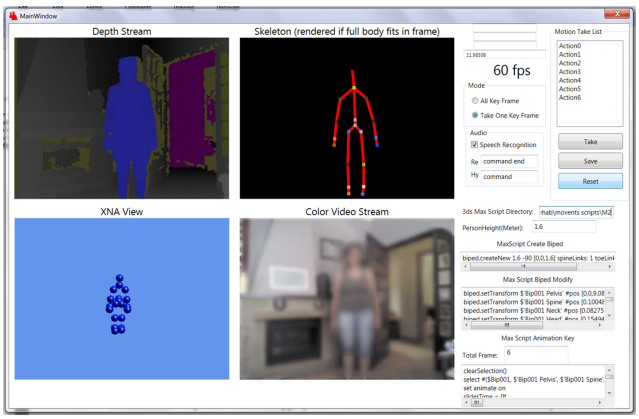

Figure 5.2: KMotion Capturer Software.

In 3ds Max, running the script created, it is obtained a biped skeleton animated with the movement captured by the KMotion Capture. Further, a skin mesh is applied to the biped in order to create a 3D model character (see Figure 5.3). Thereafter, the animated 3D model can be exported to a file possible to read in a XNA application, using the 3ds Max panda plugin[3].

5.1.2 Windows Application

The skeleton tracking system of the Microsoft Kinect, as well as the avatar previously developed, were integrated in a XNA application, to allow the evaluation of the exercise performed by the patient. Firstly, using the Game State Management sample [4], it was created a initial menu with different options - "Start rehabilitation", "Informations" and "Exit" (see Figure 5.4 (a)). Choosing the "Start rehabilitation" option, the game follows for a level selection menu (see Figure 5.4 (b)). Here, it will be possible to choose between the different exercises available on the application. Since the application is still in the initial phase of development, only one exercise model of stretching both limbs was developed. When the patient selects the

[1]http://blog.xuite.net/akira32/home
[2]http://www.autodesk.com/products/autodesk-3ds-max/overview
[3]http://www.andytather.co.uk/panda/directxmax.aspx
[4]http://xbox.create.msdn.com/en-US/education/catalog/sample/game_state_management

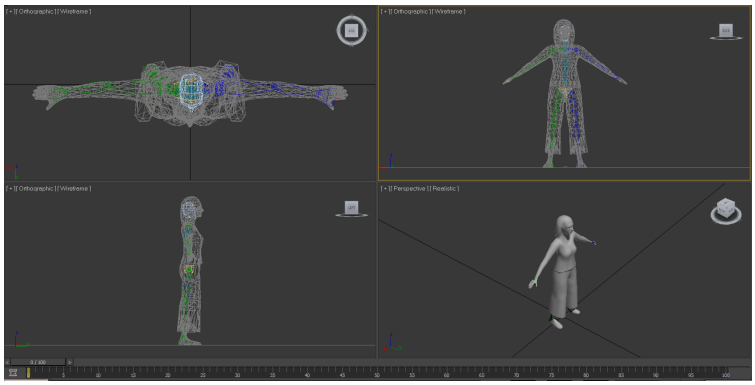

Figure 5.3: Biped skeleton with the skin mesh created in 3ds Max.

level of exercise to perform, a window is opened where is presented the avatar model, a color video stream and instructions for all the process. At first, the patients should be positioned in front of the Kinect, to allow skeleton detection (see Figure 5.4 (c)). Then, a 5 seconds countdown warns the patient to be ready, and the avatar starts to move (see Figure 5.4 (d)). The goal in this exercise is to make the women raise their arms as much as they can. Therefore, to guarantee this condition, when the avatar has the arms on the top it is verified if the patient's skeleton achieved a ROM bigger than 120º. If not, it is asked to the patient to rise more the limbs, until this condition is fulfilled. In this manner, during 5 seconds the avatar will be in pause and, afterwards, it continuous the movement as supposed. This ensures that the use of this system is not restricted for people with ROM bigger that 120º and, on the other hand, motivates patients to lift their limbs to its maximum.

The position of the skeleton joints are saved during all the process so, in the end of the movement, the evaluation of the patient's performance can be computed. This evaluation has in attention 3 different variables: the maximum height (H), the ROM at the same height (θ) and the maximum width (W) (see Figure 5.5).

In this way, for the right an left limb, it is searched the maximum height and width achieved by the hand. As explained in the previous chapter, the Shoulder Center joint is used as reference, so it is calculated the difference between this values and the Shoulder Center point. The ROM is computed at the same position of the maximum height, and will correspond to the angle between the line formed by the Head and Center Hip joints, and the line of the Elbow and Shoulder joints.

All the evaluation is performed considering that the woman has one healthy limb, which will correspond to the one that present a bigger height and, consequently, bigger ROM. Thereby, the values of this arm are used as reference for comparison. Hence, it is computed the ratio of each feature between the two limbs. To obtain an overall classification, the results of the evaluated features are considered, but with different confidence weights (Equation 5.1). In the previous Chapter, it was verified that the shoulder ROM is the feature with more relevance for the functional evaluation, so it is assigned to this variable a bigger weight. In the end, the resultant evaluation is presented in the form of percentage, which traduces the patient's performance.

$$\begin{aligned} Eval(\%) &= (\alpha_\theta \times \theta + \alpha_H \times H + \alpha_W \times W) \times 100, \\ for \quad \alpha_\theta &= 0.6, \quad \alpha_H = 0.2 \quad and \quad \alpha_W = 0.2 \end{aligned} \tag{5.1}$$

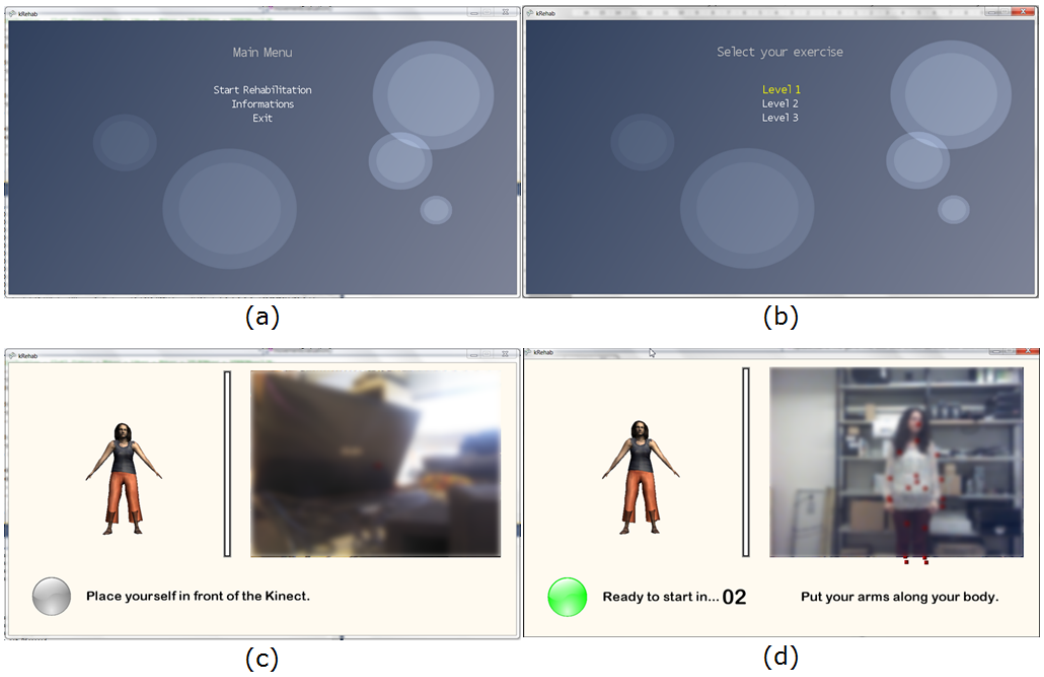

Figure 5.4: Rehabilitation App: (a) Initial menu; (b) Exercise level selection menu; (c) Window where the exercise should be performed, asking to the patient to be positioned in front of the Kinect; (d) When the skeleton is detected, a 5 seconds countdown precedes the start of the exercise.

Due to time limit problems, it was not possible to test the application with breast cancer patients. Nevertheless, experiences were made in healthy subjects, performing the abduction/adduction movement normally. Also, it was asked to the volunteers to perform another test where only one of the arms is raised completely, in order to simulate a patient with upper-body mobility problems. In the links presented below are provided two videos where is possible to see these testes.

- https://feupload.fe.up.pt/get/E7NFztIFIcJOk2l
- https://feupload.fe.up.pt/get/tkWyFEeKqOSgAVM

The application appear to have a good sensitivity to evaluate the performance of the exercise since, when the volunteers execute the movement without any difficult, the evaluation score is bigger than 90%. On the other hand, when one of the upper-limbs do not reach the maximum point, the score verified is 66% and when they do not lift one of the arms the result is around 20%.

5.2 Conclusion

In this chapter, a system that appears to be applicable for the rehabilitation at home of upper-body mobility is presented. It was developed a windows application where is possible to include different exercises recommended by an expert in physiotherapy, with an avatar performing these same exercises for the patients to mimic the movement. The Avatar was developed using the KMotion Capture free software and the 3ds Max. The application also uses the Kinect device for skeleton tracking, which allows the evaluation of the patient's performance. This evaluation is computed based on 3 features that, in the previous study, shown to

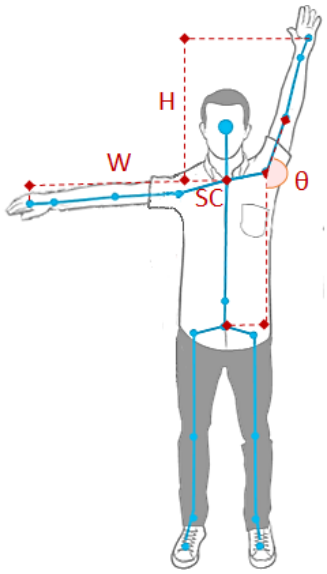

Figure 5.5: Features evaluated in the rehabilitation model.

be relevant to evaluate the UBF: the maximum height achieved by the hand, the ROM at the same height and the maximum width. The preliminary tests done to the developed system are quite satisfactory, since it was verified a good response of the evaluation method to different performances of the movement.

This part of the research is still in the initial phase of development, which means that there is a major part of the work that remains to be done. Firstly, only one exercise model was developed and so, there is the need to decide other relevant exercises to include and develop the methods for evaluation. Also, it is important to perform tests in breast cancer patients during a considerable amount of time, in order to verify if an evolution is observed regarding the upper-body function and, in this way, prove the applicability of the proposed rehabilitation model for breast cancer population. Furthermore, all the functional and visual aspects of the application has to be revisited, in order to make it more user friendly.

Chapter 6

Conclusion

Breast cancer treatment, besides the surgical removal of the tumor, also includes a radiation therapy to eradicate possible remaining cancer cells. Moreover, sometimes it is needed to remove the axillary lymph nodes by ALND. Both these procedures cause serious damage in the lymphatic system of the upper-limb, as the interruption of the lymphatic drainage. This results in the accumulation of lymph fluid in the subcutaneous tissue in the arm, which causes a decreased distensibility of the tissue around the joints and increased limb weight. Therefore, impairments as the restricted motion and arm edema are normally verified. These UBF morbidities interfere in women's daily life activities and are probably the largest source of reduced QOL in breast cancer patients.

Although its influence in women's QOL, there is no clinical standard for the diagnosis of decreased motion of UBF or arm swelling caused by breast cancer treatment. The most reported technologies used for limb volume assessment include water displacement and circumferential measurements. Regarding identification of upper-extremity reduced motion, goniometry is traditionally used. However, all these methods are operator-dependent and non-practical for clinical settings, incorrect use limits its accuracy and are not reproducible. On the other hand, several research groups studied the application of emerging 3D technologies for the human body modeling and volume assessment. Nonetheless, most of the proposed methods have high cost, complexity and are not suitable for clinical use. Furthermore, several human motion tracking systems were proposed to dynamically represent the human movement. Most of them appear to be successfully in this task, however, they have large space requirements or use complex systems of image acquisition. Moreover, almost all the studies were not developed with the specific purpose of UBF evaluation in breast cancer patients, so it is not known its sensitivity for functional problems of this population.

The main goal of this research was the study of a system for the diagnosis of upper-body functional impairments, suitable for breast cancer patients. The first step of this work was the development of an application for medical data acquisition, which allows to record color and depth frames, and the skeleton from the Kinect device. Thus, it was possible to collect a data set composed by breast cancer patients, with normal and decreased UBF, performing movements of abduction/adduction. Using the depth and skeleton data available, it was possible to obtain features of the movement performed by each patient, which relates the ROM of both shoulders, volume ratio, hand height and width, elbow flexion and movement acceleration. With this information, it was possible to test the behavior of several supervised learning algorithms (LDA, Naive Bayes and SVMs), in order to build a predictive classification model. The best classification performance was obtained using the SVM classifier, with a miss-classification error of 0.19. Therefore, these findings prove that the methodology proposed is efficient in the evaluation of the upper-body functional status in breast cancer

patients. It is important to have in attention that there is no similar work in the literature, so it is not possible to compare the results with other methods. Henceforward, more research is needed in order to progress in this direction and validate results.

Decreased mobility of the upper-limbs is a serious problem that need an early identification and prescription of appropriated exercises to prevent long-term impairments. In this manner, breast cancer patients are normally advised with a set of exercises that should perform at home. However, subjects with motor disabilities not always execute the home exercises as recommended, mainly due to lack of motivation. Thereby, other goal of this research, was the investigation of a possible home-based rehabilitation system, that uses a low-cost equipment, the Kinect device, and may help breast cancer patients to restore decreased UBF and prevent the development of chronic lymphedema. A preliminary work was performed in this direction: it was developed a windows application with a stretching exercise, which comprises an avatar model, and uses the Kinect skeleton data to perform an evaluation of the movement executed by the patient. It was not possible to explore the application performance on breast cancer population, but initial testes made with healthy subjects appear to be very promising. Nevertheless, there is still a lot of work needed in this area, to prove its applicability for the recovery of upper-limbs mobility and to prevent the progression of lymphedema on breast cancer patients.

6.1 Future Work

In this research, very promising results were accomplished regarding the method proposed for the evaluation of UBF. Nevertheless, some improvements can still be pointed.

First of all, it will be important to enrich the database with a more diversified data set, where are included multi-cultural women. In this way, it will be possible to test the feasibility of the proposed method in all kind of patients.

Lymphedema is the main cause of decreased upper-limbs motion, so there is an increased importance in the assessment of arm swelling. Since the upper-arm volume did not appear to be one of the most relevant features on this study, perhaps it is necessary to revise the methodology used. For this purpose, it can be explored a multi-Kinect system for data acquisition. On the other hand, it can also be tested an approach where the Kinect is moved around the subject.

Furthermore, it would be interesting the inclusion of the color information. It is well known that the use of radiation therapy changes the skin pigmentation, and this is verified in the upper-back when the treatment includes RT to the axilla. In this manner, another important feature could be included in the upper-body function evaluation system.

In the supervised classification models, a multi-class approach would be interesting to study. Moreover, it is important to improve the precision of the classifiers without the loss of the recall. Thus, it would be possible to decrease the false negatives and improve the classification performance. For this purpose, a continuous analysis of the UBF would be a suitable solution.

Regarding now the model of rehabilitation, a greater part of work is still needed to prove the applicability of the proposed system. More relevant exercise models should be included. Also, it remains to test its functionality with breast cancer patients, in order to verify if such a system is capable of improving the mobility of the upper-limbs.

References

[1] K. Akita. Image sequence analysis of real world human motion. *Pattern Recognition*, 17(1):73 – 83, 1984.

[2] E. Alexandre-Cortizo, M. Rosa-Zurera, and F. Lopez-Ferreras. Application of Fisher Linear Discriminant Analysis to Speech/Music Classification. In *The International Conference on Computer as a Tool*, volume 2, pages 1666–1669, Nov 2005.

[3] J.M. Armer, M.E. Radina, D. Porock, and S.D. Culbertson. Predicting Breast Cancer-Related Lymphedema Using Self-Reported Symptoms. *Nursing Research*, 52(6):370–379, 2003.

[4] J.M.G. Arroyo and M.L.D. López. Psychological Problems Derived from Mastectomy: A Qualitative Study. *International Journal of Surgical Oncology*, 2011, 2011.

[5] A.M. Baumberg and D.C. Hogg. An efficient method for contour tracking using active shape models. In *Proceedings of the 1994 IEEE Workshop on Motion of Non-Rigid and Articulated Objects, 1994.*, pages 194–199, 1994.

[6] A. Blake, R. Curwen, and A. Zisserman. A framework for spatiotemporal control in the tracking of visual contours. *International Journal of Computer Vision*, 11(2):127–145, 1993.

[7] J. Broeren, M. Rydmark, A. Björkdahl, and K.S. Sunnerhagen. Assessment and training in a 3-dimensional virtual environment with haptics: a report on 5 cases of motor rehabilitation in the chronic stage after stroke. *Neurorehabilitation and neural repair*, 21(2):180–189, 2007.

[8] C. Bulley, F. Coutts, C. Blyth, W. Jack, M.U. Chetty, M. Barber, and C.W. Tan. Prevalence and Impacts of Upper Limb Morbidity after Treatment for Breast Cancer: A Cross-Sectional Study of Lymphedema and Function. *Cancer and Oncology Research*, 1(2):30–39, 2013.

[9] C. Bulley, S. Gaal, F. Coutts, C. Blyth, W. Jack, M.U. Chetty, M. Barber, and C.W. Tan. Comparison of Breast Cancer-Related Lymphedema (Upper Limb Swelling) Prevalence Estimated Using Objective and Subjective Criteria and Relationship with Quality of Life. *BioMed Research International*, 2013.

[10] D. Burdick. Rehabilitation of the breast cancer patient. *Cancer*, 36(2):645–648, 1975.

[11] M.S. Cameirão, S. Bermúdez, and P.F.M.J. Verschure. Virtual reality based upper extremity rehabilitation following stroke: a review. *Journal of CyberTherapy & Rehabilitation*, 1(1):63–74, 2008.

[12] M.S. Cameirão, L. Zimmerli, E.D. Oller, P.F.M.J. Verschure, et al. The rehabilitation gaming system: a virtual reality based system for the evaluation and rehabilitation of motor deficits. In *Virtual Rehabilitation, 2007*, pages 29–33, 2007.

[13] K.L. Campbell, A.L. Pusic, D.S. Zucker, M.L. McNeely, J.M. Binkley, A.L. Cheville, and K.J. Harwood. A prospective model of care for breast cancer rehabilitation: Function. *Cancer*, 118(8):2300–2311, 2012.

[14] J. S. Cardoso and M. J. Cardoso. Towards an intelligent medical system for the aesthetic evaluation of breast cancer conservative treatment. *Artificial Intelligence in Medicine*, 40(2):115–126, 2007.

[15] M.J. Cardoso, J. Cardoso, N. Amaral, I. Azevedo, L. Barreau, M. Bernardo, D. Christie, S. Costa, et al. Turning subjective into objective: The BCCT.core software for evaluation of cosmetic results in breast cancer conservative treatment. *The Breast*, 16(5):456–461, 2007.

[16] G. Catanuto, A. Spano, A. Pennati, E. Riggio, G.M. Farinella, G. Impoco, S. Spoto, G. Gallo, and M.B. Nava. Experimental methodology for digital breast shape analysis and objective surgical outcome evaluation. *Journal of Plastic, Reconstructive & Aesthetic Surgery*, 61(3):314–318, 2008.

[17] C. Chang, R. Ansari, and A. Khokhar. Cyclic articulated human motion tracking by sequential ancestral simulation. In *IEEE Computer Society Conference on Computer Vision and Pattern Recognition*, 2004.

[18] Y.J. Chang, S.F. Chen, and J.D. Huang. A Kinect-based system for physical rehabilitation: A pilot study for young adults with motor disabilities. *Research in developmental disabilities*, 32(6):2566–2570, 2011.

[19] B. Cheema, C.A. Gaul, K. Lane, and M.A.F. Singh. Progressive resistance training in breast cancer: a systematic review of clinical trials. *Breast cancer research and treatment*, 109(1):9–26, 2008.

[20] J.M. Chung and N. Ohnishi. Cue circles: Image feature for measuring 3-d motion of articulated objects using sequential image pair. In *International Conference on Automatic Face and Gesture Recognition, 1998.*, pages 474–479, 1998.

[21] Pero-System Messgerate CMbH. Perometer. Wuppertal, Germany, 1999. Wuppertal, Germany.

[22] B.H. Cornish, M. Chapman, C. Hirst, B. Mirolo, I.H. Bunce, L.C. Ward, and B.J. Thomas. Early diagnosis of lymphedema using multiple frequency bioimpedance. *Lymphology*, 34(1):2–11, 2001.

[23] S. Coster, K. Poole, and L.J. Fallowfield. The validation of a quality of life scale to assess the impact of arm morbidity in breast cancer patients post-operatively. *Breast Cancer Research and Treatment*, 68(3):273–282, 2001.

[24] S. Crowley. The Effect of a Structured Exercise Program on Fatigue, Strength, Endurance, Physical Self-Efficacy, and Functional Wellness in Women With Early Stage Breast Cancer. In *Oncology Nursing Society*, 2004.

[25] D.J. Dawes, S. Meterissian, M. Goldberg, and N.E. Mayo. Impact of lymphoedema on arm function and health-related quality of life in women following breast cancer surgery. *Journal of Rehabilitation Medicine*, 40(8):651–658, 2008.

[26] I.C. De Backer, G. Schep, F.J. Backx, G. Vreugdenhil, and H. Kuipers. Resistance Training in Cancer Survivors: A Systematic review. *Int J Sports Med*, 30(10):703–712, 2009.

[27] A.K. Dixon, T.K. Wheeler, D.J. Lomas, and R. Mackenzie. Computed tomography or magnetic resonance imaging for axillary symptoms following treatment of breast carcinoma? A randomized trial. *Clinical radiology*, 48(6):371–376, 1993.

[28] Microsoft Developer Network (MSDN) Documentation. Skeletal Tracking, 2014.

[29] R. Drake, A.W. Vogl, and A.W.M. Mitchell. *Gray's Anatomy for Students*. Gray's Anatomy. Elsevier Health Sciences, 2009.

[30] R. O. Duda, P. E. Hart, and D. G. Stork. *Pattern Classification*. Wiley Interscience, 2nd Edition, 2000.

[31] F. Durand and J. Dorsey. Fast Bilateral Filtering for the Display of High-dynamic-range Images. In *Proceedings of the 29th Annual Conference on Computer Graphics and Interactive Techniques*, SIGGRAPH '02, pages 257–266, New York, USA, 2002. ACM.

[32] M. Eder, F.V. Waldenfels, A. Swobodnik, M. Klöppel, A.K. Pape, T. Schuster, S. Raith, E. Kitzler, N.A. Papadopulos, H.G. Machens, et al. Objective breast symmetry evaluation using 3-D surface imaging. *The Breast*, 21(2):152–158, 2012.

[33] J. Engel, J. Kerr, A. Schlesinger-Raab, H. Sauer, and D. Hölzel. Axilla surgery severely affects quality of life: results of a 5-year prospective study in breast cancer patients. *Breast cancer research and treatment*, 79(1):47–57, 2003.

[34] V.S. Erickson, M.L. Pearson, P.A. Ganz, J. Adams, and K.L. Kahn. Arm Edema in Breast Cancer Patients. *Journal of the National Cancer Institute*, 93(2):96–111, 2001.

[35] J. Ferlay, H.R. Shin, F. Bray, D. Forman, C. Mathers, and D.M Parkin. GLOBOCAN 2008 v2.0, Cancer Incidence and Mortality Worldwide: IARC CancerBase No. 10. Lyon, France: International Agency for Research on Cancer, 2010. Available from: http://globocan.iarc.fr, accessed on 27/10/2010.

[36] M. Fisher and D. Howell. The power of empowerment: an ICF-based model to improve self-efficacy and upper extremity function of survivors of breast cancer. *Rehabilitation Oncology*, 28(3):19–25, 2010.

[37] International Society for the Advancement of Kinanthropometry. *International Standards for Anthropometric Assessment*. National Library of Australia, 2001.

[38] R. Freitas-Silva, D.M. Conde, R. Freitas-Júnior, and E.Z. Martinez. Comparison of quality of life, satisfaction with surgery and shoulder-arm morbidity in breast cancer survivors submitted to breast-conserving therapy or mastectomy followed by immediate breast reconstruction. *Clinics*, 65(8):781–787, 2010.

[39] D.M. Gavrila. The visual analysis of human movement: A survey. *Computer vision and image understanding*, 73(1):82–98, 1999.

[40] A.E. Giuliano, K.K. Hunt, and K.V. Ballman. Axillary dissection vs no axillary dissection in women with invasive breast cancer and sentinel node metastasis: A randomized clinical trial. *JAMA*, 305(6):569–575, 2011.

[41] L. Gonçalves, E. Di Bernardo, E. Ursella, and P. Perona. Monocular tracking of the human arm in 3D. In *Proceedings of Fifth International Conference on Computer Vision, 1995.*, pages 764–770, 1995.

[42] A. Goyal, R.G. Newcombe, A. Chhabra, and R.E. Mansel. Morbidity in Breast Cancer Patients with Sentinel Node Metastases Undergoing Delayed Axillary Lymph Node Dissection (ALND) Compared with Immediate ALND. *Annals of Surgical Oncology*, 15(1):262–267, 2008.

[43] B.J. Grube and A.E. Giuliano. *Diseases of the Breast*, chapter 41: Sentinel Lymph Node Dissection. Lippincott Williams & Wilkins, 2010.

[44] J.A. Harrison, M.A. Nixon, W.R. Fright, and L. Snape. Use of hand-held laser scanning in the assessment of facial swelling: a preliminary study. *British Journal of Oral and Maxillofacial Surgery*, 42(1):8–17, 2004.

[45] S.C. Hayes, D. Battistutta, and B. Newman. Objective and subjective upper body function six months following diagnosis of breast cancer. *Breast cancer research and treatment*, 94(1):1–10, 2005.

[46] S.C. Hayes, M. Janda, B. Cornish, D. Battistutta, and B. Newman. Lymphedema After Breast Cancer: Incidence, Risk Factors, and Effect on Upper Body Function. *Journal of Clinical Oncology*, 26(21):3536–3542, 2008.

[47] S.C. Hayes, K. Johansson, N.L. Stout, R. Prosnitz, J.M. Armer, S. Gabram, and K.H. Schmitz. Upper-body morbidity after breast cancer. *Cancer*, 118(8):2237–2249, 2012.

[48] S.C. Hayes, S. Rye, D. Battistutta, T. DiSipio, and B. Newman. Upper-body morbidity following breast cancer treatment is common, may persist longer-term and adversely influences quality of life. *Health Qual Life Outcomes*, 8(1):92, 2010.

[49] D. Hayn, S. Raschhofer, M. Falgenhauer, R. Modre-Osprian, F. Fruhwald, and G. Schreier. Edema detection for heart failure patients in home monitoring scenarios. In *Computing in Cardiology (CinC), 2012*, pages 93–96, 2012.

[50] A. Henderson, N. Korner-Bitensky, and M. Levin. Virtual reality in stroke rehabilitation: a systematic review of its effectiveness for upper limb motor recovery. *Topics in stroke rehabilitation*, 14(2):52–61, 2007.

[51] H. Henseler, B.S. Khambay, A. Bowman, J. Smith, J.P. Siebert, S. Oehler, X. Ju, A. Ayoub, and A.K. Ray. Investigation into accuracy and reproducibility of a 3D breast imaging system using multiple stereo cameras. *Journal of Plastic, Reconstructive & Aesthetic Surgery*, 64(5):577–582, 2011.

[52] M.K. Holden, T.A. Dyar, L. Schwamm, and E. Bizzi. Virtual-environment-based telerehabilitation in patients with stroke. *Presence: Teleoperators and Virtual Environments*, 14(2):214–233, 2005.

[53] J.D. Huang. Kinerehab: a kinect-based system for physical rehabilitation: a pilot study for young adults with motor disabilities. In *Proceedings of the 13th international ACM SIGACCESS conference on Computers and accessibility*, pages 319–320, 2011.

[54] E. Huber. 3D real-time gesture recognition using proximity spaces. In *Proceedings 3rd IEEE Workshop on Applications of Computer Vision, 1996.*, pages 136–141, 1996.

[55] P.L. Hudak, P.C. Amadio, C. Bombardier, D. Beaton, D. Cole, A. Davis, G. Hawker, et al. Development of an upper extremity outcome measure: The DASH (disabilities of the arm, shoulder, and head). *American Journal of Industrial Medicine*, 29(6):602–608, 1996.

[56] American Cancer Society Inc. Surgery for breast cancer, September 2013.

[57] American Cancer Society Inc. What is cancer?, September 2013.

[58] Northern Digital Inc. Polaris Family of Optical Tracking Systems. Available from: http://www.ndigital.com/medical/polarisfamily.php.

[59] Polhemus Inc. FastSCAN. Available from: http://www.fastscan3d.com/.

[60] Gunnar Johansson. Visual motion perception. *Scientific American*, 1975.

[61] S.X. Ju, M.J. Black, and Y. Yacoob. Cardboard people: A parameterized model of articulated image motion. In *Proceedings of the Second International Conference on Automatic Face and Gesture Recognition, 1996.*, pages 38–44, 1996.

[62] A. Karki, R. Simonen, E. Malkia, and J. Selfe. Impairments, activity limitations and participation restrictions 6 and 12 months after breast cancer operation. *Journal of Rehabilitation Medicine*, 37(3):180–188, 2005.

[63] C.H. Kau, A. Cronin, P. Durning, A.I. Zhurov, A. Sandham, and S. Richmond. A new method for the 3D measurement of postoperative swelling following orthognathic surgery. *Orthodontics & Craniofacial Research*, 9(1):31–37, 2006.

[64] R. Kizony, P.L. Weiss, Y. Feldman, M. Shani, O. Elion, S. Harel, and I. Baum-Cohen. Evaluation of a Tele-Health System for upper extremity stroke rehabilitation. In *International Conference on Virtual Rehabilitation (ICVR), 2013*, pages 80–86, 2013.

[65] D.N. Krag, S.J. Anderson, T.B. Julian, A.M. Brown, S.P. Harlow, J.P. Costantino, T. Ashikaga, D.L. Weaver, et al. Sentinel-lymph-node resection compared with conventional axillary-lymph-node dissection in clinically node-negative patients with breast cancer: overall survival findings from the NSABP B-32 randomised phase 3 trial. *The Lancet Oncology*, 11(10):927 – 933, 2010.

[66] L. Krishnan, A.L. Stanton, C.A. Collins, V.E. Liston, and W.R. Jewell. Form or function? Part 2. Objective cosmetic and functional correlates of quality of life in women treated with breast-conserving surgical procedures and radiotherapy. *Cancer*, 91(12):2282–2287, 2001.

[67] W. Kwan, J. Jackson, L.M. Weir, C. Dingee, G. McGregor, and I.A. Olivotto. Chronic Arm Morbidity After Curative Breast Cancer Treatment: Prevalence and Impact on Quality of Life. *Journal of Clinical Oncology*, 20(20):4242–4248, 2002.

[68] M.K. Leung and Y.H. Yang. First Sight: A human body outline labeling system. *IEEE Transactions on Pattern Analysis and Machine Intelligence*, 17(4):359–377, 1995.

[69] C.I.F. Li. *Breast Cancer Epidemiology*. Springer, 2009.

[70] Charnwood Dynamics Ltd. Codamotion. Available from: http://www.charndyn.com/.

[71] Vicon Motion Systems Ltd. VICON. Available from: http://www.vicon.com/.

[72] G. Lu, G.N. DeSouza, J. Armer, B. Anderson, and C.R. Shyu. A system for limb-volume measurement using 3D models from an infrared depth sensor. In *IEEE Symposium on Computational Intelligence in Healthcare and e-health (CICARE), 2013*, pages 64–69, 2013.

[73] C.E. Matthews, S. Wilcox, C.L. Hanby, C. Ananian, S.P. Heiney, T. Gebretsadik, and A. Shintani. Evaluation of a 12-week home-based walking intervention for breast cancer survivors. *Supportive Care in Cancer*, 15(2):203–211, 2007.

[74] D.C. McKenzie and A.L. Kalda. Effect of upper extremity exercise on secondary lymphedema in breast cancer patients: a pilot study. *Journal of Clinical Oncology*, 21(3):463–466, 2003.

[75] J.G. McKinnon, V. Wong, W.J. Temple, C. Galbraith, P. Ferry, G.S. Clynch, and C. Clynch. Measurement of limb volume: Laser scanning versus volume displacement. *Journal of Surgical Oncology*, 96(5):381–388, 2007.

[76] M.L. McNeely, K. Campbell, M. Ospina, B.H. Rowe, K. Dabbs, T.P. Klassen, J. Mackey, and K. Courneya. Exercise interventions for upper-limb dysfunction due to breast cancer treatment. *Cochrane Database Syst Rev*, 6(6), 2010.

[77] M.L. McNeely, K.L. Campbell, B.H. Rowe, T.P. Klassen, J.R. Mackey, and K.S. Courneya. Effects of exercise on breast cancer patients and survivors: a systematic review and meta-analysis. *Canadian Medical Association Journal*, 175(1):34–41, 2006.

[78] I. Mikić, M. Trivedi, E. Hunter, and P. Cosman. Human body model acquisition and tracking using voxel data. *International Journal of Computer Vision*, 53(3):199–223, 2003.

[79] V. Mock, C. Frangakis, N.E. Davidson, M.E. Ropka, M. Pickett, B. Poniatowski, K.J. Stewart, et al. Exercise manages fatigue during breast cancer treatment: A randomized controlled trial. *Psycho-Oncology*, 14(6):464–477, 2005.

[80] I. Nesvold, K.V. Reinertsen, S.D. Fossa, and A.A. Dahl. The relation between arm/shoulder problems and quality of life in breast cancer survivors: a cross-sectional and longitudinal study. *Journal of Cancer Survivorship*, 5(1):62–72, 2011.

[81] Breast Care Center of Miami. Comparing Breast Conservation versus Mastectomy., 2011.

[82] H. P. Oliveira, J.S. Cardoso, A. Magalhães, and M.J. Cardoso. A 3D low-cost solution for the aesthetic evaluation of breast cancer conservative treatment. *Computer Methods in Biomechanics and Biomedical Engineering: Imaging & Visualization*, pages 1–17, 2013.

[83] H.P. Oliveira, J.S. Cardoso, A. Magalhaes, and M.J. Cardoso. Methods for the Aesthetic Evaluation of Breast Cancer Conservation Treatment: A Technological Review. *Current Medical Imaging Reviews*, 9(1):32–46, 2013.

[84] J. A. Petrek, P.I. Pressman, R.A. Smith, et al. Lymphedema: current issues in research and management. *CA: A cancer Journal for Clinicians*, 50(5):292–311, 2000.

[85] B.M. Pinto, G.M. Frierson, C. Rabin, J.J. Trunzo, and B.H. Marcus. Home-based physical activity intervention for breast cancer patients. *Journal of Clinical Oncology*, 23(15):3577–3587, 2005.

[86] B.M. Pinto, C. Rabin, and S. Dunsiger. Home-based exercise among cancer survivors: adherence and its predictors. *Psycho-Oncology*, 18(4):369–376, 2009.

[87] Hanger Prosthetics and Orthotics. Insignia Laser Scanner, 2014. Available from: http://www.hanger.com/prosthetics/services/Technology/Pages/Insignia.aspx.

[88] A.D. Purushotham, S. Upponi, M.B. Klevesath, L. Bobrow, K. Millar, J.P. Myles, and S.W. Duffy. Morbidity After Sentinel Lymph Node Biopsy in Primary Breast Cancer: Results From a Randomized Controlled Trial. *Journal of Clinical Oncology*, 23(19):4312–4321, 2005.

[89] A.L. Pusic, A.F. Klassen, A.M. Scott, J.A. Klok, P.G. Cordeiro, and S.J. Cano. Development of a New Patient-Reported Outcome Measure for Breast Surgery: The BREAST-Q. *Plastic and Reconstructive Surgery*, 124(2):–, 2009.

[90] Qualisys. Mortion Capture System. Available from: http://www.qualisys.com/.

[91] G. Rahman. Breast conserving therapy: A surgical technique where little can mean more. *J Surg Tech Case Report*, 3(1):1–4, January 2011.

[92] R. Ricciardi and L.A. Talbot. Use of bioelectrical impedance analysis in the evaluation, treatment, and prevention of overweight and obesity. *Journal of the American Academy of Nurse Practitioners*, 19(5):235–241, 2007.

[93] K. Rohr. Towards model-based recognition of human movements in image sequences. *CVGIP: Image understanding*, 59(1):94–115, 1994.

[94] R. Ronfard, C. Schmid, and B. Triggs. Learning to parse pictures of people. In *Computer Vision - ECCV 2002*, pages 700–714. Springer, 2006.

[95] R.J. Sanchez, J. Liu, S. Rao, P. Shah, R. Smith, T. Rahman, S.C. Cramer, J.E. Bobrow, and D.J. Reinkensmeyer. Automating arm movement training following severe stroke: functional exercises with quantitative feedback in a gravity-reduced environment. *Neural Systems and Rehabilitation Engineering, IEEE Transactions on*, 14(3):378–389, 2006.

[96] G. Saposnik, R. Teasell, M. Mamdani, J. Hall, W. McIlroy, D. Cheung, K.E. Thorpe, L.G. Cohen, et al. Effectiveness of Virtual Reality Using Wii Gaming Technology in Stroke Rehabilitation: A Pilot Randomized Clinical Trial and Proof of Principle. *Stroke*, 41(7):1477–1484, 2010.

[97] R.R. Seeley, P. Tate, and T.D. Stephens. *Anatomy and Physiology*. McGraw-Hill Companies, 2008.

[98] M. Shaughnessy, B.M. Resnick, and R.F. Macko. Testing a Model of Post-Stroke Exercise Behavior. *Rehabilitation nursing*, 31(1):15–21, 2006.

[99] Ashish Shingade and Archana Ghotkar. Animation of 3D Human Model Using Markerless Motion Capture Applied To Sports. *arXiv preprint arXiv:1402.2363*, 2014.

[100] R.M. Speck, K.S. Courneya, L.C. Mâsse, S. Duval, and K.H. Schmitz. An update of controlled physical activity trials in cancer survivors: a systematic review and meta-analysis. *Journal of Cancer Survivorship*, 4(2):87–100, 2010.

[101] M.A. Sprangers, M. Groenvold, J.I. Arraras, J. Franklin, A. te Velde, M. Muller, L. Franzini, et al. The European Organization for Research and Treatment of Cancer breast cancer-specific quality-of-life questionnaire module: first results from a three-country field study. *Journal of Clinical Oncology*, 14(10):2756–68, 1996.

[102] A.L. Stanton, L. Krishnan, and C.A. Collins. Form or function? Part 1. Subjective cosmetic and functional correlates of quality of life in women treated with breast-conserving surgical procedures and radiotherapy. *Cancer*, 91(12):2273–2281, 2001.

[103] A.W.B. Stanton, C. Badger, and J. Sitzia. Non-invasive assessment of the lymphedematous limb. *Lymphology*, 33(3):122–135, 2000.

[104] N.L. Stout, J.M. Binkley, K.H. Schmitz, K. Andrews, S.C. Hayes, K.L. Campbell, M.L. McNeely, et al. A prospective surveillance model for rehabilitation for women with breast cancer. *Cancer*, 118(8):2191–2200, 2012.

[105] P.W. Stratford. Assessing Disability and Change on Individual Patients: A Report of a Patient Specific Measure. *Physiotherapy Canada*, 47(4):258–263, January 1995.

[106] P.W. Stratford, J.M. Binkley, and D.M. Stratford. Development and initial validation of the upper extremity functional index. *Physiotherapy Canada*, 53 (4):259–267, 2001.

[107] A. Szuba and S.G. Rockson. Lymphedema: classification, diagnosis and therapy. *Vascular Medicine*, 3(2):145–156, 1998.

[108] R. Taylor, U.W. Jayasinghe, L. Koelmeyer, O. Ung, and J. Boyages. Reliability and validity of arm volume measurements for assessment of lymphedema. *Physical therapy*, 86(2):205–214, 2006.

[109] I. Tengrup, L. Tennvall-Nittby, I. Christiansson, and M. Laurin. Arm morbidity after breast-conserving therapy for breast cancer. *Acta Oncologica*, 39(3):393–397, 2000.

[110] C. Theobalt, M.A. Magnor, P. Schüler, and H.P. Seidel. Combining 2D feature tracking and volume reconstruction for online video-based human motion capture. *International Journal of Image and Graphics*, 4(04):563–583, 2004.

[111] C. Tomasi and R. Manduchi. Bilateral filtering for gray and color images. In *Sixth International Conference on Computer Vision*, pages 839–846, Jan 1998.

[112] P. Treleaven and J. Wells. 3D body scanning and healthcare applications. *Computer*, 40(7):28–34, 2007.

[113] C. Trombetta, P. Abundo, A. Felici, C. Ljoka, S. Di Cori, N. Rosato, and C. Foti. Computer Aided Measurement Laser (CAML): technique to quantify post-mastectomy lymphoedema. In *Journal of Physics: Conference Series*, volume 383, page 012018, 2012.

[114] Cancer Research UK, October 2012. From: http://www.cancerresearchuk.org.

[115] M. Vahdaninia, S. Omidvari, and A. Montazeri. What do predict anxiety and depression in breast cancer patients? A follow-up study. *Social Psychiatry and Psychiatric Epidemiology*, 45(3):355–361, 2010.

[116] VividGroup. VividGroup's Gesture Xtreme (GX).

[117] C. Vukotich, M.J. Geyer, and F. Erdeljac. Use of a Laser Scanning System to Measure Limb Volume in Chronic Edema. *Rehabilitation Engineering & Assistive Technology Society of North America (RESNA)*, 2011, 2011.

[118] J. Webb and J. Ashley. *Beginning Kinect Programming with the Microsoft Kinect SDK*. Expert's voice in Microsoft. Apress, 2012.

[119] P.L. Weiss, D. Rand, N. Katz, and R. Kizony. Video capture virtual reality as a flexible and effective rehabilitation tool. *Journal of neuroengineering and rehabilitation*, 1(1):12, 2004.

[120] Terese Winslow. LLC ©, 2011. U.S. Government has reuse rights.

[121] S.F. Wong and K.Y.K. Wong. Reliable and fast human body tracking under information deficiency. In *Proceedings of IEEE Intelligent Automation Conference, Hong Kong*, 2003.

[122] C.R. Wren, A. Azarbayejani, T. Darrell, and A.P. Pentland. Pfinder: Real-time tracking of the human body. *IEEE Transactions on Pattern Analysis and Machine Intelligence*, 19(7):780–785, 1997.

[123] Na-Eun Yang, Yong-Gon Kim, and Rae-Hong Park. Depth hole filling using the depth distribution of neighboring regions of depth holes in the Kinect sensor. In *IEEE International Conference on Signal Processing, Communication and Computing (ICSPCC)*, pages 658–661, Aug 2012.

[124] H. Zhang. The optimality of naive Bayes. *Proceedings of the Seventeenth International Florida Artificial Intelligence Research Society Confer ence*, 1(2):3, 2004.

[125] H. Zhou and H. Hu. Human motion tracking for rehabilitation? A survey. *Biomedical Signal Processing and Control*, 3(1):1–18, 2008.

Appendix A

Upper-body Function Evaluation

In this appendix is provided additional data for the Chapter 4, that can be useful for the understanding of the methods and results presented. Namely, it is possible to consult the UEFI questionnaire, the flowcharts of the process to obtain the points of the upper-arm and the results of the bilateral filter for noise reduction.

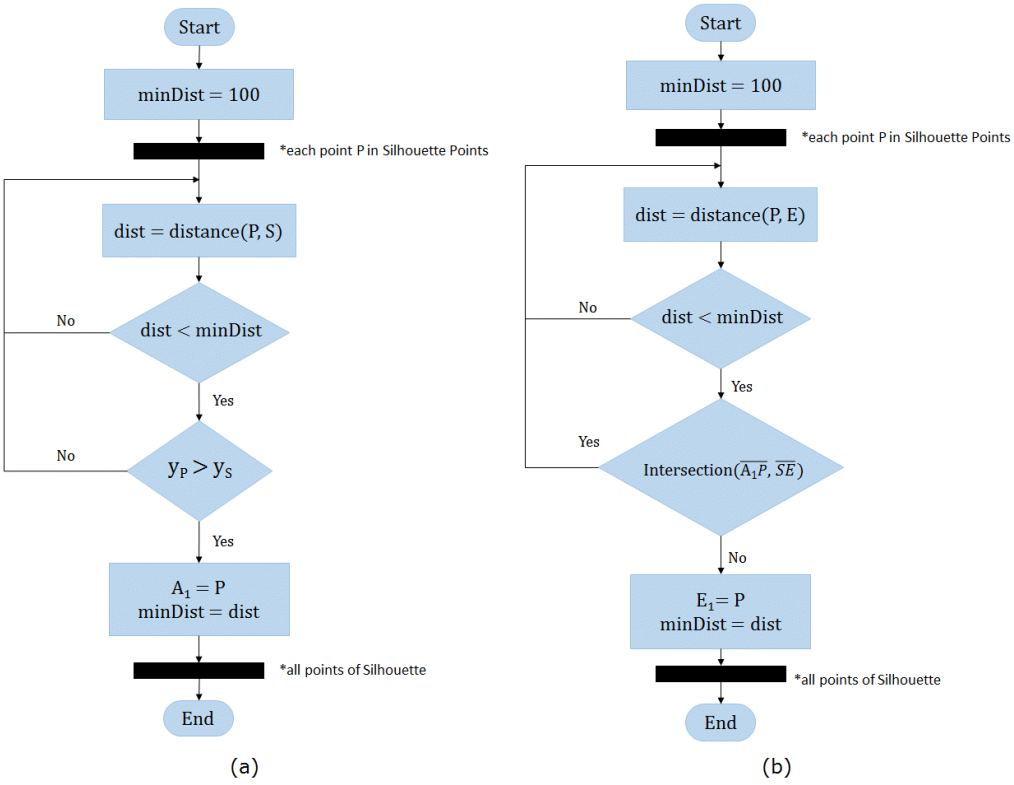

Figure A.2: Delimitation points of the upper-arm area.

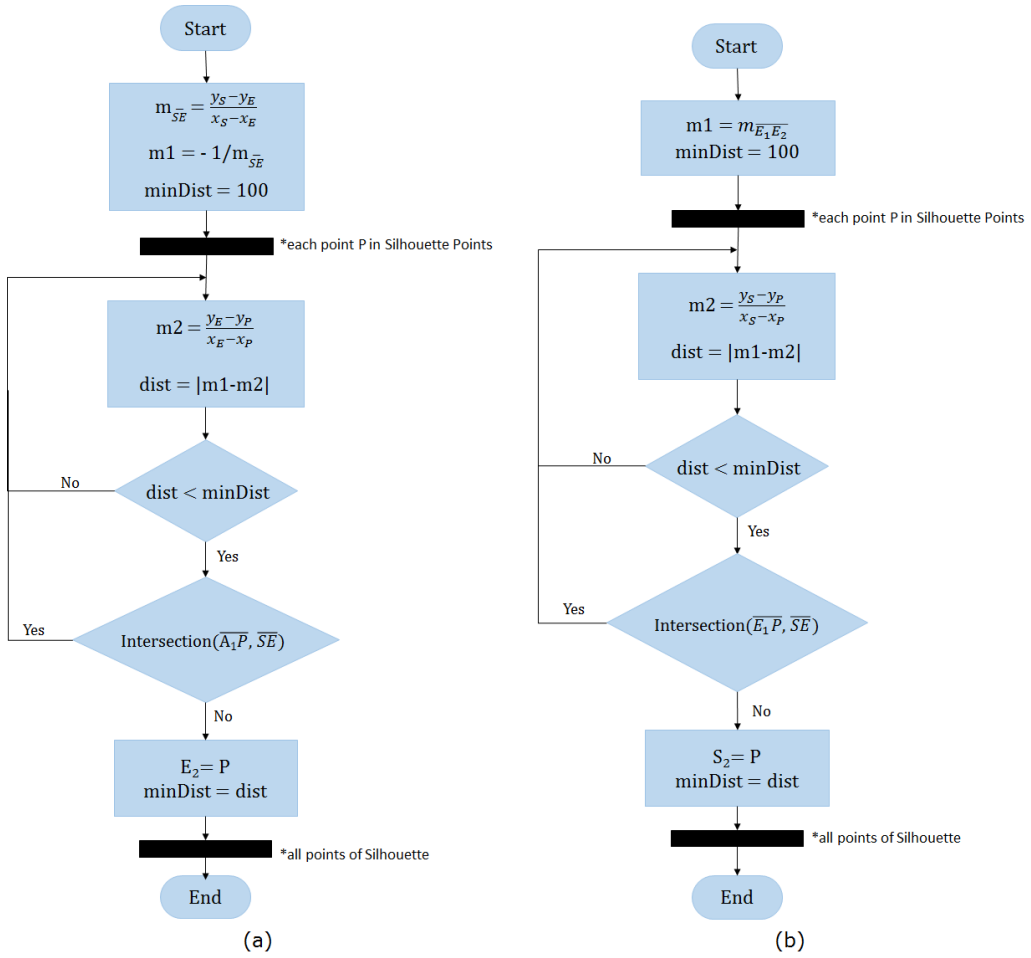

Figure A.3: Delimitation points of the upper-arm area.

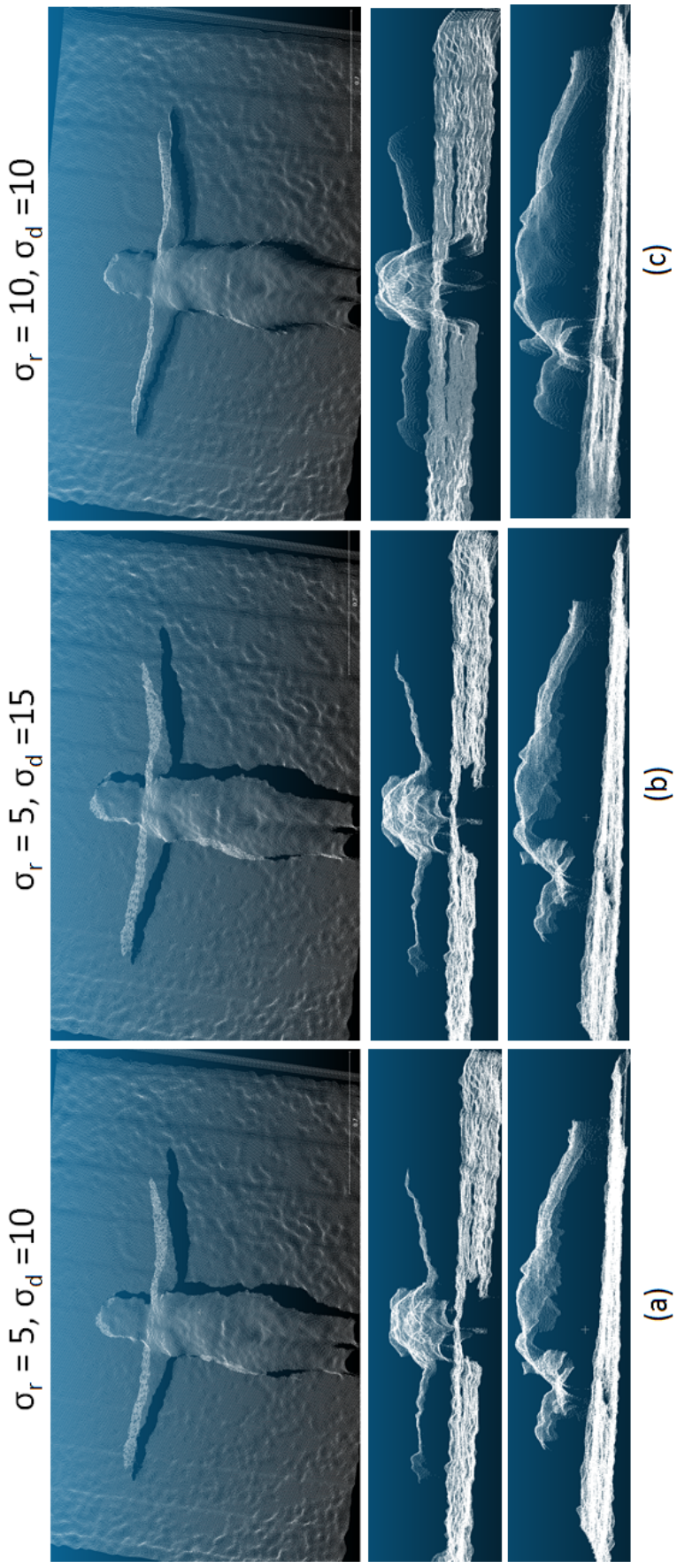

Figure A.4: Bilateral filter with a 9x9 window for differents σ_d and σ_r5.

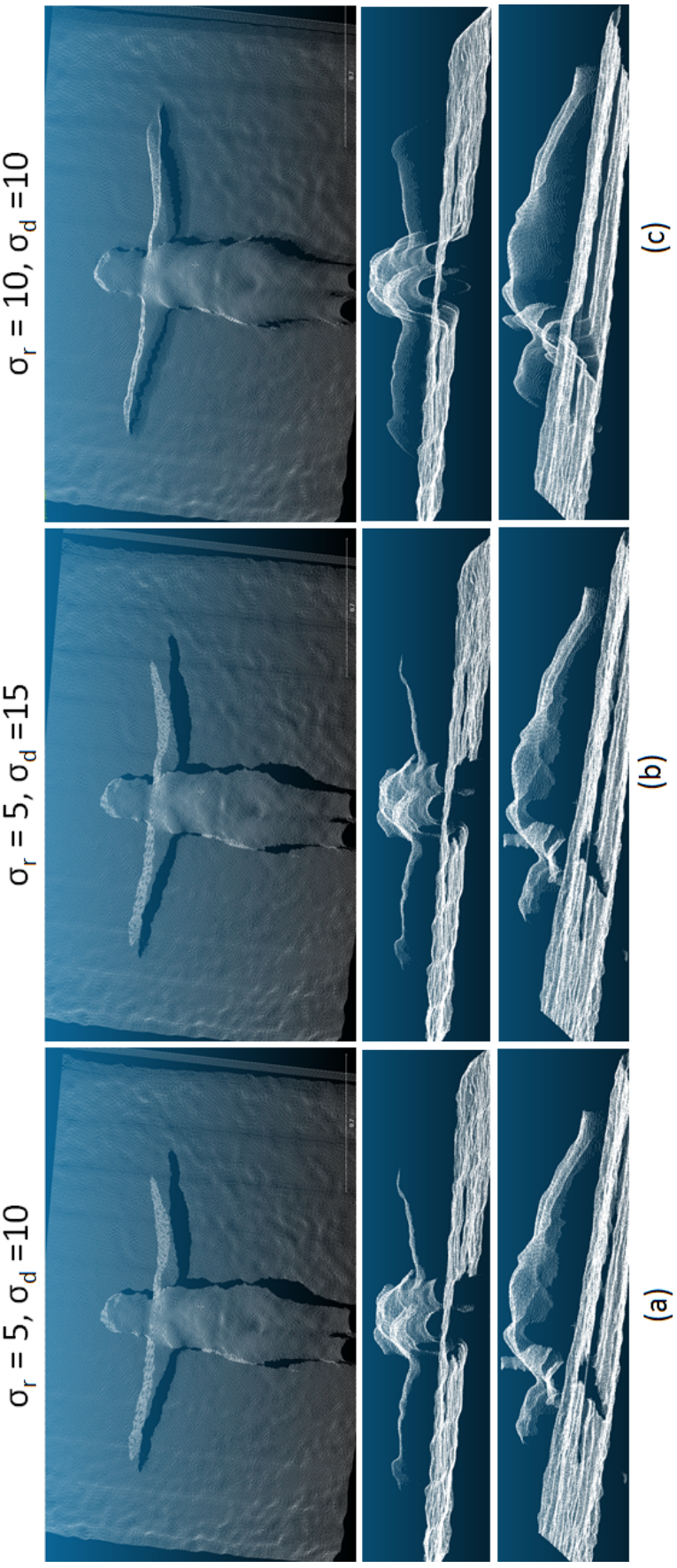

Figure A.5: Bilateral filter with a 15x15 window for differents σ_d and σ_r5.

THE UPPER EXTREMITY FUNCTIONAL INDEX (UEFI)

We are interested in knowing whether you are having any difficulty at all with the activities listed below because of your upper limb problem for which you are currently seeking attention. Please provide an answer for **each** activity.

Today, do you or would you have any difficulty at all with:

(Circle one number on each line)

	Activities	Extreme Difficulty or Unable to Perform Activity	Quite a Bit of Difficulty	Moderate Difficulty	A Little Bit of Difficulty	No Difficulty
1	Any of your usual work, housework, or school activities	0	1	2	3	4
2	Your usual hobbies, re creational or sporting activities	0	1	2	3	4
3	Lifting a bag of groceries to waist level	0	1	2	3	4
4	Lifting a bag of groceries above your head	0	1	2	3	4
5	Grooming your hair	0	1	2	3	4
6	Pushing up on your hands (eg from bathtub or chair)	0	1	2	3	4
7	Preparing food (eg peeling, cutting)	0	1	2	3	4
8	Driving	0	1	2	3	4
9	Vacuuming, sweeping or raking	0	1	2	3	4
10	Dressing	0	1	2	3	4
11	Doing up buttons	0	1	2	3	4
12	Using tools or appliances	0	1	2	3	4
13	Opening doors	0	1	2	3	4
14	Cleaning	0	1	2	3	4
15	Tying or lacing shoes	0	1	2	3	4
16	Sleeping	0	1	2	3	4
17	Laundering clothes (eg washing, ironing, folding)	0	1	2	3	4
18	Opening a jar	0	1	2	3	4
19	Throwing a ball	0	1	2	3	4
20	Carrying a small suitcase with your affected limb	0	1	2	3	4
	Column Totals:					

SCORE: _____/80

Figure A.1: Upper Extremity Functional Index.

Appendix B

Acquisition Protocol

B.1 Kinect System

Kinect has an RGB camera and a dual infrared depth sensors: a projector and an infrared sensitive camera on the same band. The default RGB video stream uses 8-bit VGA resolution (640x480 pixels) but the hardware is capable of resolutions up to 1280x1024 (at a lower frame rate). The monochrome depth sensor has a VGA resolution (640×480 pixels) with 11-bit depth that allows 2,048 sensibility levels. Both video outputs work at 30 frames per second (fps).

B.1.1 Hardware requirements

The sensor should be connect to a computer with the following requirements:

- Windows 7, Windows 8, Windows Embedded Standard 7, or Windows Embedded POSReady 7
- 32 bit (x86) or 64 bit (x64) processor
- Dual-core 2.66-GHz or faster processor
- Dedicated USB 2.0
- 2 GB RAM
- Microsoft Kinect Software Development Kit (SDK) or Kinect Runtime

B.1.2 Limits

The sensor is based on optical lenses and has some limitations, but it works well under the following ranges (all starting from the center of the Kinect):

- Horizontal viewing angle: 57°
- Vertical viewing angle: 43°
- User distance for best results: 1.2m (down to 0.4m in near mode) to 4m (down to 3m in near mode)
- Depth range: 400mm (in near mode) to 8000mm (in standard mode)
- Temperature: 5 to 35 degrees Celsius
- Elevation angle of the tilt motor in the sensor: –27° to +27°.

B.1.3 Skeleton Joints

The depth stream can be used to detect the presence of humans in front of the sensor. Skeletal tracking is optimized to recognize users facing the Kinect, so sideways poses provide some challenges because parts of the body are not visible to the sensor.

- A skeleton contains 20 positions, one for each "joint" of human body;
- The 3D position of each of the skeleton joints (if active tracking is enabled) are stored as (x, y, z) coordinates.
- Each x, y and z coordinate represents the distance in meters from the Kinect sensor, which is consider the origin, looking in the direction of the positive z-axis.
- In the default full skeleton mode, Kinect track the skeleton with 20 joints.
- In the seated mode, Kinect track the skeleton only with the 10 upper joints.
- Placing the Kinect on a surface that is not level (or tilting the sensor) to optimize the sensor's field of view can generate skeletons that appear to lean instead of be standing upright.

B.1.4 Position

- The sensor should be localized 1 – 1.8 m away from the patient and at 0.6 – 1.8 m off the floor (depending on patients height), with nothing between the patient and the sensor.
- Only the patient should be in the detection's range of the sensor.
- Nothing should prevent the sensor to automatically tilt up or down.
- The sensor shouldn't be placed on or in front of a speaker or on a surface that vibrates or makes noise.

B.1.5 Acquisition Parameters

- The Kinect is set to work in near mode
- Both the color and depth images are taken exactly at the same time.
- The RGB stream resolution is 640x480 pixels.
- The depth stream resolution is 640x480 pixels.
- The RGB and depth images were captured at 30fps.

B.1.6 Room environment

- Kinect works in all lighting situations (even darkness), but better in moderate light than in direct sunlight or full-spectrum lighting. Thus, the room should have enough light so that the patient's face is clearly visible and evenly lit. The side or back lighting, especially from a window, should be avoided.
- Ideally the light will come from behind the sensor.
- Skeleton tracking is less reliable with large amounts of natural light.

B.2 Patient

- Patients need to be at least 1 m tall and
- The acquisition will be taken while each patient is standing up.
- The patient should maintain the upper limbs in the coronal plane.

B.2.1 Arm Movement

It will be ask to the patient to start with both arms extended along the body side. Then, the subject is asked to slowly perform a movement of abduction and adduction of the limbs.

B.3 Data

The Kinect, along with the SDK, is used in order to gather the information about the patient in the form of RGB and depth frames and of a .csv file which is composed by the tridimensional coordinates of each joint.

- Color images are stored as a standard bitmap file with 32 bits per pixel and with a resolution of 640x480.
- Depth images are stored as a standard bitmap file with 16 bits per pixel grayscale channel and with a resolution of 640x480.
- Both RGB and Depth images are saved in the PNG format.
- It is possible to save a .txt file with observations about the patient.

B.3.1 Files Organization

- All the collected data is stored in a folder with the name *PatientXX_code_yyyy_mm_dd_hh_mm_ss*, where *XX* represents the patient's number, *code* the patient's code and *yyyy_mm_dd_hh_mm_ss* represents respectively the year, month, day, hour, minutes and seconds.
- RGB images file names are in the format: *PatientXX_code_Color000000N_yyyy_mm_dd_hh_mm_ss_ms.png*, where *XX* represents the patient's number, *code* the patient's code, *N* the RGB picture number and *yyyy_mm_dd_hh_mm_ss_ms* represents respectively the year, month, day, hour, minutes, seconds and milliseconds when the frame is acquired.
- Depth images file names are in the format: *PatientXX_code_Depth000000N_yyyy_mm_dd_hh_mm_ss_ms.png*, where *XX* represents the patient's number, *code* the patient's code, *N* the Depth picture number and *yyyy_mm_dd_hh_mm_ss_ms* represents respectively the year, month, day, hour, minutes, seconds and milliseconds when the frame is acquired.
- A *.txt* file is saved with the file name format: *PatientXX_code_Information.txt*, where *XX* represents the patient's number and *code* the patient's code.
- The *.csv* file name is in the format: *PatientXX_code_ SkeletonPositionData.csv*, where *XX* represents the patient's number and *code* the patient's code.

B.3.1.1 *.csv* file

- The first column of the *.csv* file contain the time stamp of the acquisition of the joint's positions.
- In the first line of the *.csv* file is listed the name of each joint which positions are saved. In the second line is present the header of the coordinates (x, y, z) that are saved.